# NEW FLORAS FROM THE TETTA CLAY PIT, UPPER LUSATIA, LATE OLIGOCENE–EARLY MIOCENE, GERMANY

**Rafał KOWALSKI [1]*, Olaf TIETZ [2], Elżbieta WOROBIEC [3] & Grzegorz WOROBIEC [3]**

[1] *Museum of the Earth in Warsaw, Polish Academy of Sciences, Na Skarpie 27, 00-488 Warsaw, Poland; e-mail: rkowalskimz@gmail.com*
[2] *Senckenberg Museum of Natural History Görlitz, Am Museum 1, 02826 Görlitz, Germany; e-mail: olaf.tietz@senckenberg.de*
[3] *W. Szafer Institute of Botany, Polish Academy of Sciences, Lubicz 46, 31-512 Kraków, Poland; e-mails: e.worobiec@botany.pl, g.worobiec@botany.pl*
* *Corresponding author*

Kowalski, R., Tietz, O., Worobiec, E. & Worobiec, G., 2024. New floras from the Tetta Clay Pit, Upper Lusatia, late Oligocene–Early Miocene, Germany. *Annales Societatis Geologorum Poloniae,* 94: 19–59.

**Abstract:** One hundred and nine taxa of carpological remains, 3 taxa of leaves, and 103 taxa of sporomorphs are identified from the late Oligocene to Early Miocene deposits at the Tetta Clay Pit, eastern Germany. Palynological analysis was performed for the first time for this site. Among the carpological remains, 82 taxa are documented for the first time for this site, including two new fossil-genera (*Paranothotsuga* Kowalski gen. nov., *Pterosinojackia* Kowalski gen. nov.), and one new fossil-species (*Sparganium tuberculatum* Kowalski sp. nov.). New combinations are also introduced (*Paranothotsuga jechorekiae* (Czaja) Kowalski n. comb., *Magnolia germanica* (Mai) Kowalski n. comb., and *Morella stoppii* (Kirchheimer) Kowalski n. comb.). Discovered microremains of *Pesavis tagluensis* fungus extend the age range of the sedimentary sequence from the previously suggested Middle Miocene to at least the latest Oligocene. Two biostratigraphic units, the Rott-Thierbach and Wiesa-Eichelskopf floristic complexes are recognized for the first time in Tetta. Beech forests are indicated as the most common vegetation type. All of these fossil assemblages evidence a warm temperate climate, but a shift toward a warmer subtropical climate is inferred in the uppermost part of the studied profile.

**Key words**: Upper Oligocene, Lower Miocene, fruits, seeds, leaves, pollen, palaeoclimate, palaeoecology.

*Manuscript received 23 November 2022, accepted 17 September 2023*

## INTRODUCTION

“Tertiary”* deposits at the northern margin of Upper Lusatia, between Kamenz, Bautzen, and Niesky, are common, but limited to small, isolated depressions called ”Marginal Basins” (Standke, 2008; Fig. 1A). Many fossil sites and macrofloras have been discovered in such Marginal Basins, including the most famous clay pit Wiesa, near Kamenz (Mai, 1995, 2000), ca. 40 km west-northwest of the Tetta clay deposit. Further explanations to definition and different views on the genesis of Marginal Basins are presented in the next chapter. The age of most of these macrofloras is imprecise or uncertain, as stratigraphic comparison between the macrofloras of different basins is difficult and radiometric and faunal correlations are lacking. For these reasons, lithostratigraphic (sequence-stratigraphic) correlation is the primary method for deriving the stratigraphic position of these fossil floras. Particularly useful are successive lignite seams, characterized by unique palynofloras (Krutzsch, 1957; Mai, 1967, 1995).

The Tetta Clay Pit is typical among the other Marginal Basins. Owing to the lack of fossil finds and lignite seams, the stratigraphy of the Tetta clay deposit long remained uncertain (Standke, 2008, p. 408). Since the opening of the Tetta Clay Pit in 1995, plant fossil discoveries have enabled the first age estimations, dating at least part of the sedimentary sequence to the Middle Miocene (Czaja and Berner, 1999; Czaja, 2000, 2001; Leder, 2007, 2009).

This paper comprehensively documents the geology and fossil floras of the sedimentary sequence exposed at Tetta in 2018–2019. In addition to macroremains (fruits and seeds, leaves), the results of palynological

* According to the International Commission on Stratigraphy, the term “Tertiary” is now only an informal term and may not be used here. Since “Paleocene and Neogene” is too long, we will simply write “Tertiary” here.

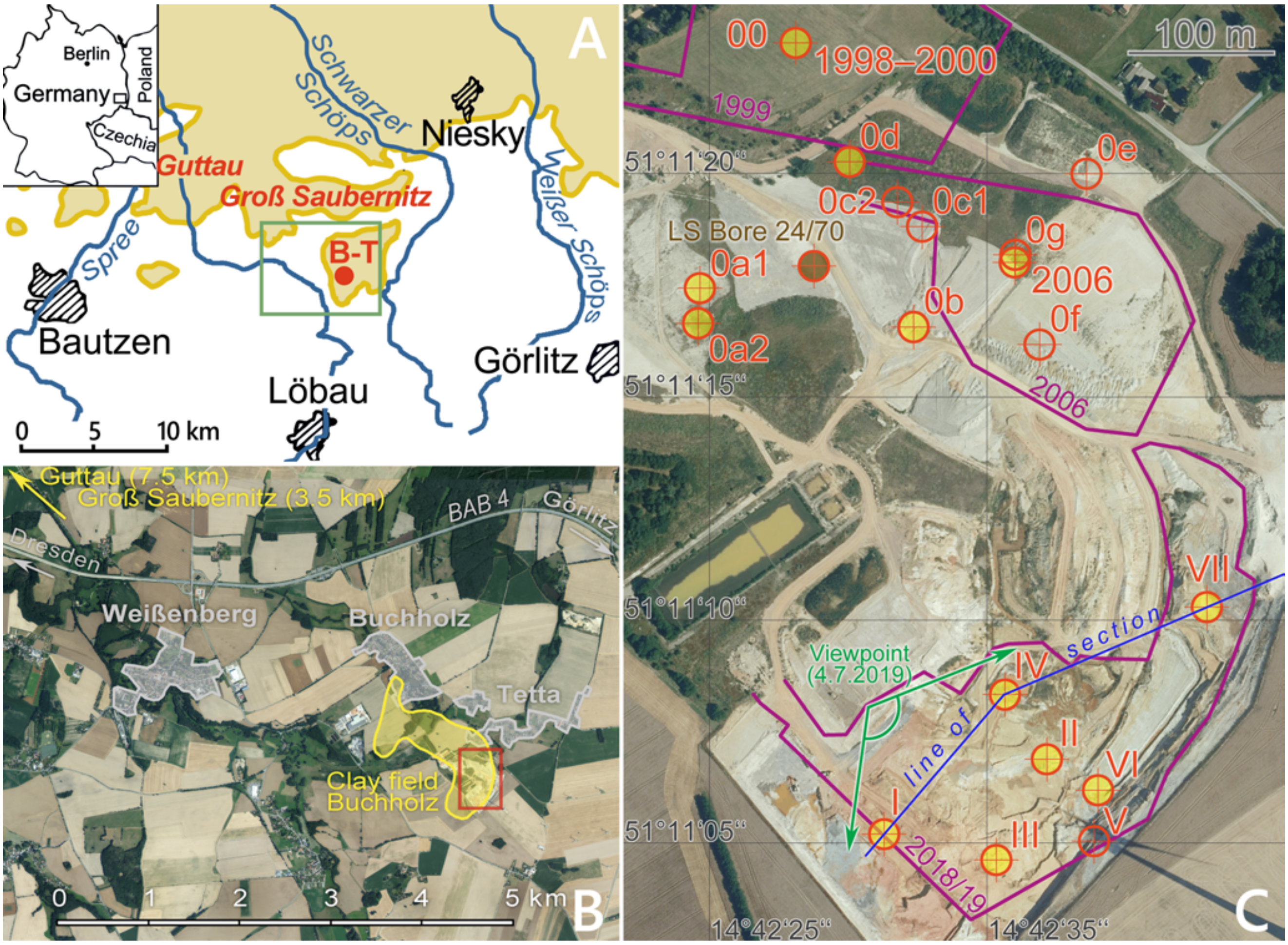


**Fig. 1.** General and specific localization of the studied area. **A.** Geographic position of the Tetta locality and distribution of the Cenozoic (based on Alexowsky and Leonhardt, 1994) with the „Marginal Basins" of Guttau, Groß Saubernitz-Dubrauke (in map only Groß Saubernitz) and Buchholz (red dot with B–T; Buchholz-Tetta), green frame see Figure 1B. **B.** Aerial photo of the close vicinity of Tetta Clay Pit with the explored distribution of the Buchholz-Tetta clay deposit, according to Adam (1974) (yellow) and the present study area (red frame, see Fig. 1C). Date of photo: 30.7.2020. Aerial photo source: District of Görlitz GIS, State Enterprise Geobasis Information and Surveying Saxony (GeoSN), https://gis-lkgr.de/. **C.** Aerial photo of Tetta Clay Pit with approximate open-cast mine boundaries from 1999, 2006 and 2018/19 (time of the present investigation) and fossil sites (red circles, yellow for important finds). LS = 0.6 m Lignite seam in borehole 24/70, approx. 9 m below ground level (Dietrich and Liebscher, 1972). For more information on each site, see Table 1. The blue line shows the profile section for Figure 3. The green arrows indicate the direction of the panorama image in Figure 4. Date of photo: 30.7.2020. Aerial photo Source: District of Görlitz GIS, State Enterprise Geobasis Information and Surveying Saxony (GeoSN), https://gis-lkgr.de/.

analysis are included for the first time for the Tetta Clay Pit. The materials and data collected lead to a new interpretation of the previously proposed age, extending the time interval of the sedimentary profile in Tetta. These new findings make Tetta one of the richest and most interesting palaeobotanical sites in the Upper Lusatia (German: Oberlausitz).

The Systematic Palaeobotany section below contains only the new taxa and new combinations, owing to the length of the publication. Lists of taxa, represented by macroscopic remains found at each site of Tetta, are included in the main text (Tabs 1–9). Descriptions of the remaining taxa and tables (Tabs S1–S4), containing a list of palaeobotanical sites in the Tetta Clay Pit, and various lists of taxa for the macro- and microscopic remains found at Tetta are included in Supplementary Materials.

## GEOLOGICAL SETTING

The so-called Marginal Basins are situated south of the continuous "Tertiary" cover of the North German-Polish Basin, at the northern margin of the uplifted Lausitz Block, consisting of consolidated Cadomian and Variscan rocks. The uplifted areas in the south are dominated by granitoids (Lausitz Granitoid Complex, approx. 540–530 Ma; Linnemann *et al.*, 2010), whereas the basement further north is mostly composed of Neoproterozoic greywackes (Lausitz Group, 555–545 Ma).

The genesis of these Marginal Basins is unclear, as primary deposition was strongly influenced by "Tertiary" relief and Pleistocene glacial deformation. Interpretations include local tectonic basins (Steding and Brause, 1969; Brause, 1990) and relief-controlled erosion relicts (Standke, 1998, p. 23, 2008, pp. 405–408). However, a younger, post-Middle Miocene subsidence also has been proposed, which would indicate post-depositional isolation of the originally contiguous areas of deposition (Göthel, 2004).

Lignite seams play a key role in the lithostratigraphic classification and correlation of Marginal Basin deposits. The most widespread groups of seams in the Marginal Basins are the 2nd (lower Middle Miocene) and 4th (lowermost Miocene) Lusatian Miocene Lignite Horizon (German: MFH; Fig. 2B). In contrast, according to Standke (1998, p. 407) the 3rd MFH (middle Lower Miocene) was not deposited at the southern sedimentation margin of the North German-Polish Basin, especially in southern Lusatia.

Buchholz-Tetta used different names for the clay deposit in the past. Adam (1964, 1974) named the clay occurrence after the village, Buchholz, because to this time there existed only a small active clay pit, directly in the area of the community Buchholz. Czaja and Berner (1999) and Leder (2007, 2009) used the district name Tetta, because the newly created mine is situated closer to this community district (Fig. 1B). In the present work, the district name Tetta is also used for the currently investigated clay mine, except for terms used historically. Furthermore, the term Buchholz-Tetta, following Standke (2008, p. 408f), is used for the entire clay basin or the entire clay deposit that was outlined by Adam (1974, fig. 18) as the Buchholz Mine area. Most geological investigations of the Tetta clay deposit (Fig. 1B) were conducted for exploration purposes and remain unpublished (Adam, 1964; Dietrich and Liebscher, 1972). The few published works focus on clay and kaolin occurrences in the whole of Upper Lusatia, only briefly characterizing the Buchholz deposit (Adam, 1974).

According to Adam (1964), the Buchholz clay deposit consists of up to 3 clay seams and up to 2 coaly clay horizons (Fig. 2). The main clay bed is the lowermost, up to 20 m thick (C3; probably partially including the 2nd seam: C2; see the work of Dietrich and Liebscher, 1972, cited below). Furthermore, sandy interbeds, up to 5 m thick, occur above and between each of these clay seams. Kaolin clay and

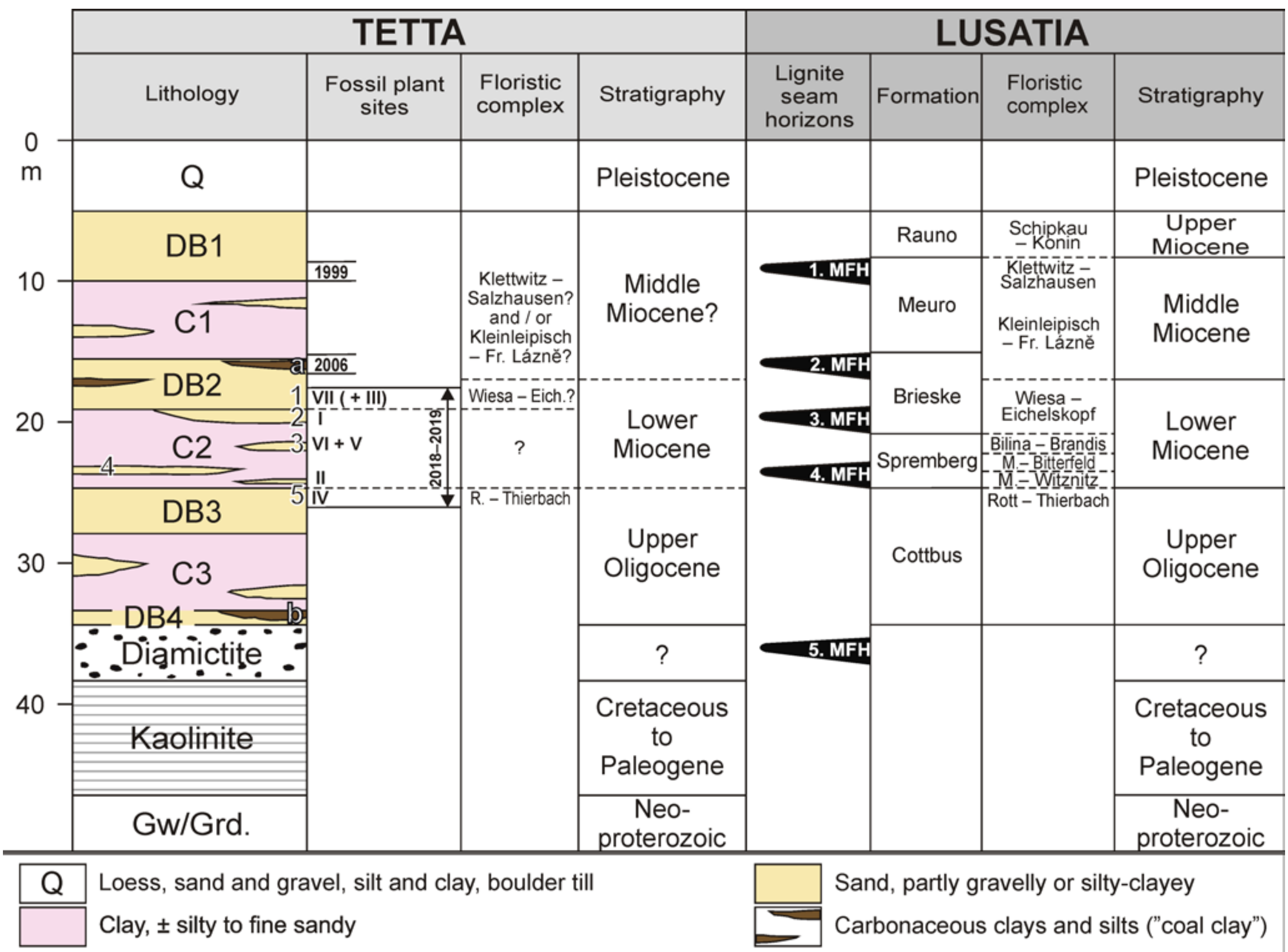


**Fig. 2.** The geological normal section of the Buchholz-Tetta clay deposit (left, TETTA) modified after Adam (1962) and Dietrich and Liebscher (1972), in comparison with the bio- and lithostratigraphic divisions of southern Lower Lusatia and Upper Lusatia (right, LUSATIA). TETTA: Average thicknesses were used, according to Dietrich and Liebscher (1972); DB – Dirt Band, C – Clay Seam (by C2 with sand bed numbers), Gw – Lusatian greywacke, Grd. – Lusatian Granodiorite; a – Upper coal clay (once as a 0.6 m lignite seam in borehole 24/70, Dietrich and Liebscher, 1972), b – Lower coal clay (Adam, 1964); carpological site number in brackets; lithostratigraphic assignment is uncertain, owing to biostratigraphy. LUSATIA: MFH – Lusatian Miocene Lignite Horizon (with number). Modified, according to Standke (2008, fig. 4.5–2, 4.5–3).

silt-sands, observed at the bottom of the sequence, can be interpreted as reworked granodiorite kaolin (Adam 1964, p. 13, App. 3.21). The thickness of the investigated "Tertiary" sequence for the whole exploration area is 5 m to 28 m (Adam, 1964, App. 4.21; excluding kaolin). The 2nd (C2) and 3rd (C3) clay seams (Adam, 1964) are relatively horizontal-bedded between the 1999 and 2006 fossil sites (Fig. 1C), while further southward to the area, exposed in 2018–2019, the strata continuously tilt to south with a dip angle of approx. 8–14° (Fig. 3). This indicates that in 2018–2019 the clay pit must have operated in deeper profile sections than in 1999 and 2006. Therefore, the clay extraction must have been based on the 2nd and/or 3rd, main seam (C2/3), while the 1st (C1, upper) clay seam crops out somewhere between the mining operation areas of 2006 and 2018/19 (for more information, see below).

The Buchholz clay area was identified by Adam (1974) as the southeastern continuation of the "Tertiary" deposit of Guttau (ca. 12 km northwest) and Groß Saubernitz-Dubrauke districts (ca. 8 km northwest; Fig. 1A, B). The Buchholz-Tetta clay area can be distinguished from the Guttau and Groß Saubernitz-Dubrauke clay fields by its lack of brown coal seams (Standke 2008, p. 408). However, according to Adam (1964, p. 26), two coaly clay beds ("Unterer Kohleton" and "Oberer Kohleton") immediately below the 3rd (C3, main clay seam) and near the top of the profile between the 1st (C1) and 2nd (C2) clay seams, documented in the Buchholz-Tetta clay area, may represent facies equivalents of lignite. Adam (1974, fig. 56d) correlated the coaly clay beds with the 3rd and 4th Lusatian Miocene Lignite Horizons, detected 8.3 km northwest in the Groß Saubernitz-Dubrauke clay deposit (according to Standke 2008: Deposit Guttau-Kleinsaubernitz-Weigersdorf-Sandförstgen). He estimated their age as being between the Oligocene and Miocene, which was in accordance with the state of knowledge at the time. According to Standke (2008, fig. 4.5–17, 19), the two lignite seams at Groß Saubernitz-Dubrauke changed in the lithostratigraphic correlation to the 2nd and 4th Lusatian Miocene Lignite Horizons (MFH). Therefore, the lignite seams (see next paragraph) or their facies equivalents in the Buchholz-Tetta clay field have an age of Early to Middle Miocene (Aquitanian–Langhian; Fig. 2).

The interpretation of the lithostratigraphic structure of the Buchholz deposit, presented by Dietrich and Liebscher (1972), is analogous to that of Adam (1964). Newly recognized in their report is a 0.6-m-thick lignite seam (Fig. 1C, bore hole 24/70), discovered between the 1st (C1) and 2nd (C2) clay seams. It was found in a single borehole, 150 m south of the 1999 fossil site, 140 m west of the 2006 location, and 300–400 m northwest of the 2018/19 investigation area. On the basis of the unpublished age estimation by D. H. Mai (in Dietrich and Liebscher, 1972, p. 26), this lignite seam was correlated with the Spremberg beds (Formation), indicating a late Oligocene age for the Buchholz deposit, according to the state of knowledge at the time (Lotsch *et al.*, 1969). The unpublished evidence of the two coaly clay beds (Adam, 1964, p. 26) and seam (Dietrich and Liebscher, 1972, borehole 24/70) for the Bucholz-Tetta deposit has never been considered in the literature. Therefore, until now, their stratigraphic position was unclear (Standke 2008, p. 408). Since the opening of the Tetta Clay Pit in 1995, fossil plant discoveries have enabled the first age estimates. All fossil floras studied so far come from the top part of the profile section (see below) and were assigned to the Middle Miocene (Czaja and Berner, 1999; Czaja, 2000, 2001; Leder, 2007, 2009).

A red clay seam, ca. 13 m thick, exposed during the 2018–2019 fieldwork in the lower part of the outcrop (Figs 3, 4), most likely represents the 2nd (C2) clay seam of the Buchholz-Tetta deposit (see above). The clay appears fat but contains large amounts of silt and smaller amounts of fine sand. The intense red to red-brown colour, in places also yellow-brown, violet, pink and light gray, is striking. The clay sometimes shows a distinctive light gray speckle ("flaming"), which may represent bleaching tubes around roots (pers. comm. I. Valeton, June 13th, 2002).

Two layers of sand were observed above (sites I and VII) and beneath (sites II and IV) the clay seam (sand bodies 1 and 5 in Fig. 3, correlated with DB2 and DB3). Moreover, three gravel-sand layers of limited extent (site III and VI) were found, embedded at different levels within the clay seam (numbered 2–4, Fig. 3). The lenticular sand layers are 0.2 to 4.5 m thick (mostly 1–3 m) and approx. 20–100 m long. The sand inclusions are predominantly fine to coarse-grained, partly also fine gravel and silty clay, light grey to dark (greyish) brown, well layered (often with cross-stratification) and partly contain organodetrital remains, including xylites and carpological fossils. The quartz grains are well to moderately sorted and clearly rounded. Some thin, dark grey to dark brown mud-like and leaf-fragment-bearing silty-sandy-clay horizon intercalations occur. Only sand layer no. 4 does not contain organodetrital residues. The sediment is also particularly coarse-grained (coarse sand to fine gravel) and has no stratification, apart from thin layers of silt and fine sand. Particularly noticeable are the sharp edges of the quartz pebbles, as well as the appearance of many kaolinized feldspars and micas and the inclusion of clay pebbles, mm to cm in size. These characteristics indicate the redeposition of granodiorite kaolin over a short distance and sedimentation from a debris flow. Similar diamictitic sediments of lesser thickness were encountered a little higher in the clay seam in the SW of the pit. All other sands, on the other hand, present organo-detrital residues and according to their structural characteristics can be interpreted as fluvial deposits in the clay basin (oblique stratification, well-sorted and rounded sands, occurrence of plant fossils).

The facies and sedimentary environment of the Marginal Basins are sparsely studied. In general, these deposits, which today are only preserved as erosion relicts, are regarded as limnic-fluviatile and interpreted as deltaic deposits (Göthel, 2004, p. 156). The observations of the present authors in the Tetta Mine confirm this interpretation. In particular, the strong alternation of fine and coarse clastic sediments (clay; sand and gravel) and the intense red-coloured clays confirm terrestrial deposition. In addition to the predominant basin and river deposits, local debris-flow (alluvial fans) and lacustrine deposits can also be assumed (see above).

The intercalated sand layers characterize the bedding conditions of the clay seam. The authors could confirm

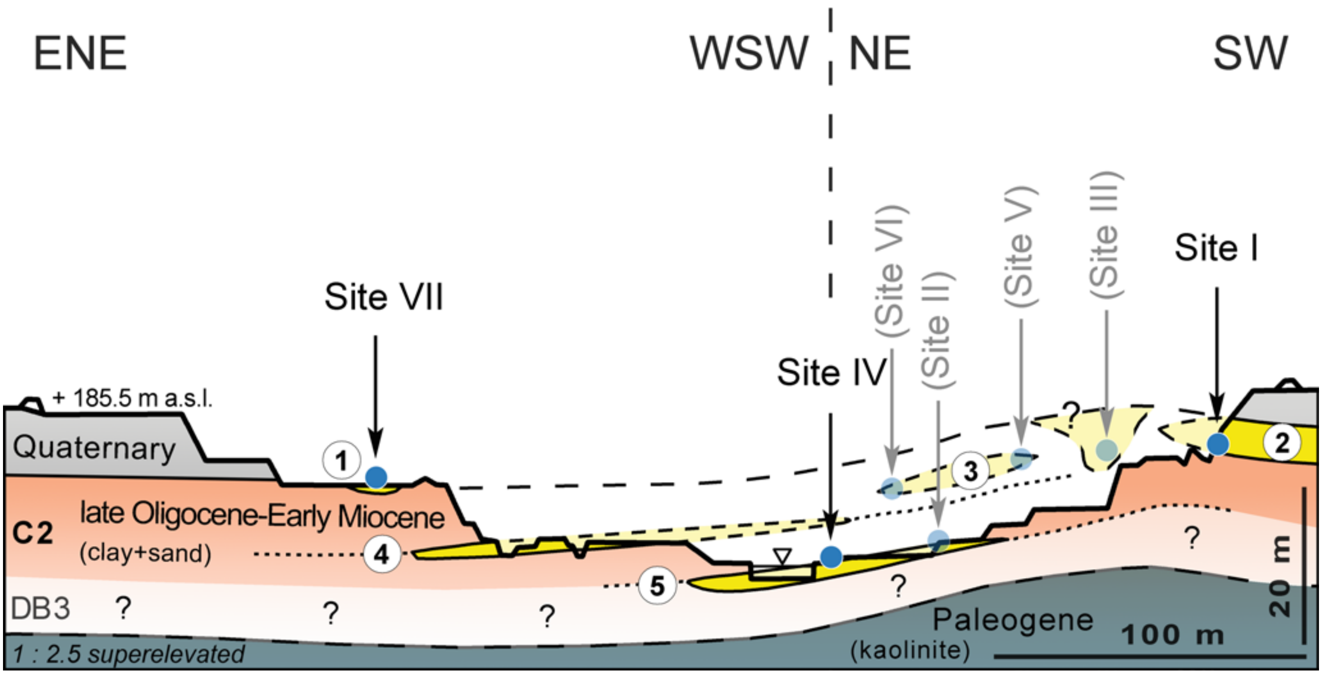


**Fig. 3.** Geological cross-section of the Tetta opencast mine, based on mapping of present authors from 2018/19. The second clay seam (C2) was mined under glacial fold conditions. The sand horizons 2–4 (circled numbers) are embedded in the clay seam. Two further sand-gravel horizons are directly situated above and below the currently mined clay seam (sand horizons 1 and 5, DB2 and DB3). Fossil plant remains could be extracted from most sand and gravel inclusions (sites I–VII). For the profile section line see Figure 1C.

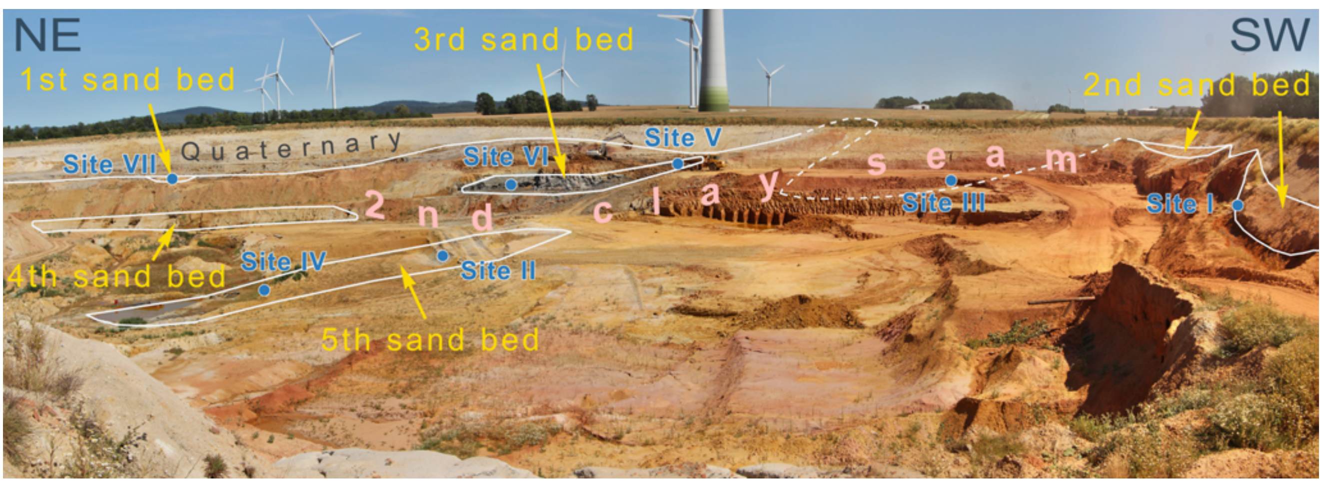


**Fig. 4.** Panoramic photo of Tetta Clay Pit, seen from NW, near the pit entrance (lower right edge of the picture). Compare sand bed numbers with Figure 3. The position, from which the photo was taken, is shown in Figure 1C (green arrows). Fossil site III no longer existed at the time the photo was taken on July 4th, 2019. The position of the site and the synclinal structure were projected onto the photo on the basis of previous mapping.

the consistently shallow dip to the north for this part of the clay deposit, reported by Adam (1964) and Dietrich and Liebscher (1972). The measured bed inclinations of 348°/12° and 20°/12° fit well with those determined from exploration boreholes (Adam, 1964). In 2018–2019 fieldwork, layers rose to their highest point and presented strong glacial deformation at the southern limit of the active pit. Clay layers were folded particularly clearly into anticlines and synclines up to 15 m deep with a clear south vergence. The top of the domal uplift shows an approx. 50–100 m depression, where overturned conditions were observed the Pleistocene sediments (likely the Elster-1 glacial) are folded in the core of the syncline. As plant remains found in site III originate from this complicated structure, their occurrence is lower than their stratigraphic position (Tab. S1) relative to site I (Fig. 3).

Another problem of correlation exists between sites II and VI. According to field observations, they belong to sand layers 5 and 3 and thus to different levels in stratification (Fig. 3). However, according to biostratigraphic evaluation, fossil finds from the two sites indicate a comparable age. This discrepancy represents the main contradiction in the present work and cannot yet be clarified. This also applies to the relatively clear lithostratigraphic correlation between sites II and IV, which show slightly different biostratigraphic ages (see below). However, this correlation (over 60 m) could not be observed directly because between the two outcrops (each with approx. 1–2 m high cutting walls) lies an area of leveled ground with a poor degree of exposure (Fig. 4). Therefore, strata displacement (e.g., due to Pleistocene deformation) cannot be ruled out completely. The authors attempted to localize previously published floras (see above) in the geological profile and describe their relation to the fossiliferous layers documented in the present paper. The carpological flora, described by Czaja and Berner (1999) and Czaja (2000, 2001), was found in the ca. 3-m-thick upper sand-gravel-horizon (DB1, for position and stratigraphy see Fig. 2A, site "1999") situated at the top of the clay pit. This fossiliferous layer was clearly stratified and consisted of clayish-silty fine to coarse sand, with fine gravel intercalations. It was rich in varied plant detritus, including continuous layers of driftwood, up to 1 m long. The exact location of this site cannot be established, as coordinates are lacking, but using a combination of aerial photos and the coordinates of Leder (2007), it is approx. 470–590 m north-northwest of the 2018–2019 clay pit operation area (Fig. 1C, site 00). The fossiliferous layer was located 180–183 m a.s.l. and can be correlated with the sand bed (DB1) above the 1st (C1) clay seam, according to Adam (1964, App. 4.21, 5.4).

The fossil flora described by Leder (2007, 2009) was found about 200 m southeast of the site, described by Czaja and Berner (1999; Fig. 1C, site 0g). Fossil plant remains were discovered in a carbonaceous clay lens, up to 20 cm thick and up to 500 cm long, embedded in a sand-gravel lens, located 0.8 m above the base of the pit and 16 m below ground level, 170 m a.s.l. (Leder, 2007). It was a part of an approx. 10-m-long sand-gravel channel within the lower section of the clay seam C1 (Fig. 2), approx. 10 m below the upper sand-gravel horizon (DB1) where Czaja and Berner's (1999) fossil flora occurred. A second sand-gravel horizon found ca. 5 m below (joint field trip O. Tietz, R. Leder and J. Czossek, 6.12.2006; see also Leder, 2007) was mostly lacking in fossils, except for one location at the NW margin of the pit. Here, numerous leaves and carpological remains were found in dark brown to dark gray silty-clay lenticular intercalations, up to 26 cm in thickness and 600 and 300 cm in length (Fig. 1C, site 0f). It appears that the second sand-gravel horizon (DB2) corresponds to the horizon, described by Leder (2007). Both horizons lay within or immediately below the basal section of clay bed C1 (Fig. 2, site "2006"). They are at least 15 m long and 1.2 m thick (the base of clay bed C1 was unavailable for Leder, 2007).

Considering the exploration reports by Adam (1964) and Dietrich and Liebscher (1972), the fossiliferous layer, described by Leder (2007, 2009), most likely lies between the 1st and 2nd Tetta clay seams (C1/C2). Its stratigraphic position and lithological characteristics indicate that it may correspond with the upper coal-clay horizon (according to Adam, 1964 and Dietrich and Liebscher, 1972). According to Standke (2008), the upper coal-clay horizon may represent the 2nd MFH and therefore a late Early Miocene age (late Burdigalian). However, biostratigraphic dating of the coaly intercalations in the higher section of Tetta with the 2nd MFH, based on a purely lithostratigraphic correlation, is problematic. Furthermore, the regional distribution of the coaly intercalations at Tetta has not been proven. An alternative interpretation could be local limnic-fluviatile deposits that cannot be age-correlated with the Lusatian paralic-lacustrine lignite seams (MFH).

## MATERIAL AND METHODS

The basis for this research paper is a collection of fossil plant remains, mainly fruits and seeds (ca. 4,000 specimens), gathered by R. Kowalski and O. Tietz during four joint excursions to the Tetta Clay Pit in the years 2018–2019. The Tetta Clay Pit is located near Buchholz, Upper Lusatia, Germany (51°11′08.3″N, 14°42′34.0″E; Fig. 1A, B), a district in the municipality of Vierkirchen. Twelve samples, representing different layers, were taken directly from the geological profile at seven sites (numbered I–VII, Tab. S1). Six samples provided both micro- (spores, pollen grains, and non-pollen palynomorphs – Tab. S4) and macrofossil remains (mainly fruits, seeds, cones, leaves, Tabs 1–5, and wood, not included in this paper), two only microfossils (Tab. S4), four only macrofossils (Tabs 6–9), and two were barren. The locations of the sites are shown in Figure 1C.

Site IV was in the deepest and middle part of the clay pit. Three samples with diverse fossil assemblages of macro and microremains were collected here at an altitude of 162 m from the highest part of the sand bed DB3. Sample IV/1 was taken from a silt-flaseric fine sand layer (Tab. 1). Samples IV/2 (Tab. 2) and IV/3 (Tab. 3) were collected from layers ca. 40 cm above sample IV/1. These layers were black, brown and fine-flaser-bedded, clayey with fine sandy silt. Sediment samples of ca. 20 cm in thickness were taken one above the other (IV/1 to IV/3).

At site II, two samples were taken from close to the base of the clay pit. The dark clay layer, from which sample II/5 (Tab. 4) was taken, was at an altitude of 165 m, with the sand-silt-clay layer with flaser bedding, source of sample II/4 (Tab. 5), lying ca. 40 cm below. Both provided macro- and microremains.

Site V was in the southeastern part of the Tetta Clay Pit, ca. 80 m east-northeast of site III. Here, sample V/10 was taken from the clay at an elevation of 179 m and provided only microremains. In June and July 2019, it was possible to see the bedding connection between sediments of site V and site VI, significantly deeper in terms of elevation.

Site VI was in the southeastern part of the Tetta Clay Pit, ca. 50 m north of site V. Two samples were collected here. Sample VI/6, which was taken from sands at an altitude of 172 m, provided only macroremains (Tab. 6), and sample VI/7 (Tab. S4), taken from grey silt-clays, provided only microremains.

Site I was on the southern margin of the Tetta Clay Pit. The fossiliferous layer occurred in a 4-m-thick gravel-sand-silt-clay sequence between the main clay seam (C2) and the Pleistocene cover. Along with site VII, site I represents the upper part of the sedimentary sequence exposed in Tetta in the years 2018–2019. Sample I/8, which was taken from a sand-silt layer at an elevation of 179 m, provided only

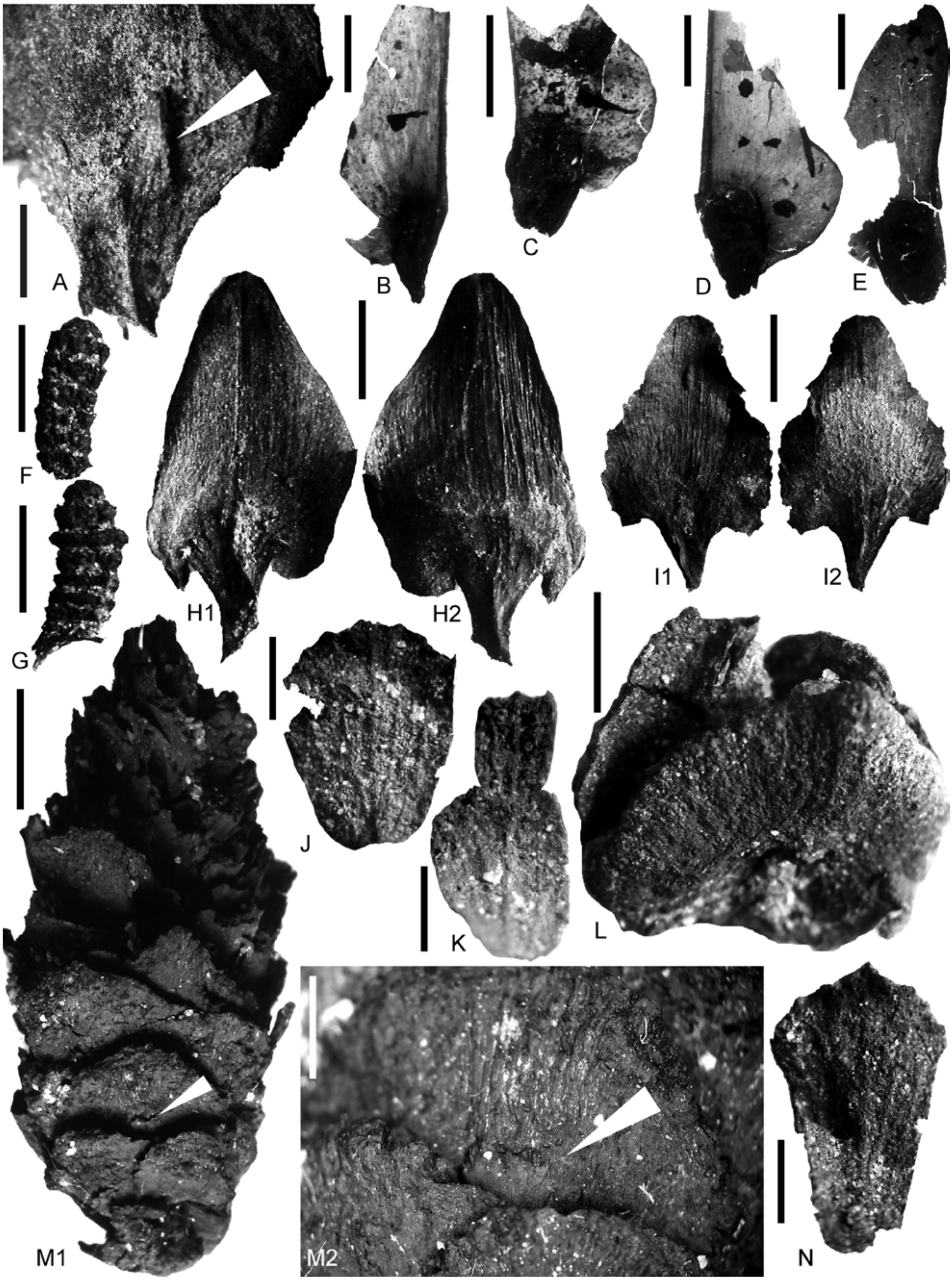


**Fig. 5.** Carpological remains from Tetta. **A.** *Pseudolarix schmidtgenii* Kräusel, bract-scale complex close-up, arrow indicates the bract, MZ VII/134/4, 2 mm. **B–E.** *Pseudolarix schmidtgenii* Kräusel, seeds, MZ VII/134/150, 151, 5 mm. **F, G.** *Pseudolarix schmidtgenii* Kräusel, brachioblasts, MZ VII/134/10, 5 mm. **H1, H2, I1, I2.** *Pseudolarix schmidtgenii* Kräusel, bract-scale complex, opposite sides of the same specimen, MZ VII/134/4, 5 mm. **J, K, N.** *Tetraclinis salicornioides* (Unger) Kvaček, branch segments, MZ VII/134/14, 1 mm. **L.** *Tetraclinis salicornioides* (Unger) Kvaček, seed cone, MZ VII/134/9, 2 mm. **M1.** *Tsuga moenana* Kirchheimer, seed cone, MZ VII/134/6, 10 mm. **M2.** *Tsuga moenana* Kirchheimer, close-up of M1, arrow indicates the bract, MZ VII/134/6, 1 mm.

macroremains (Tab. 7). Sample I/9, taken from a clay layer ca. 2.5 m above the position of sample I/8, provided a relatively rich microfossil assemblage but only a few macrofossils (not included in this paper).

Site III, in the southeastern part of the clay pit, only exposed in 2018 was at an elevation of 176 m. The sand layer, from which sample III/11 was obtained, provided only macroscopic plant remains (Tab. 8).

Site VII was in the eastern part of the Tetta Clay Pit, ca. 150 m north of site VI. It was cut from the highest mining level at an altitude of 180 m, a small sandy syncline above clay seam C2. This level was covered by Pleistocene gravel-sands and till, as shown by various till slices, embedded in the sediments of the fossil site and a mining slope 8 m to the east. Sample VII/12, which was taken from organo-detritic sand, provided only macroremains (Tab. 9).

Fossil remains from sands were either picked directly from the layer, or sediment samples were collected in bulk and sieved in the laboratory. Remains from silt and clay were isolated in the laboratory in the following way: 1) sediment samples were dried at room temperature, 2) washed with boiling water and laundry detergent, and 3) after cooling, the disaggregated sediment was sieved and dried.

The here documented collection of fossil macroremains from the Tetta Clay Pit is stored at the Polish Academy of Sciences, Museum of the Earth, Warsaw, Poland. Specimens were numbered consecutively MZ VII/134/1-311.

Unpublished material from Senckenberg Museum of Natural History Görlitz, collected by Alexander Czaja and Olaf Tietz in the years 1998–2000, is also included in this article. According to Czaja and Berner (1999), smaller plant remains were extracted from sediment samples, using sieves, and larger specimens were collected in-situ from naturally washed accumulations at foot of the walls of the pit. Most specimens have been identified and are stored in the geoscientific collection of the Senckenberg Museum of Natural History Görlitz, Germany, under the numbers Tet. K 1193–1257 (consecutive numbers with 74 counting units and a total of 580 individual specimens).

Comparative studies are based on the fossil and carpological collections from the PAS, the Museum of the Earth in Warsaw, the Senckenberg Museum of Natural History Görlitz, the Museum of Natural History Berlin, and W. Szafer Institute of Botany, Polish Academy of Sciences, Kraków.

Ten sediment samples from sites I, II, IV, V and VI were used for the palynological study. The samples were prepared in the laboratory of the W. Szafer Institute of Botany PAS, using HCl, KOH, and HF (Moore *et al.*, 1991). Three to eight slides were studied for each sample. Nine samples (IV/1, IV/2, IV/3, II/4, II/5a, II/5b, VI/7, I/9 and V/10, Tab. S4) yielded more than 500 well-preserved sporomorphs (pollen grains and spores; in these samples all co-occurring non-pollen palynomorphs were also counted). The palynological slides and residues are stored in the W. Szafer Institute of Botany, Polish Academy of Sciences, Kraków.

All carpological remains, some leaves and important palynomorphs (spores, pollen grains and a fungus), gathered by R. Kowalski and O. Tietz during four joint excursions to the Tetta Clay Pit in the years 2018–2019, are illustrated on Figures 5–22. Only new, macroscopic fossil-taxa are fully described here (Figs 6A, B, 7P, Q, 8F, 13I, L, 17G, M, N). Other taxa, including macroscopic plants remains and microremains of fungi, are only illustrated on the figures (Figs 5A–N, 7A–O, 8A–E, G–H, 9A–J, 10A–P, 11A–J, 12A–O, 13A–H, J–K, M–T, 14A–U, 15A–T, 16A–H, 17A–F, H–L, O, 18A–K, 19A–H, 20A–G, 21A–J, 22Z–BB), but described in the supplementary materials.

## SYSTEMATIC PALAEOBOTANY

Family Pinaceae Sprengel ex F. Rudolphi, 1830
Genus *Paranothotsuga* Kowalski gen. nov.

**Type species:** *Paranothotsuga jechorekiae* (Czaja) Kowalski gen. nov et sp. nov comb., monotypic.
**Etymology:** Generic name indicates the resemblance to *Nothotsuga*.
**Amended diagnosis**: Distal part of the ovulate scale with two extended downwards lobes, proximal part with lateral auricles. Bract and scale of equal length. Bract lanceolate, with two cusps at midpoint.
**Description:** As for the species, below.
**Remarks:** As for the species, below.

*Paranothotsuga jechorekiae* (Czaja) n. comb.
Fig. 6A, B

v*2000 *Pseudotsuga jechorekiae* sp. nov. – Czaja, pp. 129–134, pl. 1, fig. 6.
2001 *Pseudotsuga jechorekiae* (Czaja) – Czaja, p. 30, pl. 2, figs 1–2.
(?) 2014 *Pseudotsuga jechorekiae* (Czaja) – Kunzmann, pp. 397–400, pl. 4.
2017 *Cathaya vanderburghii* sp. nov. – Gossmann ex Winterscheid and Gossmann, pp. 188–192, figs 2A–I.

**Epitype:** Specimen MZ VII/134/7 designated here as epitype is stored in PAS the Museum of the Earth in Warsaw.
**Materials:** Holotype – Tet.k 799; Tetta IV/3–1 specimen (MZ VII/134/7).
**Diagnosis:** As for the genus, above.
**Description:** Single bract-scale complex. Ovulate scale slightly abraded on the margin of distal part. 1.1 cm long, 0.9 cm wide, obovate in outline. Proximal (basal) section triangular, ca. half the full length of the scale, auriculate extension preserved on one side. Distal section abruptly extended, semicircular with two lobes directed toward the base. Scale longitudinally wrinkled. Bract narrowly lanceolate, gradually narrowing toward the apex, ca. 1.1 cm long and 1.5 mm wide at its widest point, slightly below the middle of its length two laterally directed short (0.5 mm long) remains of cusps.
**Remarks:** Bulges on the ovulate scale margin of *Pseudotsuga jechorekiae* were not mentioned in the protologue but are visible on the specimen illustrated by Czaja (2000, pl. 1, fig. 6) and were seen by the first author in type material (17.10.2018). This clearly indicates that the

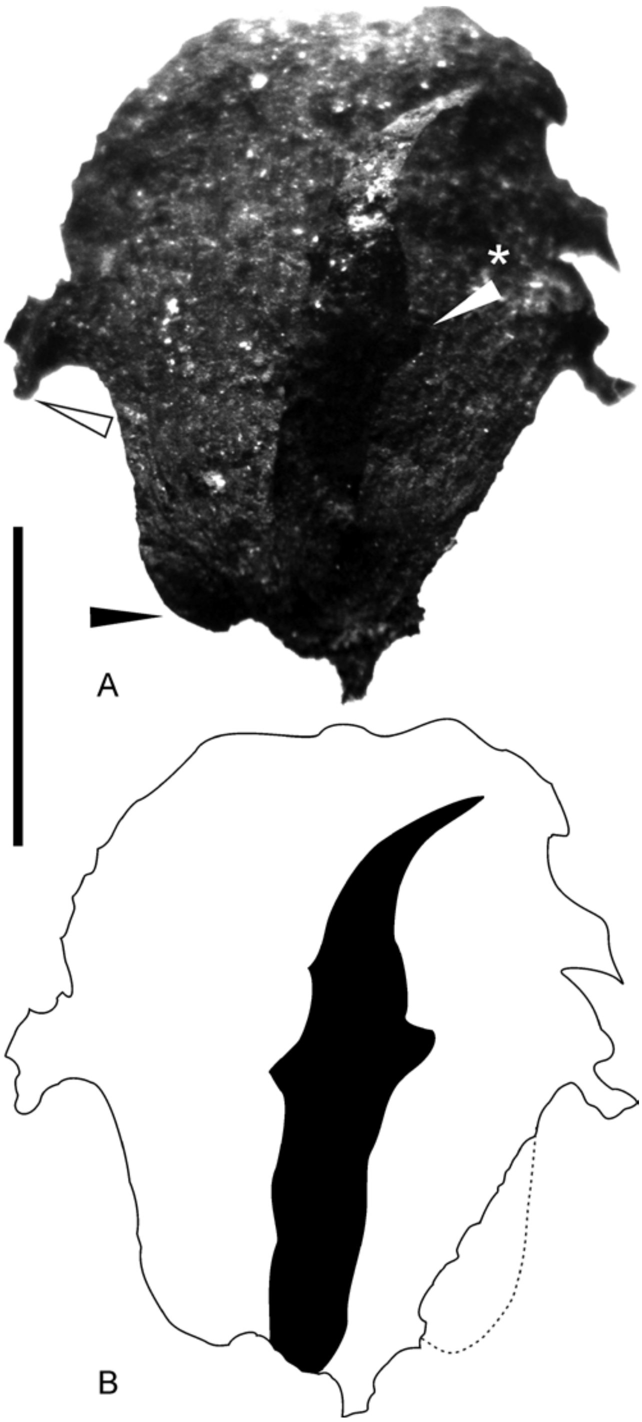


**Fig. 6.** Carpological remains from Tetta. **A, B.** *Paranothotsuga jechorekiae* (Czaja) Kowalski gen. nov et sp. nov comb., bract-scale complex, black arrow indicates auriculate extension, white arrow indicates downward lobe, white arrow with asterisk indicates cusp on the bract, MZ VII/134/7, 10 mm.; B – outline of A.

specimen of the present authors and the one described by Czaja belong to the same species. There is also a noticeable similarity in the shape of the bracts, but nothing is known about lateral cusps in *Pseudotsuga jechorekiae*. Auricles on the distal part of ovulate scales in the materials presented by Czaja are not visible, but probably could be revealed by breaking the scales off.

The shape of the ovulate scale in the specimen of the present authors corresponds with living *Nothotsuga* Page, 1989 (Frankis, 1988; Fu *et al*., 1999; Farjon, 2010). However, in *Nothotsuga*, the bract is shorter and broader, has only a short median cusp and lacks lateral lobes. On the other hand, it is possible that lateral cusps are not the bases of longer lateral structures, but represent remnants of broader (spatulate), proximal part of bract, which were broken during fossilization or extraction. Another difference is that in living *Nothotsuga*, cones may disintegrate on the tree (Farjon, 2010), while materials described by Czaja (2000) indicate that *Paranothotsuga* sheds whole cones.

Despite a striking resemblance to *Nothotsuga* in the shape of ovulate scale, the erection of a new genus is justified, owing to the major difference in the shape of bract.

Considering the shape of ovulate scales, the cones described by Winterscheid and Gossmann (2017) from the Lower Pliocene of Lower Rhine Basin (North Rhine-Westphalia, Germany) as *Cathaya vanderburghii* Gossmann ex Winterscheid and Gossmann, undoubtedly represent *Paranothotsuga jechorekiae*. In the opinion of the present authors, the ligulate-spathulate shape of bracts, which according to Winterscheid and Gossmann indicate a relationship with *Cathaya*, are incompletely preserved. The authors believe that they are lacking a long, lanceolate distal part of bract, as can be seen in materials from Tetta, described here and by Czaja (2000). The present authors are uncertain whether *Pseudotsuga jechorekiae,* found in Wiesa (Kunzmann, 2014), can be assigned to *Paranothotsuga*, owing to its poor preservation.

**Type locality:** Tetta near Buchholz, Upper Lusatia, Germany.

**Type level:** Cottbus Formation**;** sample IV/3.

**Stratigraphic distribution:** Upper Oligocene to Lower Pliocene.

Family Magnoliaceae Jussieu, 1789

Genus *Magnolia* Linnaeus, 1753

*Magnolia germanica* (Mai) Kowalski n. comb.

Fig. 7P, Q

1971 *Manglietia germanica* sp. nov. – Mai, pp. 444–446, pl. 42, figs 9–14.

**Material:** Tetta IV/2 – 2 specimens (MZ VII/134/35).

**Description:** Seeds flat, 4–5 mm long, 3.5–3.8 mm wide, cordate in outline. Sclerotesta indistinctly knobbed, wall very thin. Chalazal end with small, unraised pore, always on one side of the seed. Sinus inconspicuous.

**Remarks:** Considering size, shape, morphology, the thickness of sclerotesta, and the pore on the chalazal end, these seeds represent *Manglietia germanica*. Mai (1971) assigned seeds of this type to *Manglietia* based mainly on the presence of the terminal pore. According to Tiffney (1977) and Xu (2003), the chalaza of the pore type is also typical of *Pachylarnax* Dandy, 1927 [= Section *Manglietiastrum* (Y.W. Law) Nooteboom, 1985], *Aromadendron* Blume, 1825 (= Subsection *Aromadendron* Figlar and Nooteboom, 2004), *Elmerrillia* Dandy, 1927 [= subgenus *Yulania* Spach sect. *Michelia* (L.) Baill. Subsect. *Elmerrillia* (Dandy) Figlar and Nooteboom, 2004] and *Liriodendron*, also commonly

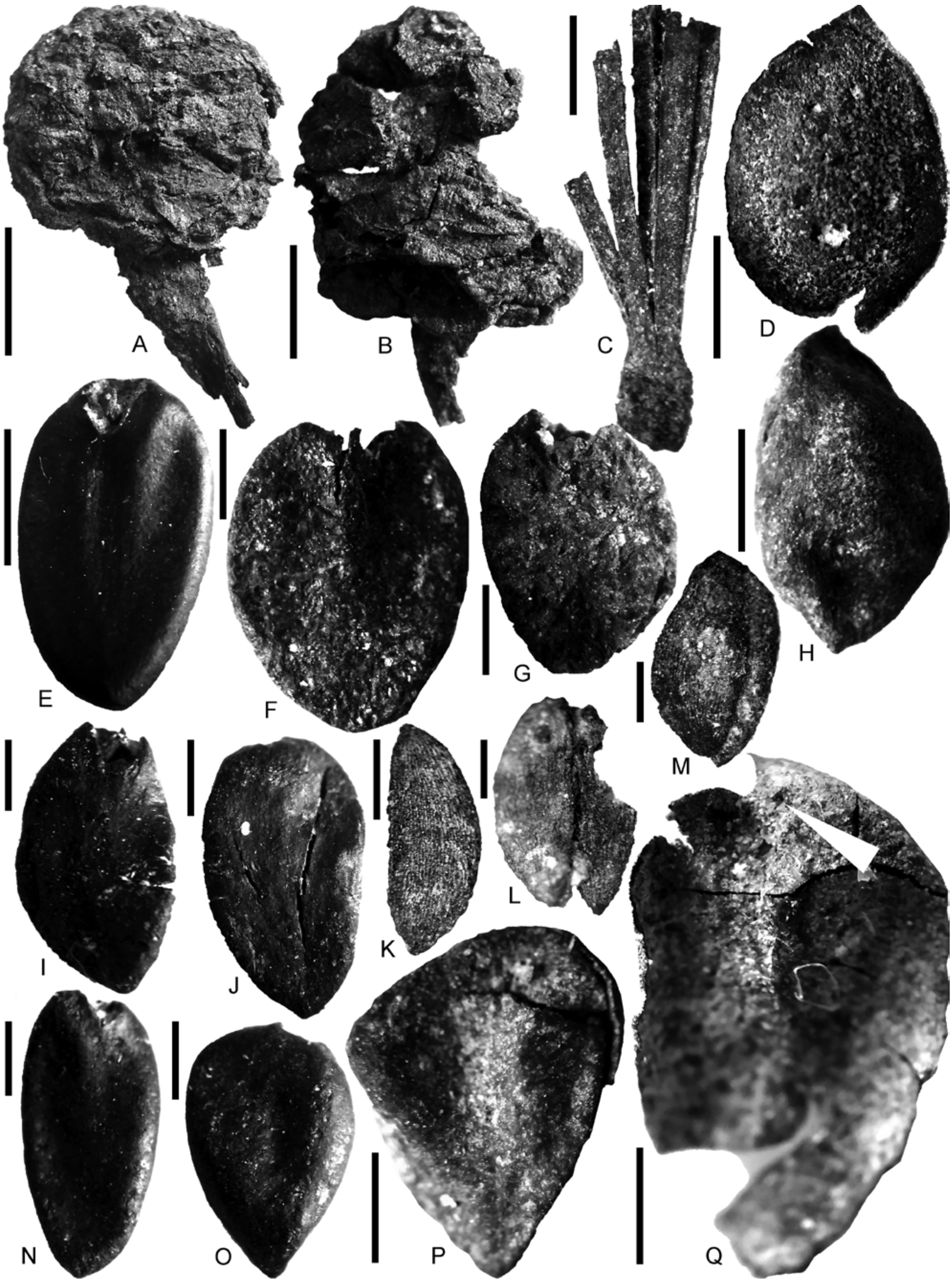


**Fig. 7.** Carpological remains from Tetta. **A, B.** *Sequoia abietina* (Brongn.) Knobloch, seed cones, MZ VII/134/22, 5 mm. **C.** *Pinus palaeostrobus* Ettingshausen**,** dwarf shoot and needles, MZ VII/134/19, 2 mm. **D, H.** *Cephalotaxus miocenica* (Krausel) Gregor, seeds, MZ VII/134/16, MZ VII/134/17, 5 mm. **E.** *Magnolia ludwigii* Ettingshausen, seed, MZ VII/134/31, 5 mm. **F, G.** *Magnolia burseracea* (Menzel) Mai, seeds, MZ VII/134/33, MZ VII/134/30, 2 mm. **I, J.** *Magnolia ludwigii* Ettingshausen, seed, MZ VII/134/32, 2 mm. **K–M.** *Liriodendron geminata* Kirchheimer, seeds, MZ VII/134/37, MZ VII/134/36, 1 mm. **N, O.** *Magnolia ludwigii* Ettingshausen, seeds, MZ VII/134/32, 2 mm. **P, Q.** *Magnolia germanica* (Mai) Kowalski, seeds, MZ VII/134/35, seeds, 1 mm.

occurs in *Talauma* Jussieu, 1789 (sect. Talauma Baillon, 1866), and can be found in some *Kmeria* (Pierre) Dandy, 1927 [= Section *Kmeria* (Pierre) Figlar and Nooteboom, 2004] species. However, this type of chalaza, in combination with the small size of seeds, clearly visible raphal sinus, and papillate sclerotesta surface are all characteristics of *Manglietia* Blume, 1823 [subgenus *Magnolia* sect. *Manglietia* (Blume) Baillon, 1866] species (Xu, 2003). Among fossil-species, distinguished by Mai (1971), only *M. hercynica* combines all these features, whereas *M. zinkeisenii* (Geinitz) Mai and *M. germanica* Mai are smooth or only poorly ornamented, which is rare in living *Manglietia* (Tiffney, 1977; Xu 2003). Nevertheless, considering its exceptionally small seeds, this fossil type can be assigned to *Manglietia* (Xu, 2003).

In the last twenty years, the classification of Magnoliaceae has undergone substantial changes (Figlar and Nooteboom, 2004; Wang *et al.*, 2020). As a result, only *Liriodendron* and *Magnolia* are now accepted, while the remaining genera were subdivided into 15 sections and included in *Magnolia.*

Following the current classification (Wang *et al.,* 2020), the present authors propose a new combination, *Magnolia germanica* [section *Manglietia* (Blume) Baill.].

**Distribution:** It is known from the middle Oligocene to the Middle Miocene, but relatively rare (Mai, 1997).

Family TYPHACEAE Jussieu, 1789
Genus *Sparganium* Linnaeus, 1753
*Sparganium tuberculatum* Kowalski sp. nov.
Fig. 8F1, F2

**Holotype:** MZ VII/134/44.
**Etymology:** The species name refers to the tubercles, visible on the endocarp surface.
**Material:** 28 endocarps (MZ VII/134/44, 45, 46).
**Diagnosis:** Endocarps small, broadest in the subapical part, stalked, longitudinally folded or not, apex with a short neck; surface covered with slightly elongated tubercles. Endocarp wall relatively thick.
**Description:** Endocarps small, 1.2–2.2 mm long and 0.9–1 mm wide, urceolate-asymmetrical, sometimes angular at ca. $^2/_3$ endocarp's height (= widest point). Base gradually narrows to a short stalk. Surface uneven, slightly longitudinally folded, poorly visible vascular bundles, conspicuous small, round or slightly elongated tubercles.
**Remarks:** The newly described species represents the subgenus *Xanthosparganium* and shows similarities with *S. camenzianum* Kirchheimer, 1941*, S. tambovicum* Dorofeev, 1979, *S*, *nanum* Dorofeev, 1979 and *S. tomskianum* Dorofeev, 1979. Few specimens with more expressed longitudinal folds also resemble *S. tanaiticum* Dorof. From the Miocene of Bolshaya Orlovka, Russia (Dorofeev, 1979).
**Type locality:** Tetta near Buchholz, Upper Lusatia, Germany.
**Type level:** Spremberg Formation**;** sample Tetta II/5.
**Stratigraphic distribution:** Lower Miocene.

Family Myricaceae Richard ex Kunth, 1817
Genus *Morella* Loureiro, 1790
*Morella stoppii* (Kirchheimer) Kowalski n. comb.
Fig. 13I, L

1942 *Myrica stoppii* sp. nov. – Kirchheimer, pp. 430–432, fig. 8.

**Material:** Tetta VII/12 – 1 specimen (MZ VII/134/287).
**Description:** For detailed description, see Kirchheimer (1942).
**Remarks:** Its large size, the shape of the locule, and the surface ornamentation relate this endocarp with *Myrica stoppii.* This species has been documented in only a few Lower/Middle Miocene floras of Central Europe (Mai, 1999). With respect to the size and thickness of the endocarp wall, *Myrica stoppii* corresponds with *Morella*, which was formerly treated as a section (Chevalier, 1901) or subgenus (Elias, 1971) of *Myrica* until being designated as a separate genus (Wilbur, 1994). The present authors propose a new combination, according to the current classification.

Considering its general characteristics, *Morella stoppii* most closely resembles species of the genus *Morella* in the sense of Wilbur (1994), especially *M. rubra* Siebold and Zuccarini, 1846 and *M. nagi* Thunberg, 1784 (Mai, 1999).

Family Styracaceae Candolle and Sprengel, 1821
Genus *Pterosinojackia* Kowalski gen. nov.

**Type species:** *Pterosinojackia lusatica* Kowalski gen. et sp. nov.
**Etymology:** The generic name suggests close relationship to *Pterostyrax* and *Sinojackia*, whereas the specific name refers to Lusatia.
**Diagnosis:** Fruits with caudate rostrum, hypanthium not adnate to the full length of fruit; sepals 5, fully exposed, long and narrow, triangular; exo-mesocarp thin, wings lacking.

*Pterosinojackia lusatica* Kowalski sp. nov.
Fig. 17G, M, N

**Holotype:** MZ VII/134/228.
**Material:** Tetta IV/1 – 78 specimens (MZ VII/134/231, 232); Tetta IV/2 – 40 specimens (MZ VII/134/228, 229); Tetta IV/3 – 10 specimens (MZ VII/134/237); Tetta VI/6 – 2 specimens (MZ VII/134/235); Tetta I/8 – 1 specimen (MZ VII/134/239); Tetta III/11 – 10 specimens (MZ VII/134/235).
**Diagnosis:** As for the genus.
**Description**: Fruits narrow, fusiform, highly compacted, 12–19 mm long and 5–6.5 mm wide. Longitudinal ribs thin, variable in number and height, 5–6 main ribs, 0–2 lower midribs and wrinkles between each pair of main ribs. Ribs run from the base to $^2/_3$ of the fruit length. Fruits gradually narrow to a short, rib-free base, with a short and thin pedicel, mostly not preserved. Calyx 5-lobed and hairy. Apical rostrum broad ($^1/_2$–$^2/_3$ the width of the fruit) at the base, abruptly narrowing at $^1/_3$ its length into a long, thin cone. Pericarp consists of a thick and highly coalified endocarp, covered with a thin and frequently detached external layer of meso- and exocarp. Exocarp surface hairy. Locules >2.
**Remarks:** Superficially, these fossil fruits may be confused with *Halesia crassa* Kirchheimer, 1943a endocarp, as they are similar in size, shape and general morphology

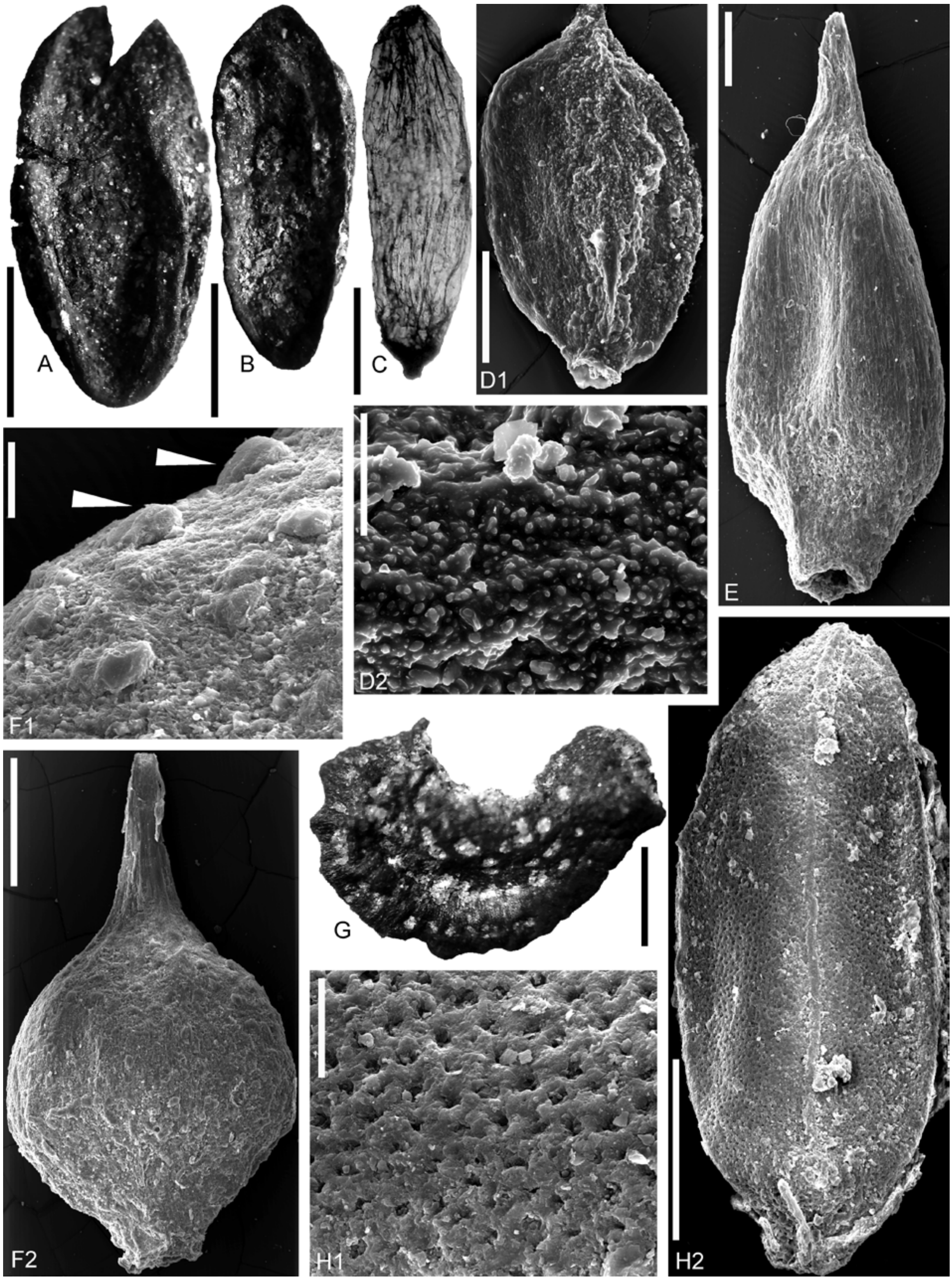


**Fig. 8.** Carpological remains from Tetta. **A, B.** *Cinnamomum costatum* (Mai) Pingen, Ferguson & Collinson, seeds, MZ VII/134/41, MZ VII/134/42, 3 mm. **C.** *Vallisneria vittata* Mai, seed, MZ VII/134/297, 500 µm. **D1.** *Cyperus* aff. *leptodermis* Mai, achene, MZ VII/134/50, 200 µm. **D2.** *Cyperus* aff. *leptodermis* Mai, achene, MZ VII/134/50, 50 µm. **E.** *Sparganium* aff. *pusilloides* Mai, endocarp, MZ VII/134/58, 200 µm. **F1.** *Sparganium tuberculatum* Kowalski, endocarp surface close-up, arrows indicate tubercles, MZ VII/134/46, 100 µm. **F2.** *Sparganium tuberculatum* Kowalski, endocarp, MZ VII/134/46, 500 µm. **G.** *Urospathites visimensis* (Dorofeev) Gregor and Bogner, seed, MZ VII/134/43, 500 µm. **H1.** *Dulichium hartzianum* Mai, achene surface close-up, MZ VII/134/48, 50 µm. **H2.** *Dulichium hartzianum* Mai, achene, MZ VII/134/48, 500 µm.

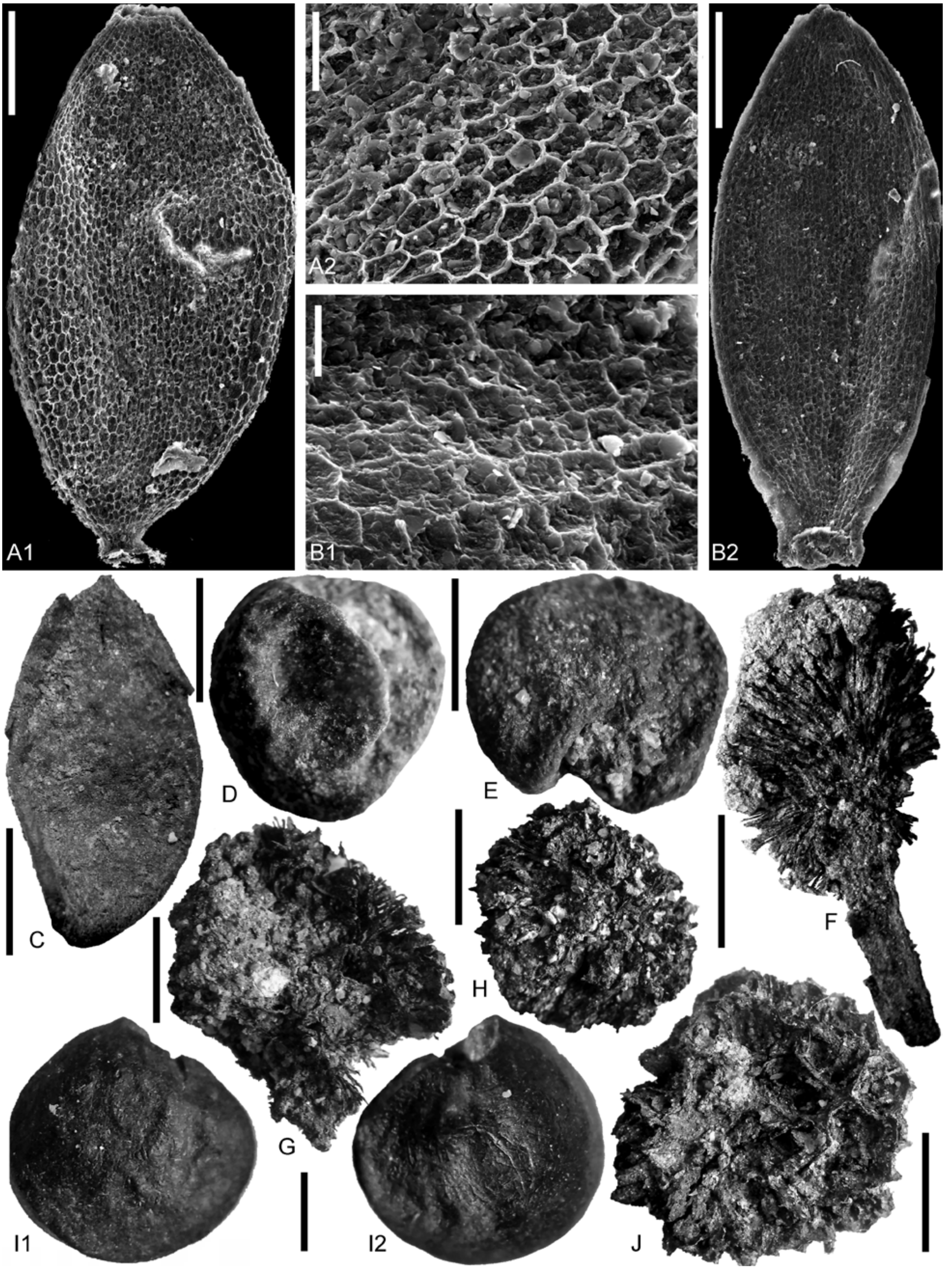


**Fig. 9.** Carpological remains from Tetta. **A1.** *Carex plicata* Łancucka-Środoniowa, achene, MZ VII/134/51, 200 µm. **A2.** *Carex plicata* Łancucka-Środoniowa, achene surface close-up, MZ VII/134/51, 50 µm. **B1.** *Scirpus brevicornis* Mai, achene surface close-up, MZ VII/134/56, 20 µm. **B2.** *Scirpus brevicornis* Mai, achene, MZ VII/134/56, 200 µm. **C.** *Decaisnea bornensis* Mai, seed, MZ VII/134/57, 2 mm. **D, E.** *Meliosma pliocaenica* (Szafer) Gregor, endocarps, MZ VII/134/63, MZ VII/134/65, 2 mm. **F–H.** *Platanus neptuni* (Ett.) Bůžek, Kvaček & Holý, staminate inflorescences, MZ VII/134/68, MZ VII/134/66, MZ VII/134/75, 4 mm. **I1, I2.** *Meliosma miessleri* Mai, endocarp, opposite sides of the same specimen, MZ VII/134/62, 1 mm. **J.** *Liquidambar europaea* A. Braun, infructescence, MZ VII/134/69, 5 mm.

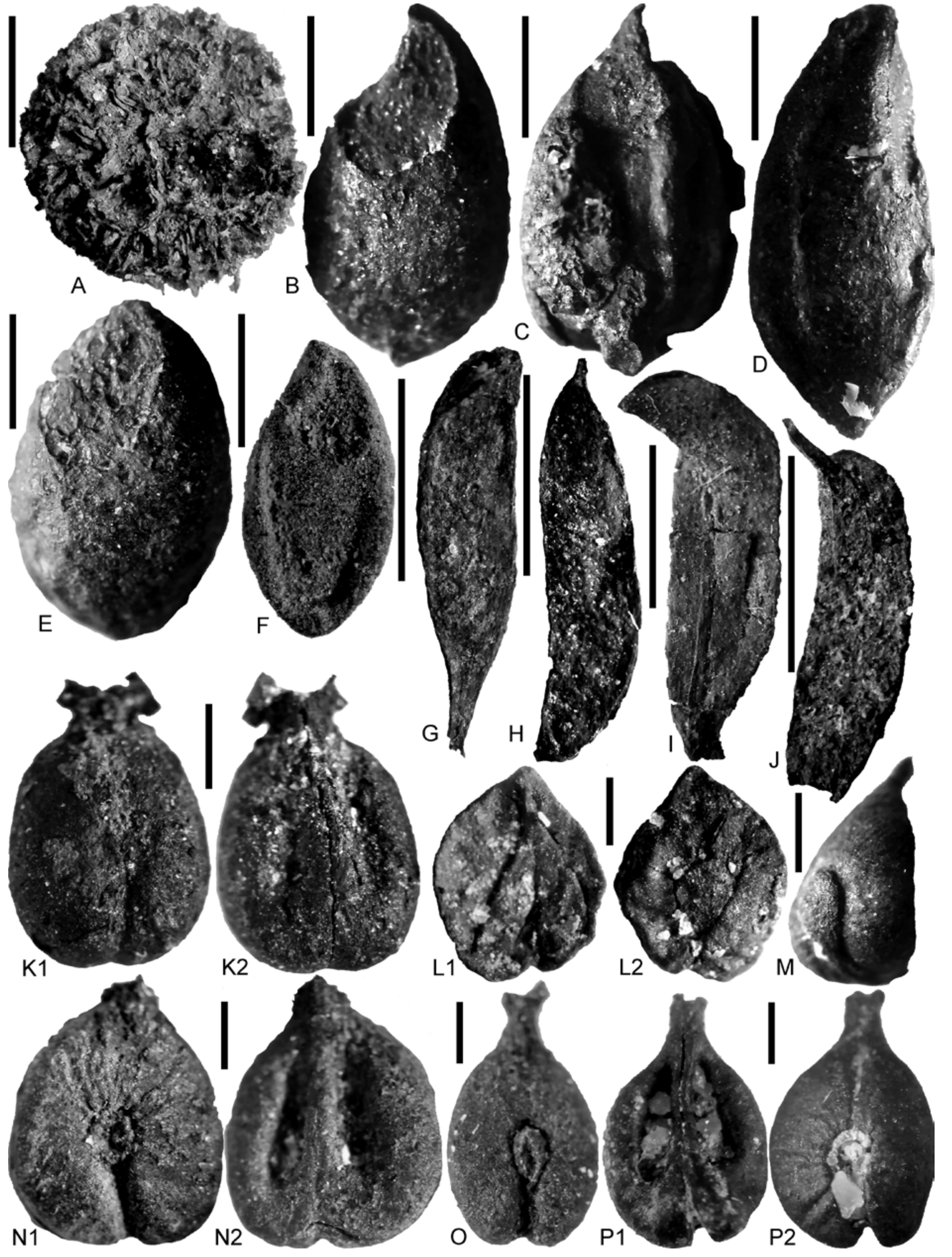


**Fig. 10.** Carpological remains from Tetta. **A.** *Liquidambar europaea* A. Braun, infructescence, MZ VII/134/69, 5 mm. **B, C.** *Distylium protogaeum* Mai, seeds, MZ VII/134/78, 2 mm. **D.** *Distylium uralense* Kolesnikova, seed, MZ VII/134/72, 2 mm. **E.** *Fothergilla europaea* Szafer, seed, MZ VII/134/307, 2 mm. **F.** *"Fortunearia" altenburgensis* Mai, seed, MZ VII/134/80, 2 mm. **G–J.** *Cercidiphyllum helveticum* (Heer) Jähnichen, Mai & Walther, follicles, MZ VII/134/83, MZ VII/134/82, 5 mm. **K1, K2.** *Vitis parasilvestis* Kirchheimer, seed, both sides of the one specimen, MZ VII/134/88, 1 mm. **L1, L2.** *Ampelopsis rotundata* Chandler, seed, opposite sides of the same specimen, MZ VII/134/84, 1 mm. **M.** *Ampelopsis rotundata* Chandler, seed, MZ VII/134/85, 1 mm. **N1, N2.** *Vitis parasilvestis* Kirchheimer, seed, opposite sides of the same specimen, MZ VII/134/88, 1 mm. **O.** *Vitis* aff. *teutonica* A. Braun, seed, MZ VII/134/95, 1 mm. **P1, P2.** *Vitis* aff. *teutonica* A. Braun, seed, MZ VII/134/97, 1 mm.

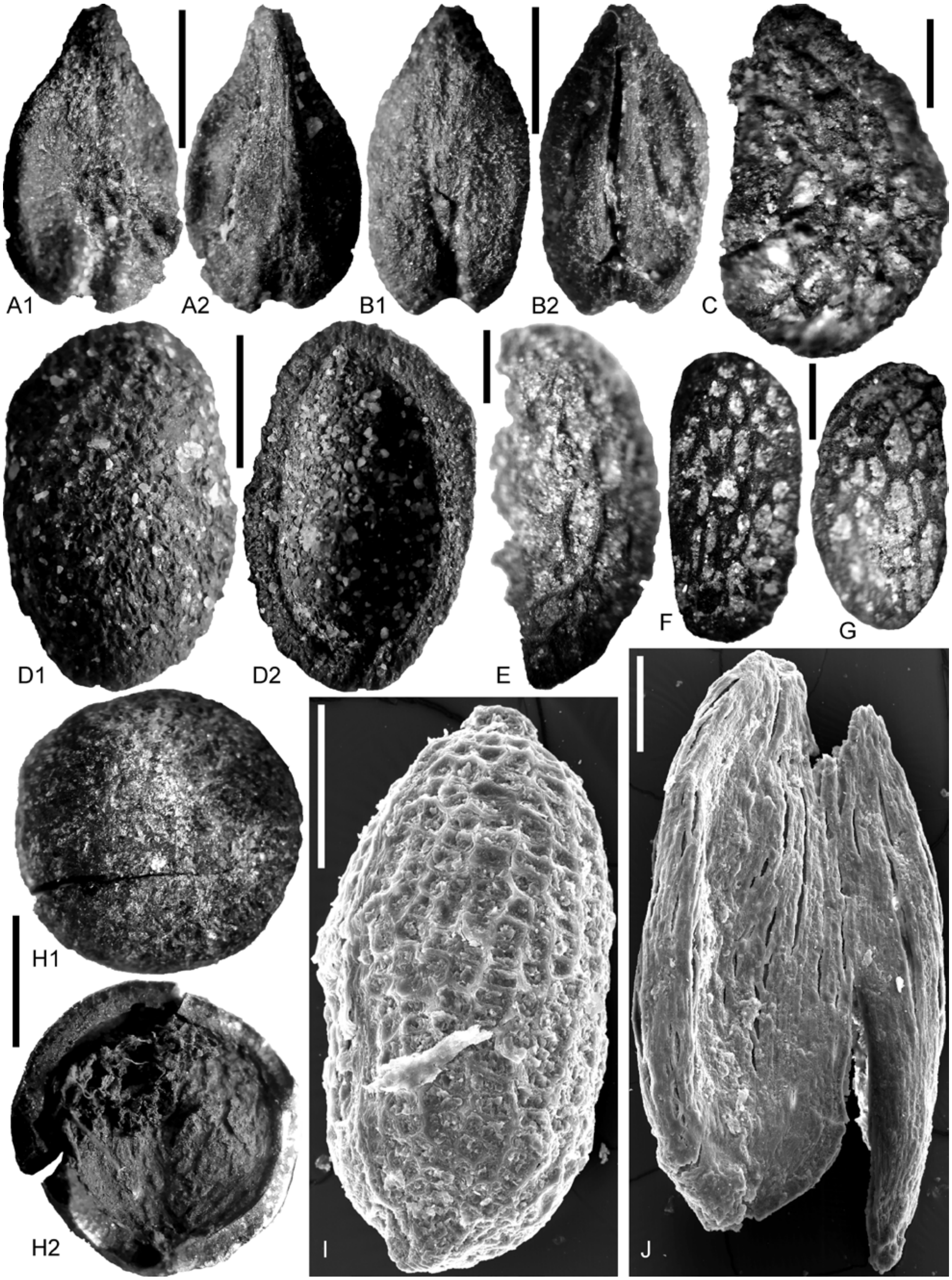


**Fig. 11.** Carpological remains from Tetta. **A1, A2, B1, B2.** *Parthenocissus britannica* (Heer) Chandler, seeds, opposite sides of the same specimen, MZ VII/134/98, 2 mm. **C.** *Rubus semirotundatus* Łancucka-Środoniowa, endocarp, MZ VII/134/107, 500 µm. **D1, D2.** *Prunus scharfii* Gregor, drupe, internal and external side, MZ VII/134/102, 5 mm. **E.** *Rubus semirotundatus* Łancucka-Środoniowa, endocarp, MZ VII/134/106, 500 µm. **F, G.** *Rubus microspermus* C. & E. M. Reid, endocarps, MZ VII/134/105, 500 µm. **H1, H2.** *Prunus lepori-montana* Mai, drupe, internal and external side, MZ VII/134/103, 3 mm. **I.** *Hypericum septestum* Nikitin, seed, MZ VII/134/100, 200 µm. **J.** *Poliothyrsis eurorimosa* Mai, seed, MZ VII/134/290, 200 µm.

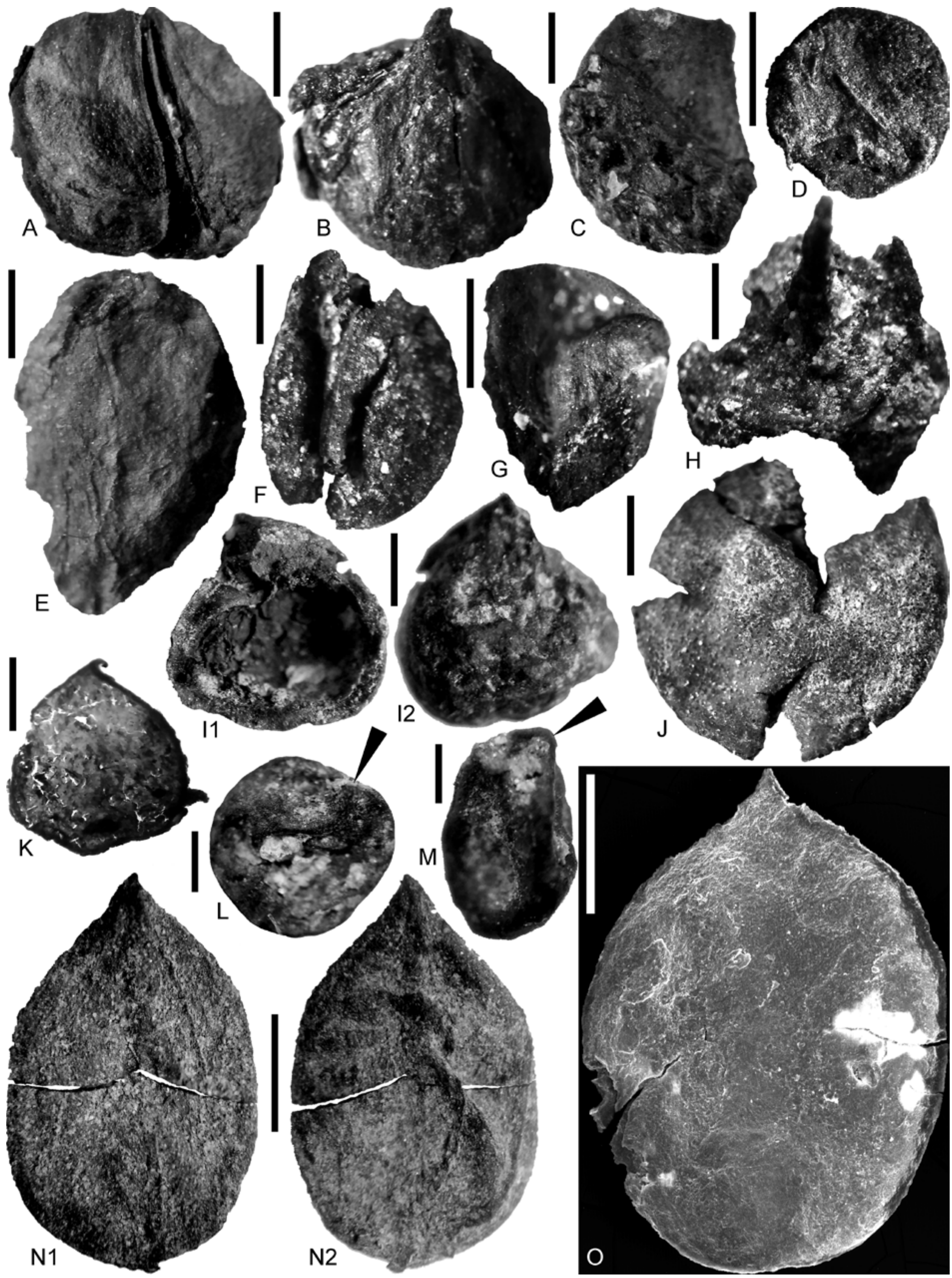


**Fig. 12.** Carpological remains from Tetta. **A–C.** *Pyracantha acuticarpa* (C. & E. M. Reid) Szafer, pyrenes, MZ VII/134/111, 1 mm. **D.** *Paliurus favonii* Unger, seed, MZ VII/134/116, 1 mm. **E.** *Cotoneaster wackersdorfensis* Gregor, pyrene, MZ VII/134/304, 1mm. **F.** *Frangula solitaria* Gregor, drupe, MZ VII/134/115, 1 mm. **G.** *Pyracantha acuticarpa* (C. & E. M. Reid) Szafer, pyrene, MZ VII/134/111, 1 mm. **H.** *Paliurus favonii* Unger, basal part of the fruit, MZ VII/134/116, 1 mm. **I1, I2.** *Gironniera carinata* Mai, drupe, internal and external side, MZ VII/134/118, 1 mm. **J.** *Gironniera verrucata* Mai, drupe, MZ VII/134/122, 1 mm. **K.** *Laportea europaea* Dorofeev, achene, MZ VII/134/276, 1 mm. **L.** *Ficus lutetianoides* Mai, vertically compressed achene, arrow indicates mucro, MZ VII/134/126, 500 μm. **M.** *Ficus lucida* Chandler, achene, arrow indicates mucro, MZ VII/134/124, 500 μm. **N1, N2.** *Comptonia* aff. *goniocarpa* Mai, nut, MZ VII/134/143, 1 mm. **O.** *Laportea nemejcii* Mai, achene, arrow indicates basal stipe attachment, MZ VII/134/283, 500 μm.

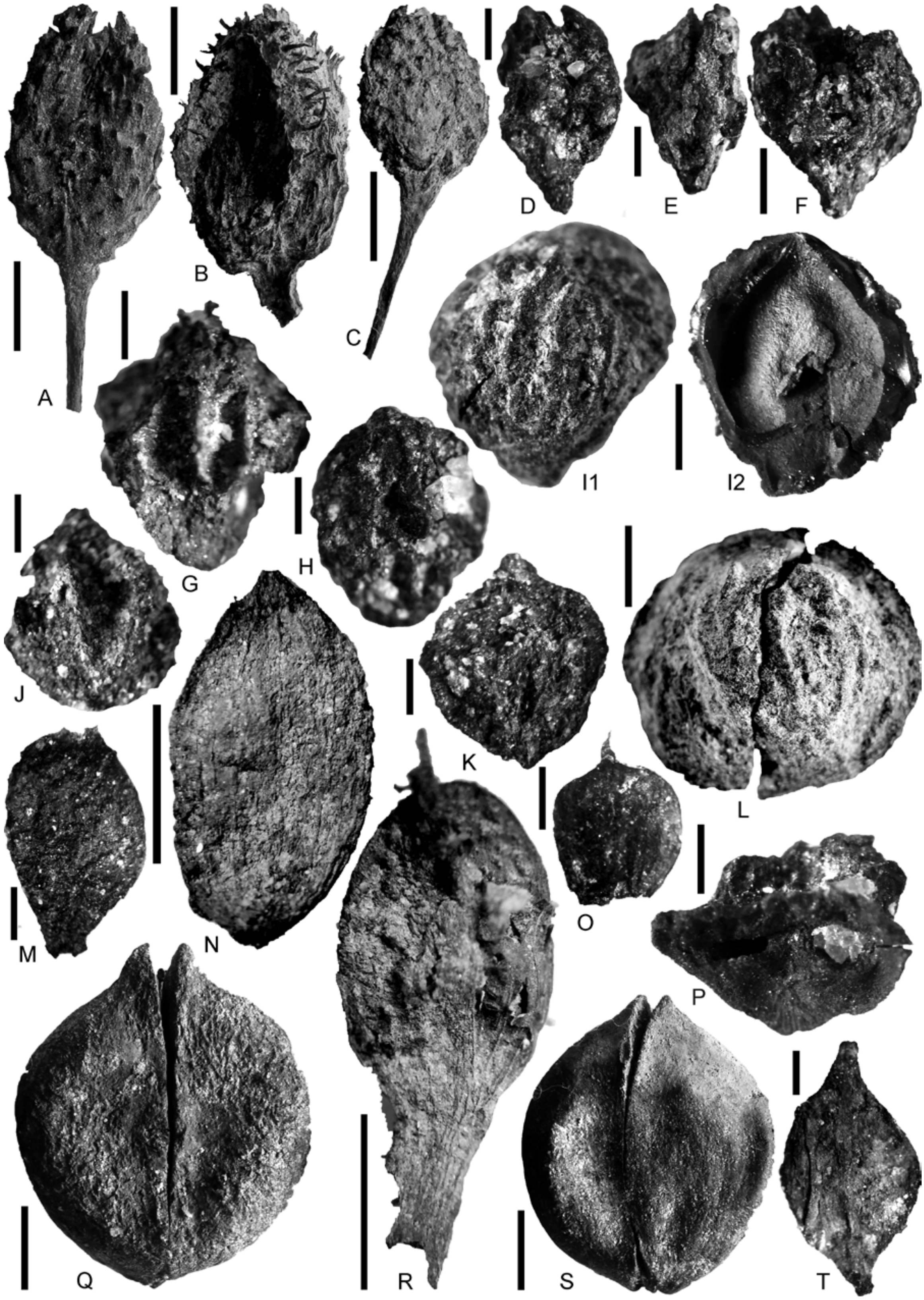


**Fig. 13.** Carpological remains from Tetta. **A–C.** *Fagus deucalionis* Unger emend. Denk & Meller, cupules, MZ VII/134/138, MZ VII/134/136, MZ VII/134/138, 5 mm. **D–F.** *Trigonobalanopsis exacantha* (Mai) Kvaček & Walther, cupules, MZ VII/134/274, 2 mm. **G, H.** *Pterocarya* aff. *margaritana* Mai, nutlets, MZ VII/134/146, MZ VII/134/149, 1 mm. **I1, I2.** *Morella stoppii* (Kirchheimer) Kowalski, one half of endocarp, internal and external side, MZ VII/134/287, 2 mm. **J, K.** *Pterocarya* aff. *margaritana* Mai, nutlets, MZ VII/134/149, MZ VII/134/148, 1 mm. **L.** *Morella stoppii* (Kirchheimer) Kowalski, second half of endocarp, external side, MZ VII/134/287, 2 mm. **M.** *Betula* cf. *longisquamosa* Madler, wingless nutlet, MZ VII/134/164, 500 µm. **N, R.** *Carpinus cordataeformis* Mai, fruit, MZ VII/134/152, 2 mm. **O.** *Alnus latibracteosa* Mai & Walther, seed, MZ VII/134/165, 1 mm. **P.** *Pterocarya* aff. *margaritana* Mai, nutlet, MZ VII/134/146, 1 mm. **Q, S.** *Carya ventricosa* (Sternb.) Unger, nuts, MZ VII/134/144, 5 mm. **T.** *Betula* cf. *dryadum* Brongniart, wingless nutlet, MZ VII/134/163, 500 µm.

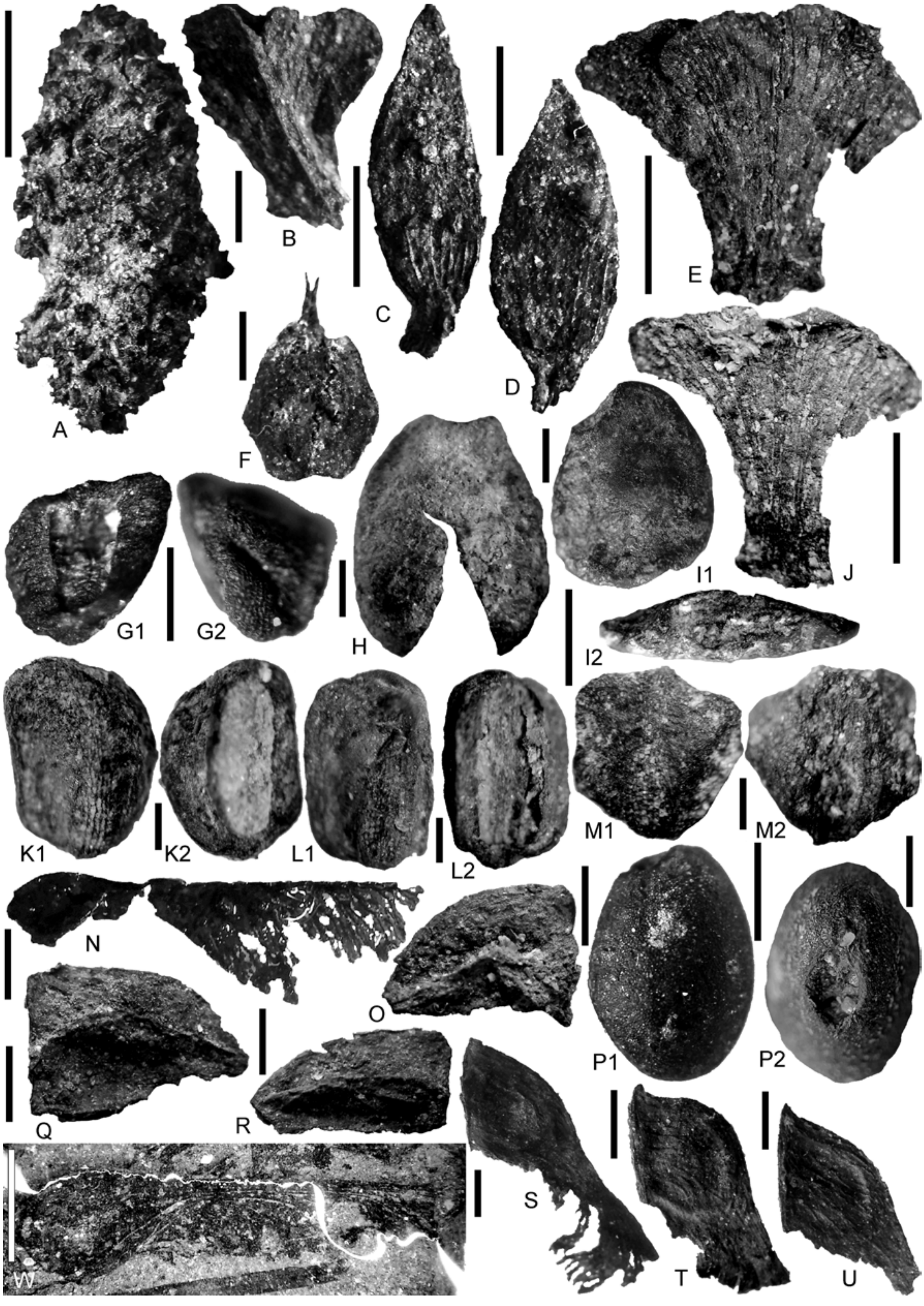


**Fig. 14.** Carpological remains from Tetta. **A.** *Alnus lusatica* Mai, infructescence, MZ VII/134/169, 5 mm. **B.** *Alnus lusatica* Mai, scale, MZ VII/134/170, 1 mm. **C, D.** *Ostrya scholtzii* Gregor, nutlets, MZ VII/134/156, 2 mm. **E, J.** *Alnus latibracteosa* Mai & Walther, scales, MZ VII/134/165, 2 mm. **F.** *Alnus lusatica* Mai, seed, MZ VII/134/170, 1 mm. **G1, G2.** *Microdiptera minor* (Chandler) Mai, seed, opposite sides of the same specimen, MZ VII/134/306, 500 µm. **H.** *Staphylea rotundata* Dorofeev, seed, MZ VII/134/300. **I1, I2.** *Staphylea rotundata* Dorofeev, seed – lateral view, apical view, MZ VII/134/301, 1 mm. **K1, K2, L1, L2.** *Microdiptera lusatica* Mai, seeds, opposite sides of two specimens, MZ VII/134/171, 300 µm. **M1, M2.** *Microdiptera* aff. *parva* Chandler, seed, opposite sides of the same specimen MZ VII/134/172, 500 µm. **N, W.** *Acer* aff. *angustilobum* Heer, fruit, MZ VII/134/176, 5 mm. **O, Q, R.** *Acer hercynicum* Mai, nutlets, MZ VII/134/186, MZ VII/134/189, 2 mm. **P1.** *Turpinia ettingshausenii* (Engelh.) Mai, seed - lateral view, MZ VII/134/175, 2 mm; **P2.** *Turpinia ettingshausenii* (Engelh.) Mai, seed - apical view, MZ VII/134/175, 1 mm. **S–U.** *Acer* sp. 2 Mai, nutlets, MZ VII/134/179, 2 mm.


**Fig. 15.** Carpological remains from Tetta. **A–D.** *Acer* sp. 1, nutlets, MZ VII/134/185, MZ VII/134/190; A, C = 1 mm; B, D = 2 mm. **E, I.** *Acer* sp. 2 Mai, nutlets, MZ VII/134/178, 2 mm. **F.** aff. *Burretia* sp., flower bud, MZ VII/134/305, 2 mm. **G.** *Craigia bronnii* (Unger) Kvaček, Bůžek et Manchester, fruit, MZ VII/134/195, 5 mm. **H.** *Zanthoxylum giganteum* Gregor, micropylar end of the seed, MZ VII/134/299, 1 mm. **J, L.** *Moehringia miocaenica* Mai, seeds, Tet.k 1287, 200 µm. **K, M.** *Eurya stigmosa* (Ludwig) Mai, seeds, MZ VII/134/281, 500 µm. **N–P.** *Symplocos casparyi* Ludwig, endocarp, MZ VII/134/213, 1 mm. **Q.** *Ternstroemia sequoioides* (Engelhardt) Bůžek & Holý, seed, MZ VII/134/293, 2 mm. **R.** *Mastixia amygdalaeformis* (Schloth.) Kirchheimer, endocarp in type of *M. amygdalaeformis*, MZ VII/134/206, 10 mm. **S.** *Mastixia amygdalaeformis* (Schloth.) Kirchheimer, endocarp in type of *M. meyeri*, MZ VII/134/209, 5 mm. **T.** *Mastixia amygdalaeformis* (Schloth.) Kirchheimer, endocarp in type of *M. thomsoni*, MZ VII/134/205, 10 mm.

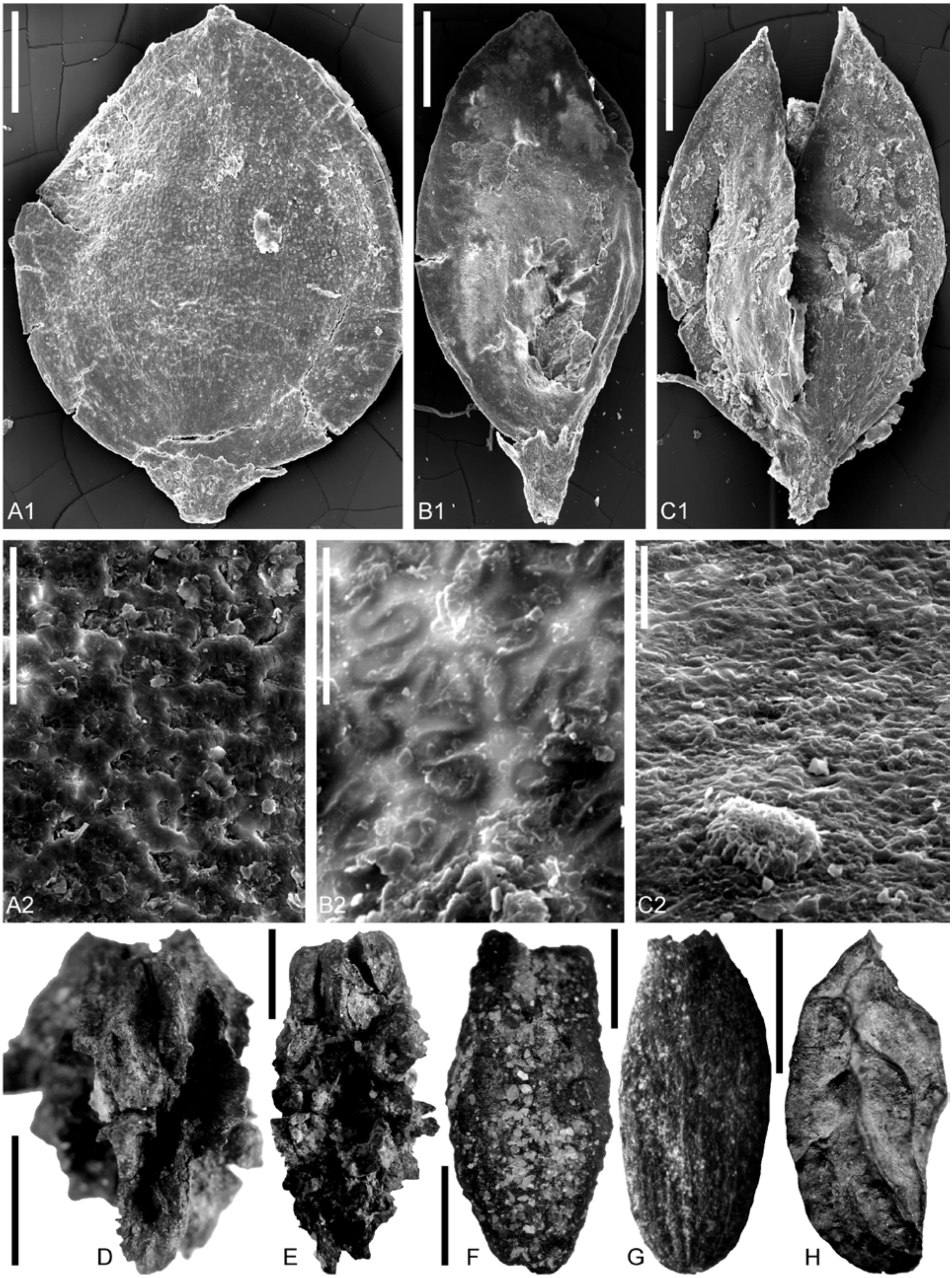


**Fig. 16.** Carpological remains from Tetta. **A1.** *Persicaria* aff. *polesieana* Arbuzova, fruit, MZ VII/134/196, 500 µm. **A2.** *Persicaria* aff. *polesieana* Arbuzova, pericarp surface close-up shows epidermal cells, MZ VII/134/196, 100 µm. **B1.** *Polygonum* sp. 2, fruit, MZ VII/134/201, 500 µm. **B2.** *Polygonum* sp. 2, pericarp surface close-up shows epidermal cells, MZ VII/134/201, 20 µm. **C1.** *Polygonum* sp. 1, fruit, MZ VII/134/198, 500 µm. **C2.** *Polygonum* sp. 1, pericarp surface close-up shows epidermal cells, MZ VII/134/198, 20 µm. **D, E.** *Symplocos schereri* Kirchheimer, endocarps, MZ VII/134/225, 3 mm. **F.** *Symplocos pseudogregaria* Kirchheimer, endocarp, MZ VII/134/227, 3 mm. **G.** *Symplocos minutula* (Sternberg) Kirchheimer, endocarp, MZ VII/134/221, 2 mm. **H.** *Ilex saxonica* Mai, pyrene, MZ VII/134/254, 2 mm.

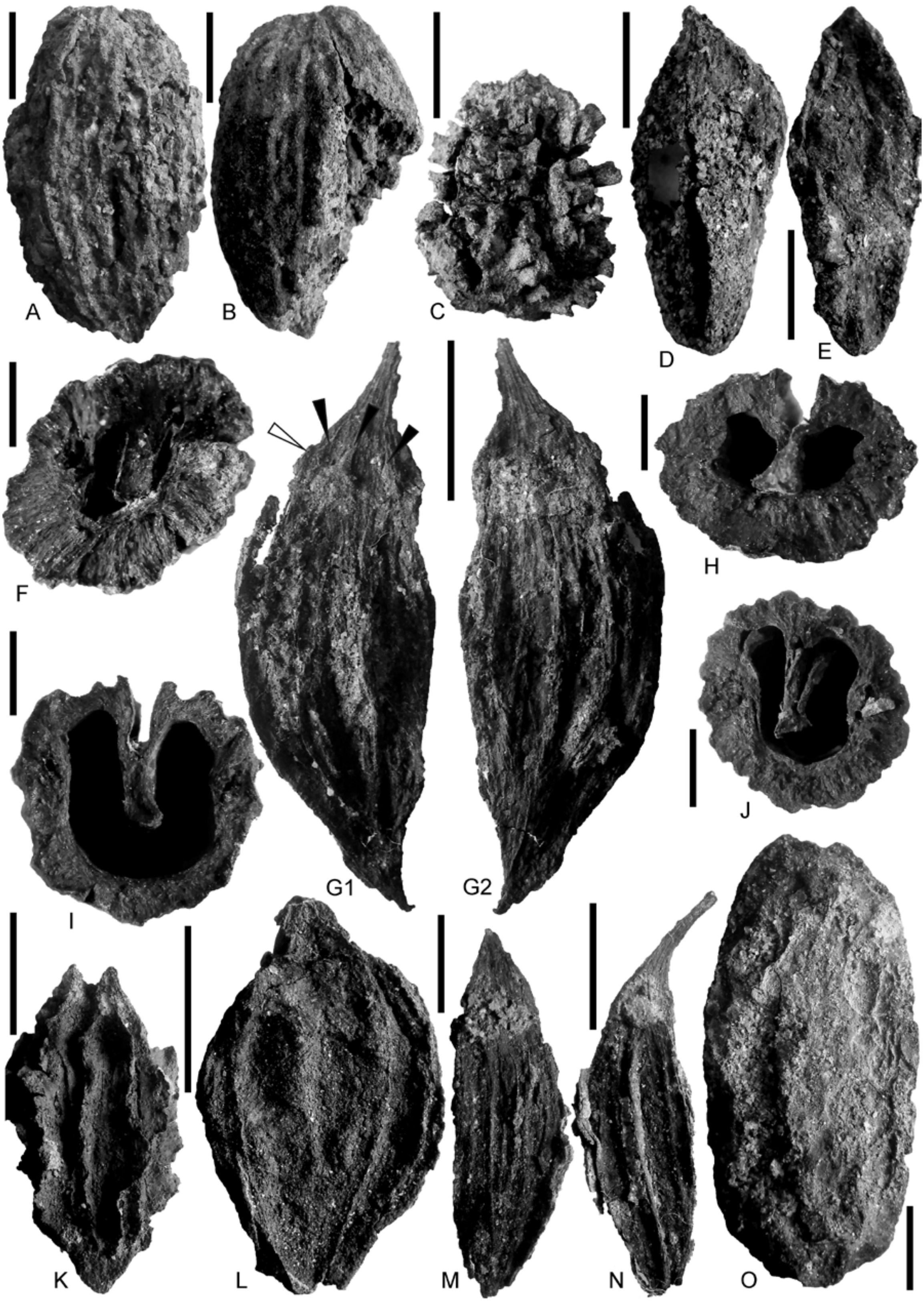


**Fig. 17.** Carpological remains from Tetta. **A–C.** *Eomastixia saxonica* (Menzel) Holy, endocarps, MZ VII/134/270, 10 mm. **D, E.** *Nyssa ornithobroma* Unger, endocarps, MZ VII/134/269, 5 mm. **F.** *Mastixia amygdalaeformis* (Schloth.) Kirchheimer, endocarp of *M. amygdalaeformis* type, MZ VII/134/209, 2 mm. **G1, G2.** *Pterosinojackia lusatica* Kowalski gen. et sp. nov., holotype, opposite sides of fruit, black arrows indicate 3 sepals and white arrow indicates hypanthium margin, MZ VII/134/228, 5 mm. **H.** *Mastixia amygdalaeformis* (Schloth.) Kirchheimer, endocarp of *M. meyeri* type, MZ VII/134/209, 2 mm. **I.** *Mastixia amygdalaeformis* (Schloth.) Kirchheimer, endocarp in type of *M. meyeri*, MZ VII/134/209, 5 mm. **J.** *Mastixia amygdalaeformis* (Schloth.) Kirchheimer, endocarp of *M. amygdalaeformis* type, MZ VII/134/204, 2 mm. **K, L.** *Rehderodendron ehrenbergii* (Kirchheimer) Mai, endocarp, MZ VII/134/240, 10 mm. **M, N.** *Pterosinojackia lusatica* Kowalski gen. et sp. nov., fruits, MZ VII/134/229, 5 mm. **O.** *Tectocarya elliptica* (Ung.) Holý, endocarp, MZ VII/134/272, 5 mm.


**Fig. 18.** Carpological remains from Tetta. **A.** *Pterostyrax coronatus* Mai, variability of size and shape of endocarps, MZ VII/134/233, 5 mm. **B–D.** *Pterostyrax coronatus* Mai, endocarps, MZ VII/134/238, MZ VII/134/236, 2 mm. **E.** *Pterostyrax coronatus* Mai, endocarp in cross-section, arrows indicate locules, MZ VII/134/236, 1 mm. **F, G.** *Leucothoe narbonensis* (Saporta) Weyland, capsules, MZ VII/134/284, MZ VII/134/285, 2 mm. **H–J.** *Actinidia faveolata* C & EM Reid, seeds, MZ VII/134/288, **K1, K2.** *Oxydendrum europaeum* Van der Burgh, capsule, opposite sides of the same specimen, arrow indicates basal placenta, MZ VII/134/242, 2 mm.

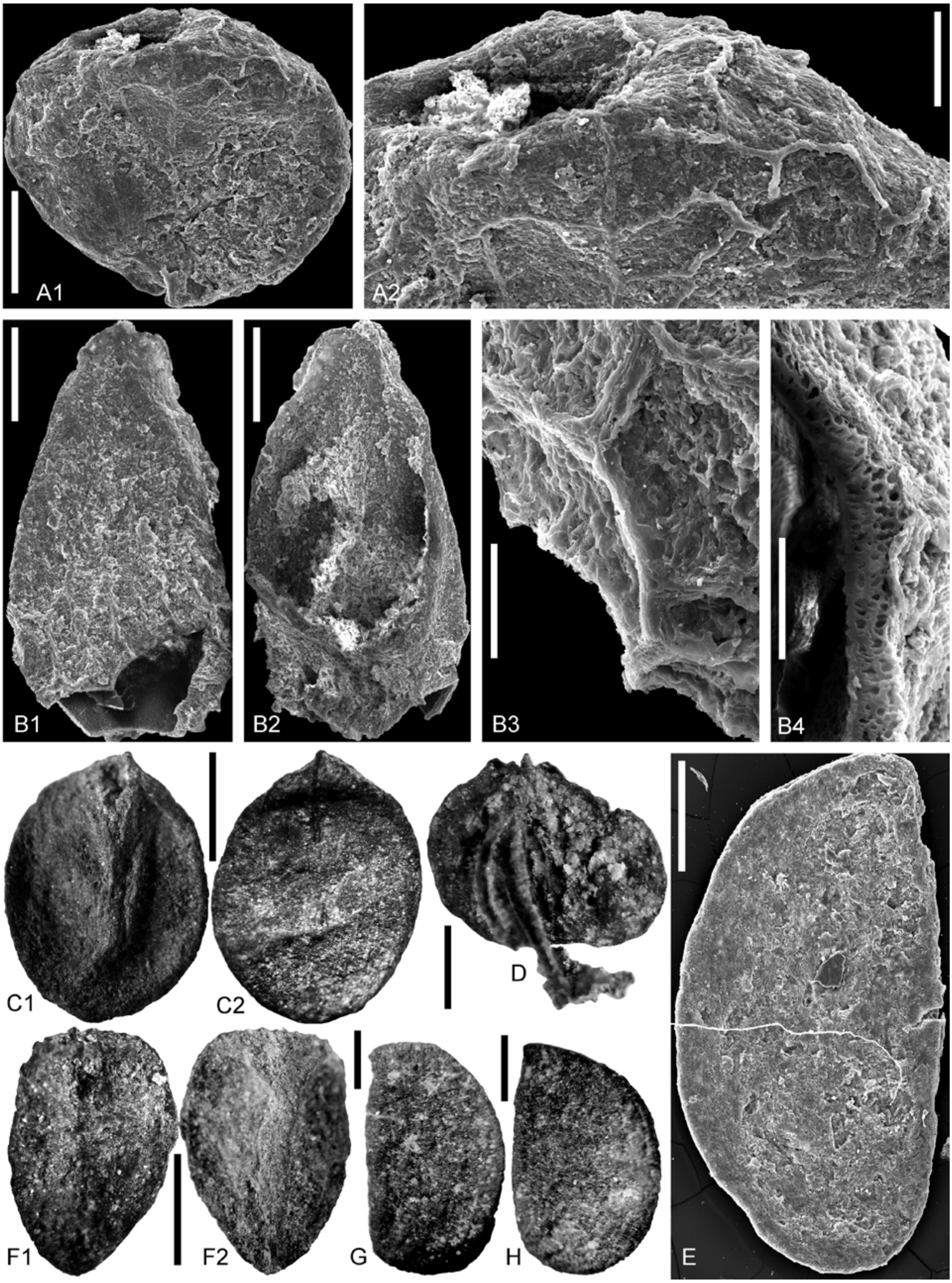


**Fig. 19.** Carpological remains from Tetta. **A1.** *Collinsonia* cf. *europaea* Mai, nutlet, MZ VII/134/246, 500 µm. **A2.** *Collinsonia* cf. *europaea* Mai, nutlet close-up shows delicate reticulum on the surface, MZ VII/134/246, 200 µm. **B1, B2.** *Teucrium* aff. *martinae* Mai, nutlet, opposite sides of the same specimen, MZ VII/134/243, 500 µm. **B3.** *Teucrium* aff. *martinae* Mai, nutlet close-up shows ornamentation on the surface, MZ VII/134/244, 100 µm. **B4.** *Teucrium* aff. *martinae* Mai, pericarp wall in cross-section, MZ VII/134/244, 100 µm. **C1, C2.** *Ilex ovidrupacea* Mai, pyrene, ventral and dorsal side, MZ VII/134/250, 2 mm. **D.** *Umbelliferopsis molassicus* Gregor, fruit, MZ VII/134/298, 1 mm. **E.** *Aralia lusatica* Mai, endocarp, MZ VII/134/261, 500 µm. **F1, F2.** *Ilex ovidrupacea* Mai, pyrene, dorsal and ventral side, MZ VII/134/250, 2 mm. **G, H.** *Aralia rugosa* Dorofeev, endocarps, MZ VII/134/257, MZ VII/134/259, 500 µm.


**Fig. 20.** Carpological remains from Tetta. **A.** *Ilex* aff. *lotschii* Mai, pyrene, MZ VII/134,248, 2 mm. **B, C.** *Sambucus lucida* Dorofeev, seeds, MZ VII/134/291, 1 mm. **D.** *Aralia lusatica* Mai, endocarp, MZ VII/134/260, 1 mm. **E.** *Aralia intermedia* Dorofeev, endocarp, MZ VII/134/256, 1 mm. **F.** *Schefflera dorofeevii* Łańcucka-Środoniowa, endocarp, MZ VII/134/264, 1 mm. **G.** *Pentapanax tertiarius* Mai, endocarp, MZ VII/134/263, 1 mm.

(Kirchheimer, 1943b). Nevertheless, several features clearly indicate that our fossils cannot be assigned to *Halesia*: The caudate rostrum observed in our fossils suggests the hypanthium was not adnate to the full length of fruit and, as a result, both the apical section of the fruit and the base of the style can be seen above calyx ring. Comparable rostra can be observed in *Melliodendron* Handel-Mazzetti, 1921*, Pterostyrax corymbosum* Siebold and Zuccarini, 1835, *Sinojackia* Hu, 1928 and *Changiostyrax* Chen, 1995 (Ying *et al.*, 1993; Hwang and Grimes, 1996). In contrast, in *Halesia* J. Ellis ex Linnaeus, 1759, and *Perkinsiodendron* P.W. Fritsch, 2016 (Fritsch *et al.*, 2016) the hypanthium fuses to the fruit along its full length and only the base of the style protrudes beyond the calyx ring. Therefore, the rostrum generally takes the form of a regular, slim and gradually narrowing cone (Fritsch *et al.*, 2016).

Several delicate structures, including sepals, epidermal hairs, and fragments of pedicel have been preserved in the present specimens. The layer with hairs is thin and lies directly on the endocarp. This indicates that at least part of the most external layer of fruits is preserved, in turn leading the authors to believe that unlike in *Halesia*, the present fossil fruits were devoid of a noticeable mesocarp. The endocarp covered with only a thin exo-mesocarp hypanthium sheath resembles *Pterostyrax* Siebold and Zuccarini, 1835 (see Hwang and Grimes, 1996) and *Sinojackia microcarpa* (Chen and Li, 1997).

As none of the examined specimens present a fully preserved calyx, the authors cannot be sure about the original number of sepals. However, the arrangement of the remaining sepals indicates that there may have been five, which is rather unusual for *Halesia*, but typical of *Pterostyrax*, *Sinojackia*, *Melliodendron*, and *Rehderodendron* (Hwang and Grimes, 1996).

The course of the calyx ring in the present specimens is close to straight, whereas in *Halesia* it is sinuous due to the presence of wings (personal observation). Sepals in the present specimens are well exposed and relatively long and narrow, comparable to those in *Sinojackia*. In contrast, in *Halesia* sepals are rather short and mostly concealed by wings, rendering them barely visible in mature fruit (first author observation).

Even considering the fact that fossil fruits are usually smaller than their living relatives, the present specimens still seem too small for *Halesia*. Furthermore, they cannot be considered to be abraded endocarps of *Halesia*, because, in the opinion of the present authors, the *Halesia* mesocarp could not be removed naturally without destroying the aforementioned delicate structures. The authors believe the present-day size may be close to the original. Fruits of this size can be found among living *Pterostyrax* (1.2–2.5 cm long) and some *Sinojackia* (*S. xylocarpa* Hu, 1928, 1.8–2 cm; Hwang and Grimes, 1996; Yao *et al.*, 2007).

In the light of the aforementioned evidence, the described fossils can be compared only with *P. psilophyllus* Diels ex Perkins, 1907 and *S. henryi* (Dummer) Merrill, 1937. Evidence collected did not allow the authors to ascertain which is closer; probably it combines features of both recent taxa, therefore the authors propose to assign these fossils to a new fossil-genus *Pterosinojackia*.

**Type locality:** Tetta near Goerlitz, Upper Lusatia, Germany.

**Type level:** Cottbus and Spremberg Formation; samples IV/1–III/11.

**Stratigraphic distribution:** upper Oligocene to Lower Miocene.

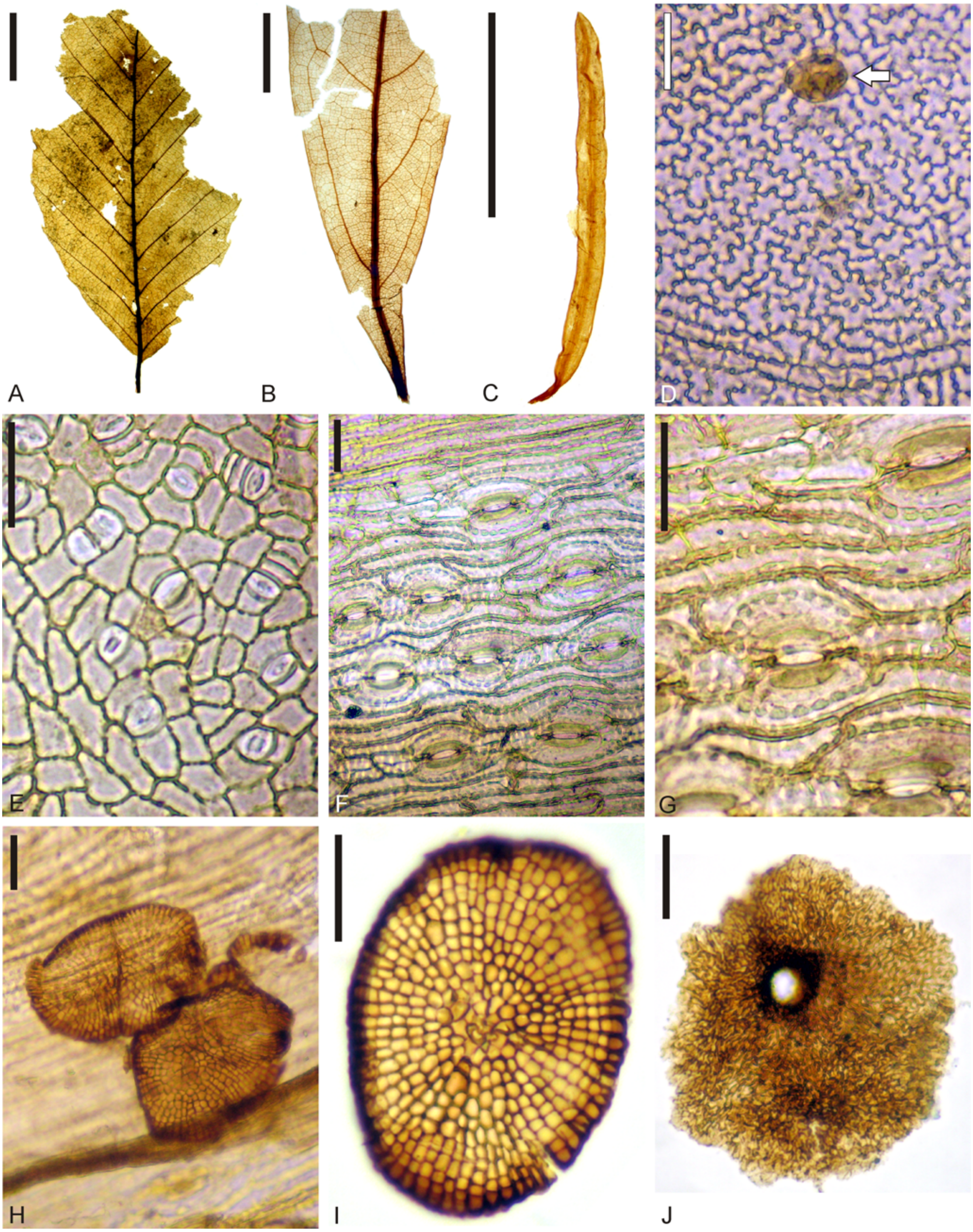


**Fig. 21.** Leaves and fungi from Tetta. **A.** *Fagus castaneifolia* Unger, leaf (MZ VII/134/312). **B, D, E.** *Daphnogene polymorpha* (Al. Braun) Ettingshausen (MZ VII/134/313); B – leaf; D – adaxial epidermis; note secretory idioblast (arrow); E – abaxial epidermis with stomata. **C, F, G.** *Tsuga* sp. (MZ VII/134/314); C – needle; F, G – epidermis with stomata; note pitted cell walls. **H, I.** *Phragmothyrites* cf. *concentricus* Carlie J. Phipps & Rember (MZ VII/134/319$_1$); H – three sporocarps on epidermis of needle of *Tsuga* sp. (MZ VII/134/319$_1$); I – details of porocarp (MZ VII/134/319$_2$). **J.** *Plochmopeltinites* cf. *masonii* Cookson, sporocarp (MZ VII/134/319$_3$). Scale bar: A – C – 1 cm,D–J – 50 µm.

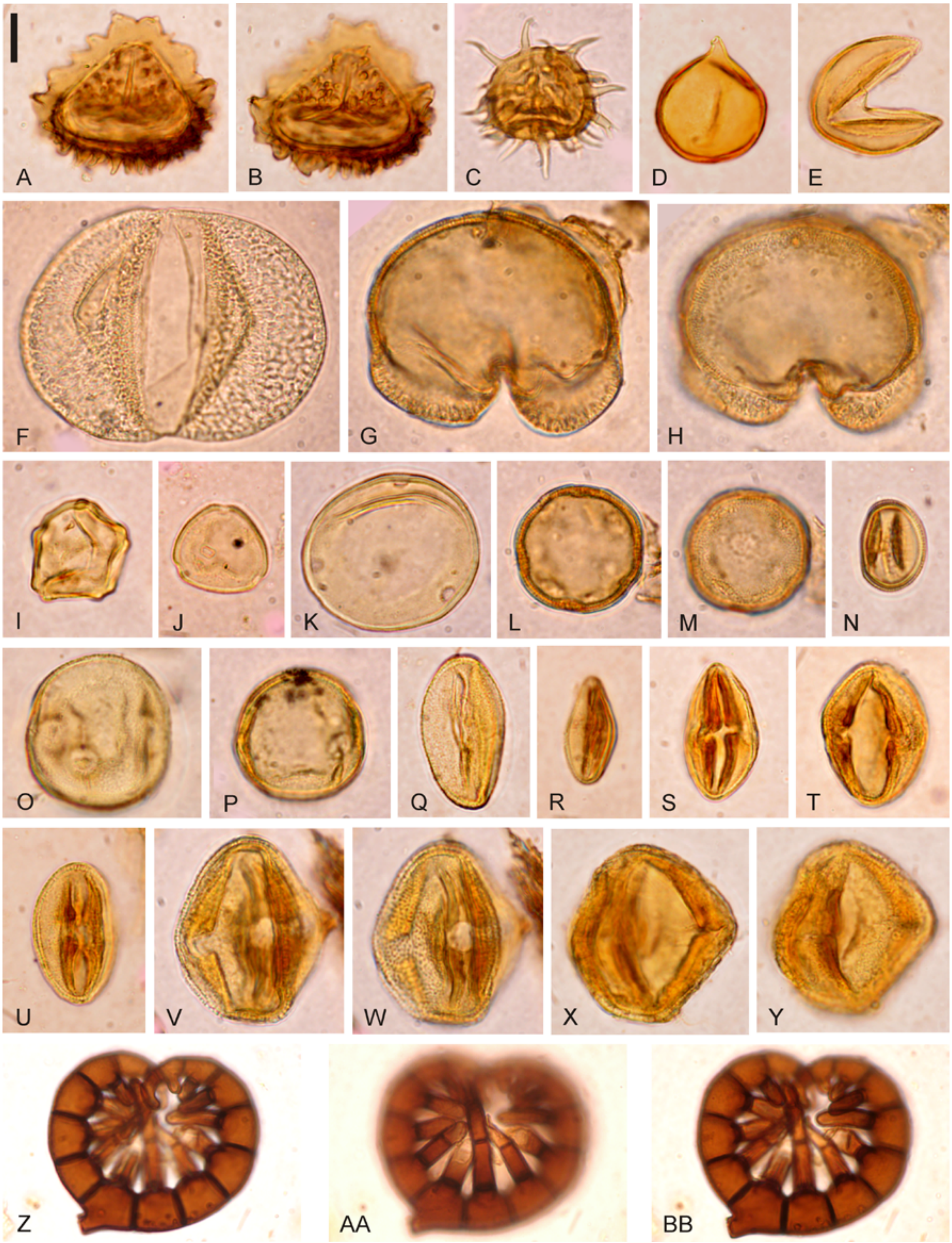


**Fig. 22.** Palynomorphs (spores, pollen grains and a fungus) from Tetta. **A, B.** *Muerrigerisporis* sp. 1 Grabowska, same specimen, various foci, site II. **C.** *Echinatisporis longechinus* Krutzsch, site IV. **D.** *Sequoiapollenites rotundus* Krutzsch, site IV. **E.** *Inaperturopollenites concedipites* (Wodehouse) Krutzsch, site IV. **F.** *Cathayapollis wilsonii* (Sivak) Ziembińska-Tworzydło, site II. **G, H.** *Cedripites parvisaccatus* (Zauer) Krutzsch, same specimen, various foci, site IV. **I.** *Alnipollenites verus* Potonié, site IV. **J.** *Momipites* sp., site II. **K.** *Caryapollenites simplex* (Potonié) Raatz, site II. **L, M.** *Periporopollenites stigmosus* (Potonié) Pflug & Thomson, same specimen, various foci, site IV. **N.** *Platanipollis ipelensis* (Pacltová) Grabowska, site II. **O.** *Faguspollenites* cf. *bockwitzensis* (Walter & Z&ter) Kohlman-Adamska & Ziembińska-Tworzydło, site II. **P.** *Faguspollenites minor* Nagy, site IV. **Q.** *Quercoidites henricii* (Potonié) Potonié, Thomson & Thiergart, site II. **R.** *Quercoidites microhenricii* (Potonié) Potonié, Thomson & Thiergart, site II. **S.** *Tricolporopollenites villensis* (Thomson) Thomson & Pflug, site IV. **T.** *Tricolporopollenites pseudocingulum* (Potonié) Thomson & Pflug, site II. **U.** *Tricolporopollenites dolium* (Potonié) Pflug & Thomson, site II. **V, W.** *Araliaceoipollenites amplus* Słodkowska, same specimen, various foci, site IV. **X, Y.** cf. *Edmundipollis* sp., site II. **Z–BB.** *Pesavis tagluensis* Elsik & Jansonius, same specimen, various foci, site IV. Scale bar = 10 µm. One scale for all photographs.

## DISCUSSION

### General characteristics of the collected materials

Among the materials collected in Tetta between 2018–2019, the present authors identified 109 taxa belonging to 45 families, of which 81 taxa are documented for the first time for Tetta, including two new species. In addition, among disseminules (fruit and seeds) collected by Alexander Czaja and Olaf Tietz, the present authors identified or verified 46 taxa, of which nine are new to Tetta and were not found in materials gathered between 2018–2019 (Tab. S2).

Among the 2018–2019 samples, many leaves, mostly gymnosperm needles (especially in samples IV/1–IV/3) were extracted, but only 2 angiosperm and 1 gymnosperm taxa were identified. Moreover, several Bryophyta, fungi and wood fragments were found, but not all identified. The taxonomic composition of each fossil assemblage is summarized in Tables 1–9.

Considering this and previous reports, a total of 152 taxa have so far been documented in the fossil flora from Tetta (Tab. S3).

Palynological analysis revealed the presence of 103 fossil-species of sporomorphs, including 18 species of plant spores, 19 species of gymnosperm pollen grains, and 66 species of angiosperm pollen grains (Tab. S4). These results are generally consistent with results for the plant macroremains fossil assemblages. Many of the macroremain taxa of trees, shrubs and herbs (e.g., *Sequoia*, *Alnus*, *Cercidiphyllum*, *Fagus*, *Ilex*, *Mastixia*, *Platanus*, *Sparganium*, and *Symplocos*) are represented by pollen grains. These macroremain and pollen assemblages are complementary rather than equal, as the palynological assemblages represent a broader context, but pollen grains and spores can only be assigned to a family or genus level, while the macroremains represent plant species growing onsite. In addition, the spores of ferns and lycopods plus some non-pollen palynomorphs, including freshwater algae and fungal microremains, were recorded.

### Taphonomical remarks

The sedimentary succession at Tetta is characterized by a limnic sedimentary environment with fluvial and partly lacustrine intercalations. The lowermost section studied at site IV (sample IV/1, DB3) and the uppermost section at site III (sample III/11) and VII (sample VII/12, DB2) represent a highly energetic, fluvial environment (see Geological setting), which facilitated the transportation of bigger and heavier disseminules over a greater distance. Conversely, deposits that occur at site II (samples II/4–II/5) were formed in low-energy environments.

Sediments at site IV, where samples 1–3 were collected consist of frequently alternating thin, light, and dark grey layers of sand and silt. However, in sample IV/1 the sediments are coarser, and the authors frequently observed pyrite concretions and small, armoured mud balls, composed of light grey or orange clay. Plant remains occurred in dark, up to 5 cm thick layers separated by light-coloured sediments. The authors observed fruits, seeds, cones, leaves, needles, twigs, and many larger wood fragments (up to 1 m in length), as well as extensive microscopic remains, including spores, pollen grains, and non-pollen palynomorphs. However, in all site IV samples, disseminules of any kind were generally less common than leaves. In terms of taxonomic composition, the three samples from site IV indicate similar fossil assemblages. Gymnosperm needles, anemochorous disseminules, and wood fragments (up to 1 m in length) are more common in sample 1, whereas angiosperm leaves appear more frequent in samples IV/2 and IV/3.

The fact that various types of remains with different transportation potentials co-occur at site IV may reflect poor sorting and short distance transport (Gastaldo and Ferguson, 1998). Therefore, all fossil assemblages from this site are considered allochthonous to paraautochthonous.

The plant assemblage, found in sample II/4 (Tab. 4), comes from dark gray silt-clay with an admixture of sand. Sand particles are mostly represented by sharp quartz (including automorphic crystals), but mica was also present. Wood (up to 1 m in length) and leaf fragments dominate this sample, whereas disseminules were scarce and represented by larger woody plant remains. Sample II/5 provided mostly leaves that occurred in a dark clay lens within a grey clay. Plant remains identified here represent various organs of *Fagus* and small disseminules of herbs (Tab. 4). The fact that leaves and fruits of *Fagus* co-occurred, despite distinct transportation potential, indicates that sample II/5 represents an autochthonous to paraautochthonous fossil assemblage.

Samples from site VI appear lithologically and taphonomically comparable to site IV samples.

Fossil assemblages extracted from samples III/11 (Tab. 8) and VII/12 (Tab. 9) were found in lenses of coarse sand in the apical section of a red/yellow clay bed. Most remains found here are either moderately or poorly preserved. Large and woody disseminules of *Carya*, *Eomastixia*, *Mastixia*, and *Fagus* are most conspicuous, but the smaller *Eurya* is equally abundant. This indicates that the disseminules have not been sorted according to size. The characteristics of deposits and concentration of fossils in samples III and VII indicate that they were formed in a high-energy environment, for example, during flood events. Poor sorting and roundness of sedimentary particles indicate short transportation. Therefore, remains can be attributed to vegetation in relatively close proximity. However, it is clear that the taxonomic composition of these fossil assemblages is taphonomically biased, which is evidenced by the scarcity of anemochorous disseminules of woody plants and complete lack of herb remains.

### Vegetation reconstruction

Most plant macroremains found at Tetta belong to temperate, deciduous, and woody angiosperms. Among the most common is *Fagus*, which was found in all samples except VII/12. Conifers are characteristic of the lowermost part of the profile (samples IV/1–3, Tabs 1–3), where up to five genera per sample may be observed. They are rare in the middle section (samples II/4, Tab. 4, VI/6, Tab. 6), represented by only a few remains of one species and completely absent in the uppermost part of the profile (samples III/11, VII/12). Overall, conifers outnumber flowering plants in the number of macroremains.

Macroremains of aquatic and swamp plants are very rare. Floating hydrophytes are lacking, while submerged plants are represented only by *Vallisneria* (Fig. 8C). Amphibious hydrophytes are more common, including obligate aquatic *Dulichium, Sparganium*, and *Urospathites*, as well as facultative aquatic *Carex* (Fig. 9A), *Scirpus* (Fig. 9B), *Persicaria* (Fig. 16A), *Polygonum* (Fig. 16B, C), also possibly *Hypericum* (Fig. 11I), and *Umbelliferopsis molassicus* (Fig. 19D). Only a few pollen grains of Sparganiaceae/Typhaceae and Cyperaceae are present (Tab. S4). Common Cenozoic obligate swamp trees, such as *Taxodium* or *Glyptostrobus* are completely lacking among macroremains, but *Alnus* is observed in most samples. Other swamp elements, including *Nyssa* (Fig. 17D, E) and *Microdiptera,* were found in up to two samples. *Alnus* pollen grains were found regularly, while *Nyssa* pollen was scarce. Disseminules of herbaceous and woody wetland plants never appear together in a sample, which at least partially results from their different transportation potentials.

The complete absence of floating hydrophytes indicates a lack of large, open water bodies. The limited presence of submerged plant remains may indicate either small or ephemeral ponds (site II) and flowing water environments (site IV). Fast-flowing water events also occurred sporadically, as evidenced by the sediments in site III and VII. The relative abundance of anemochorous, early successional trees in most studied sites may indicate a high frequency of habitat disturbance. Unstable, frequently changing conditions around sedimentary basin would promote pioneering angiosperm trees. A dynamic environment also might have hindered locally the development of *Taxodium* and *Glyptostrobus* communities. Stable floodplains appear absent, especially during the clay deposit stage (see below), which could, for example, indicate steep (tectonic) basin margins.

Cupressaceae pollen grains without distinct papillae, usually of the *Taxodium/Glyptostrobus* type (Fig. 22E), are present in all studied samples (min. 3% in site II and max. 22% in site IV, Tab. S4). Their occurrence could indicate the presence of swamp forests, composed of *Taxodium* and/or *Glyptostrobus* in the vicinity of the sampled sites. Nevertheless, it is difficult and often impossible to identify the genera of Taxodioideae and Sequoioideae based on pollen morphology (Bouchal and Denk, 2020). Therefore, the entire composition of pollen assemblages should be considered in their interpretation.

The most diverse group of macroremains include mesophytic and/or riparian vegetation types. Conifers represent a particularly rich group, consisting of *Cephalotaxus*, *Paranothotsuga*, *Pinus* (Fig. 7C), *Pseudolarix*, *Sequoia*, *Tetraclinis*, and *Tsuga* (Figs 5M, 21C, F, G). They are mostly considered mesophytes, but *Sequoia*, for example, can be variously interpreted as either riparian or mesophytic (Kovar-Eder and Meller, 2001; Kunzmann and Mai, 2005). Observation of living sequoias indicates, however, that they reach their maximum development on alluvial flats, where considerable sediment accumulation rates significantly reduce competition from other species (Burns and Honkala, 1990).

Most macroremains of deciduous angiosperm trees and shrubs found in Tetta represent riparian elements, including *Acer* (Figs 14N, O, R–W, X, 15A–E, I), *Liquidambar*, *Platanus neptuni* (Fig. 9F–H), *Pterocarya*, *Cercidiphyllum* (Fig. 10G–J), and *Craigia* (Fig. 15G, aff. *Burretia* sp. – Fig. 15F; Kvaček and Walther, 2004; Mai, 2000). Others, such as *Aralia*, *Betula*, *Cotoneaster* (Fig.12E), *Liriodendron* (Fig. 7K–M), *Poliothyrsis* (Fig. 11J), *Pterostyrax*, and *Rubus*, *Staphylea* (Fig. 14H, I) can be considered as both riparian and mesophytic elements. Considering the autecology of most modern representatives, *Fagus* could be regarded as the only true mesophyte among deciduous trees, but in Tetta it occupied more riparian areas. Exclusively evergreen trees and shrubs, and those which today are represented by both evergreen and deciduous species, including *Cinnamomum* (Fig. 8A–B), *Daphnogene* (Fig. 21B, D, E), *Distylium* (Fig. 10B–D), *Eurya* (Fig. 15K, M), *Ficus* (Fig. 12L–M), *Gironniera* (Fig. 12I–J), *Ilex* (Figs 16H, 19C, F20A), *Leucothoe* (Fig. 18F, G), *Magnolia* (Fig. 8A–B), *Mastixia* (Figs 7E–G, I, J, N–O), *Meliosma* (Fig. 9I, D, E), *Prunus* (Fig. 11D, H), *Pyracantha* (Fig. 12A–C, G), *Schefflera* (Fig. 20F), *Symplocos*, *Ternstroemia*, and *Turpinia* (Fig. 14P) are usually considered mesophytic (Mai, 1995).

Lianas are represented by *Actinidia* (Fig. 18H–J), *Ampelopsis* (Fig. 10L, M), *Decaisnea* (Fig. 9C), *Parthenocissus* (Fig. 11A, B) and *Vitis* (Fig. 10K, N, O, P). Probably, they were most common in riparian forests, but especially in forest gaps or thickets on the sunny edges along rivers (Collinson *et al.*, 2012).

Disseminules of herbaceous, meso- or xerophytes are exceptionally rare, represented by *Collinsonia* (Fig. 19A), *Moehringia* (Fig. 15J, L), and *Teucrium* (Fig. 19B) and the role they played in local plant communities is difficult to determine. Only *Laportea* can be considered as important herbaceous element of the forest ground, but especially in the riparian habitats.

The vegetation reconstruction discussed below is based only on the most conspicuous samples with clear mutual stratigraphic relations. Using traditional, subjective, and intuitive interpretation, the zonal vegetation of site IV (Tabs 1–3) could be generally described as an ecotone between Mixed mesophytic forests (MMF) and Broad-leaved evergreen forests (BLEF), owing to the high proportion of broad-leaved evergreen elements (see Wang, 1961). The presence of *Fagus* in all studied samples supports the assumption of the present authors that this tree was common in mesic forests at that time. Today *F. grandifolia* is probably the only species of this genus which can be found in riparian environments. Considering the characteristics of the fossil assemblages of site IV and phytosociological relations of modern *Fagus*, beech forests appear to have been the most common mesic vegetation at this time. They were characterized by a diverse array of conifer trees and rich broad-leaved evergreen plants in the understory. In terms of the diversity of conifers the authors see some resemblance between the beech forest of site IV and the modern Japanese beech forest (Hukusima *et al.*, 2013).

Beech forests are well documented in the European Neogene. They begin to be evidenced by macrofloras from the late Oligocene, but only become common from the Late Miocene onwards (Mai, 1995).

Many of the aforementioned genera were recorded during the palynological analysis by the authors (Fig. 22; Tab. S4). Site IV samples contain numerous pollen grains of *Sequoia/Sequoiadendron/Metasequoia/Cryptomeria* (Fig. 22D), *Pinus*, *Cathaya*, *Picea*, *Fagus*, *Quercus* (mainly *Quercoidites henricii* and *Q. microhenricii*), fossil-species *Tricolporopollenites villensis*, *T. dolium*, *T. pseudocingulum*, Castaneoideae, other Fagaceae (including *Fususpollenites*), Mastixiaceae (*Cornaceaepollis satzveyensis*), *Ilex*, Engelhardioideae, *Platanus*, *Betula*, as well as some pollen grains of *Acer*, *Cercidiphyllum*, Cornaceae, Cyrillaceae/Clethraceae, *Corylopsis*, other Hamamelidaceae (*Tricolporopollenites staresedloensis*), Ericaceae, Fabaceae, *Liquidambar*, Oleaceae, *Pterocaya*, Rosaceae, *Cedrus*, *Sciadopitys*, and others.

In the slightly younger part of the sequence, exposed at site II, carpological remains of *Fagus* occur alone (sample II/5, Tab. 4) or with *Sequoia* (sample II/4, Tab. 5). Considering this evidence alone, these fossil assemblages indicate two possible types of plant communities: monodominant *Sequoia* forests and poorly diversified beech forests. However, the diversity of the leaves found at this site (not studied in this paper) indicates that the forest must have been much more diverse, an assumption confirmed by palynological analysis. *Fagus* pollen is abundant in all site II samples (up to 25%), but these samples are also rich in various other pollen grains. *Pinus*, *Cathaya*, *Sequoia/Sequoiadendron/Metasequoia/Cryptomeria*, *Picea*, *Keteleeria/Pseudolarix*, *Quercus* (mainly *Quercoidites henricii*), the fossil-species *Tricolporopollenites pseudocingulum*, Mastixiaceae, Engelhardioideae, *Platanus*, *Liquidambar*, *Carya*, Ericaceae, *Platycarya*, *Symplocos*, and *Ulmus* are most frequent. In addition, some pollen grains of Castaneoideae, *Cercidiphyllum*, *Corylopsis*, Cyrillaceae/Clethraceae, Fabaceae, *Ilex*, Myricaceae, *Cedrus*, *Sciadopitys*, *Tsuga*, and others were encountered. Most of these taxa could represent components of mesophytic and/or riparian forests in the surrounding area.

The sedimentary succession, exposed at sites III (sample III/11, Tab. 8) and VII (sample VII/12, Tab. 9), provided fossil assemblages that significantly differ in taxonomic composition from those in the lower part of the sequence (see above). Unlike the other sites at Tetta, sites III and VII lack aquatic plants and conifers. Swamp vegetation is scarce, represented only by *Alnus* (sample III/11), while *Carya* (Fig. 13Q, S) and *Liquidambar* constitute the only riparian forest elements. Lianas, specifically *Parthenocissus* and *Vitis*, could represent riparian and/or mesophytic elements.

Most plant remains found in samples III/11 and VII/12 can be related to mesic habitats, including the exclusively evergreen trees/shrubs: *Symplocos* (Figs 15N–P, 16D–F), *Mastixia* (Figs 15R–T, 17F, H–J), *Eurya* (Fig. 15K, M), *Distylium* (Fig. 10B–D), *Pyracantha* (Fig. 12A–C, G), *Eomastixia* (Fig. 17A–C), *Zanthoxylum* (Fig. 15H), *Gironniera* (Fig. 12I, J), *Tectocarya*, *Ternstroemia*, *Trigonobalanopsis*, *Morella*, evergreen or deciduous trees/shrubs: *Ilex*, *Magnolia* (Fig. 7E–G, I, J, N, O), *Meliosma*, *Prunus*, and *Turpinia* and the deciduous trees/shrubs: *Aralia*, *Carpinus*, *Fagus*, *Pterostyrax*, *Pterosinojackia*, *Rehderodendron*, and *Sambucus* (Fig. 20B, C). This floristic composition indicates the dominance of a broad-leaved evergreen forest. However, the absence of Lauraceae, abundance of *Fagus* and very limited contribution of evergreen Fagaceae is unusual for Early Miocene broad-leaved evergreen forests. Therefore, a species-rich beech forest, potentially resembling modern beech forests in mountainous regions of South-Central China, seems more likely (Hukusima *et al.*, 2013).

The differences in taxonomic composition between samples III/11, VII/12 and the samples from site IV may indicate a substantial change in the physiognomy and composition of plant communities. However, a wide variety of taphonomic factors may be responsible, given the clear difference between the depositional environments of these sites (see section Taphonomical remarks).

IPR-vegetation analysis was used (Kovar-Eder and Kvaček, 2007; Teodoridis *et al.*, 2020) to test vegetation types, determined by the intuitive method. The present authors only tentatively analyzed sample III/11 and three samples from sites IV, which were analyzed as one site. The results obtained from samples I/8 and VI/6 were comparable to those from site IV, therefore they were ignored.

Using "Drudge 1" and based on best-fitted modern analogs - "Results - Mix", the authors found that assemblages of site IV and sample III/11 generally represent broad-leaved evergreen forests (Teodoridis *et al.*, 2011), but show the closest similarity to the modern evergreen/deciduous broad-leaved mixed forest zone (1500–2000 m alt.) at Mount Emei (Tang and Ohsawa, 1997; Teodoridis *et al.*, 2020), which however, cannot be seen as a modern equivalent. Despite general resemblance, the assemblage of sample III/11 has a higher percentage of broad-leaved evergreen components than the assemblages of site IV (50.3% to 44.8%).

When considered major biome types, the results obtained with IPR-vegetation analysis do not indicate significant change between samples from site IV and sample III/11. The results of IPR-vegetation analysis slightly differ from those, obtained by intuitive analysis, since they do not show physiognomical alteration in vegetation. However, the increase (real or apparent) in the proportion of broad-leaved evergreen components was indicated. Nevertheless, in the opinion of the present authors, the intuitive method appears more accurate in this case, as it places a stronger emphasis on taxonomical changes and the importance of *Fagus* in the forest composition.

### Age estimation of Tetta floras

Despite determined efforts, the authors did not find evidence that would enable absolute dating of any part of the sequence. Nor did the authors find any lignite deposits in the area studied 2018–2019 that could be used as a lithostratigraphic reference layer. Therefore, the authors were forced to base their age estimation exclusively on available plant taxa. The authors compared their fossil assemblages with other Lusatian floras and correlate them with the units of the biostratigraphic division, the so-called "Florenkomplexe" (floristic complexes) proposed by Mai and Walther (Mai and Walther, 1978; Mai, 1995, 1997), as well as palynofloras

**Table 1**

The list of taxa found at the site Tetta IV/1.

| | | |
|---|---|---|
| *Acer hercynicum* | *Ficus lutetianoides* | *Pterocarya margaritana* |
| *Acer* sp. 2 | *"Fortunearia" altenburgensis* | *Pterosinojackia lusatica* |
| *Alnus lusatica* | *Gironniera verrucata* | *Pterostyrax coronatus* |
| *Ampelopsis rotundata* | *Ilex ovidrupacea* | *Rubus microspermus* |
| *Aralia intermedia* | *Laportea europaea* | *Sequoia abietina* |
| *Aralia lusatica* | *Leucothoe narbonensis* | *Symplocos casparyi* |
| *Cephalotaxus miocenica* | *Liriodendron geminata* | *Symplocos schereri* |
| *Cercidiphyllum helveticum* | *Magnolia burseracea* | *Ternstroemia sequoioides* |
| *Cinnamomum* cf. *costatum* | *Mastixia amygdalaeformis* | *Tetraclinis salicornioides* |
| *Collinsonia* cf. *europaea* | *Meliosma miessleri* | *Tsuga moenana* |
| *Distylium protogaeum* | *Meliosma pliocaenica* | *Turpinia ettingshausenii* |
| *Eurya stigmosa* | *Platanus neptuni* | *Umbelliferopsis molassicus* |
| *Fagus deucalionis* | *Prunus scharfii* | *Vitis* aff. *teutonica* |
| *Ficus lucida* | *Pseudolarix schmidtgenii* | *Vitis parasilvestis* |

**Table 2**

The list of taxa found at the site Tetta IV/2.

| | | |
|---|---|---|
| *Acer hercynicum* | *Fagus deucalionis* | *Poliothyrsis eurorimosa* |
| *Acer* sp. 1 | *Ficus lutetianoides* | *Pseudolarix schmidtgenii* |
| *Acer* sp. 2 | *"Fortunearia" altenburgensis* | *Pterocarya margaritana* |
| *Actinidia faveolata* | *Gironniera verrucata* | *Pterosinojackia lusatica* |
| *Alnus lusatica* | *Ilex saxonica* | *Pterostyrax coronatus* |
| *Betula* cf. *dryadum* | *Laportea europaea* | *Sequoia abietina* |
| *Cephalotaxus miocenica* | *Leucothoe narbonensis* | *Symplocos casparyi* |
| *Cercidiphyllum helveticum* | *Liriodendron geminata* | *Symplocos schereri* |
| *Cinnamomum* cf. *costatum* | *Magnolia germanica* | *Tetraclinis salicornioides* |
| *Decaisnea bornensis* | *Mastixia amygdalaeformis* | *Turpinia ettingshausenii* |
| *Distylium protogaeum* | *Meliosma miessleri* | *Vallisneria vittata* |
| *Dulichium hartzianum* | *Pinus palaeostrobus* | *Vitis* aff. *teutonica* |
| *Eurya stigmosa* | *Platanus neptuni* | *Vitis parasilvestis* |

**Table 3**

The list of taxa found at the site Tetta IV/3.

| | | |
|---|---|---|
| *Acer* aff. *angustilobum* | *Gironniera verrucata* | *Pterosinojackia lusatica* |
| *Acer hercynicum* | *Laportea europaea* | *Pterostyrax coronatus* |
| *Acer* sp. 1 | *Liriodendron geminata* | *Rubus semirotundatus* |
| *Acer* sp. 2 | *Mastixia amygdalaeformis* | *Schefflera dorofeevii* |
| *Alnus lusatica* | *Oxydendrum europaeum* | *Sequoia abietina* |
| *Aralia lusatica* | *Pentapanax tertiarius* | *Staphylea rotundata* |
| *Betula* cf. *dryadum* | *Platanus neptuni* | *Symplocos casparyi* |
| *Cercidiphyllum helveticum* | *Poliothyrsis eurorimosa* | *Ternstroemia sequoioides* |
| *Craigia bronnii* | *Pseudolarix schmidtgenii* | *Tetraclinis salicornioides* |
| *Eurya stigmosa* | *Paranothotsuga jechorekiae* | *Vitis* aff. *teutonica* |
| *Fagus deucalionis* | *Pterocarya margaritana* | *Vitis parasilvestis* |

**Table 4**

The list of taxa found at the site Tetta II/5.

| | |
|---|---|
| *Ampelopsis rotundata* | *Sequoia abietina* |
| *Fagus deucalionis* | *Symplocos casparyi* |
| *Ilex saxonica* | |

**Table 5**

The list of taxa found at the site Tetta II/4.

| | | |
|---|---|---|
| *Carex plicata* | *Laportea nemejcii* | *Scirpus brevicornis* |
| *Cyperus leptodermis* | *Microdiptera lusatica* | *Sparganium pusilloides* |
| *Fagus deucalionis* | *Microdiptera minor* | *Sparganium tuberculatum* |
| *Hypericum septestum* | *Polygonum* sp. 2 | |
| *Laportea europaea* | *Polygonum* sp.1 | |

**Table 6**

The list of taxa found at the site Tetta VI/6.

| | | |
|---|---|---|
| *Actinidia faveolata* | *Mastixia amygdalaeformis* | *Rubus semirotundatus* |
| *Alnus latibracteosa* | *Meliosma miessleri* | *Sequoia abietina* |
| *Cephalotaxus miocenica* | *Meliosma pliocaenica* | *Symplocos casparyi* |
| *Distylium protogaeum* | *Nyssa ornithobroma* | *Symplocos pseudogregaria* |
| *Eurya stigmosa* | *Parthenocissus britannica* | *Symplocos schereri* |
| *Fagus deucalionis* | *Platanus neptuni* | *Tectocarya elliptica* |
| *Gironniera carinata* | *Pseudolarix schmidtgenii* | *Tetraclinis salicornioides* |
| *Gironniera verrucata* | *Pterocarya margaritana* | *Vitis parasilvestis* |
| *Liriodendron geminata* | *Pterosinojackia lusatica* | |
| *Magnolia burseracea* | *Pterostyrax coronatus* | |

**Table 7**

The list of taxa found at the site Tetta I/8.

| | | |
|---|---|---|
| *Alnus latibracteosa* | *Laportea europaea* | *Pyracantha acuticarpa* |
| *Aralia rugosa* | *Liquidambar europaea* | *Rubus microspermus* |
| *Betula* cf. *longisquamosa* | *Magnolia ludwigii* | *Sambucus lucida* |
| *Carpinus cordataeformis* | *Mastixia amygdalaeformis* | *Symplocos casparyi* |
| *Cephalotaxus miocenica* | *Meliosma miessleri* | *Symplocos minutula* |
| *Comptonia goniocarpa* | *Meliosma pliocaenica* | *Ternstroemia sequoioides* |
| *Distylium protogaeum* | *Microdiptera* aff. *parva* | *Teucrium* aff. *martinae* |
| *Eurya stigmosa* | *Moehringia miocaenica* | *Urospathites visimensis* |
| *Fagus deucalionis* | *Ostrya scholtzii* | *Vitis* aff. *teutonica* |
| *Frangula solitaria* | *Paliurus favonii* | *Vitis parasilvestis* |
| *Ilex* aff. *lotschii* | *Pentapanax tertiarius* | |
| *Ilex ovidrupacea* | *Persicaria* aff. *polesieana* | |
| *Ilex saxonica* | *Pterosinojackia lusatica* | |

**Table 8**

The list of taxa found at the site Tetta III/11.

| | | |
|---|---|---|
| *Alnus latibracteosa* | *Gironniera verrucata* | *Sambucus lucida* |
| *Aralia rugosa* | *Ilex ovidrupacea* | *Symplocos casparyi* |
| aff. *Burretia* sp. | *Liquidambar europaea* | *Symplocos pseudogregaria* |
| *Carpinus cordataeformis* | *Magnolia burseracea* | *Symplocos schereri* |
| *Carya ventricosa* | *Magnolia ludwigii* | *Tectocarya elliptica* |
| *Cotoneaster wackersdorfensis* | *Mastixia amygdalaeformis* | *Ternstroemia sequoioides* |
| *Distylium protogaeum* | *Meliosma pliocaenica* | *Turpinia ettingshausenii* |
| *Distylium uralense* | *Ostrya scholtzii* | *Vitis* aff. *teutonica* |
| *Eomastixia saxonica* | *Parthenocissus britannica* | *Vitis parasilvestis* |
| *Eurya stigmosa* | *Pterostyrax coronatus* | *Zanthoxylum giganteum* |
| *Fagus deucalionis* | *Pyracantha acuticarpa* | |
| *Fothergilla europaea* | *Rehderodendron ehrenbergii* | |

**Table 9**

The list of taxa found at the site Tetta VII/12.

| | | |
|---|---|---|
| *Carya ventricosa* | *Myrica stoppii* | *Symplocos* cf. *pseudogregaria* |
| *Eomastixia saxonica* | *Prunus leporimontana* | *Symplocos schereri* |
| *Ilex ovidrupacea* | *Pyracantha acuticarpa* | *Trigonobalanopsis exacantha* |
| *Mastixia amygdalaeformis* | *Rehderodendron ehrenbergii* | *Vitis parasilvestis* |
| *Meliosma miessleri* | *Staphylea rotundata* | |
| *Meliosma pliocaenica* | *Symplocos casparyi* | |

and schemes of the spore-pollen zones in the Paleogene and Neogene (Krutzsch *et al.*, 1992; Piwocki and Ziembińska-Tworzydło, 1997; Krutzsch, 2000).

Except for the lowermost section (site IV), exclusively Paleogene taxa were absent from the sedimentary succession. Considering macroremains only, fossil assemblages from the lower part of the sedimentary succession appear older than those obtained from the upper part. Both "old" (unreported after Lower Miocene), and enduring (Eocene–Miocene or Pliocene and upper Paleogene/Neogene) taxa are abundant, while the so-called "young" exclusively Neogene elements (Mai, 1995, 1997, 2000, 2001, 2008) are rare (Tabs 1–9). In Lusatia, features like these are typically encountered among transitional floras, from the upper Oligocene to the Lower Miocene.

The percentage of palaeotropical elements among the macroremains exceeds 50% only in samples III/11 and VII/12. There is a marked increase in the participation of palaeotropical elements between the lowermost (represented by sites IV and II) and the upper sections of the profile. This progression may correspond to climate warming. Equivalent climatic change is observed between central European floras from the upper Oligocene and upper Lower Miocene (Friis, 1975; Mai, 1965).

Crucial for estimating the upper age limit of macrofloras is the absence of extant elements and the scarcity of herbaceous, aquatic and swamp vegetation elements in all studied samples. In the Lusatia region, modern European tree species and aquatic and non-woody swamp plants begin to appear in the Middle Miocene (Mai, 1985, 1995), especially among floras of the Schipkau - Konin floristic complex (Mai, 2001).

Therefore, the most likely time frame for the fossil assemblages of the authors is between the latest Oligocene and the latest Early Miocene.

The results of palynological analysis led to the same conclusion. All sporomorphs, recorded in the Tetta samples, can be found in Oligocene – Middle Miocene strata (Grabowska, 1996; Krutzsch, 2000; Stuchlik *et al.*, 2001, 2002, 2009, 2014). Among them, "the oldest taxa" are *Fususpollenites* sp., *Intratriporopollenites insculptus*, *Momipites quietus*, and *Quercoidites microhenricii*. The lack of such taxa as *Aglaoreidia cyclops*, *Boehlensipollis hohlii*, *Cicatricosisporites dorogensis*, *Cupanieidites eucalyptoides*, and pollen grains from the Normapolles group is also an important feature of the palynoflora. These taxa have their upper stratigraphical limits in the lower/upper Oligocene or the lower part of the upper Oligocene (Grabowska, 1996; Grabowska and Słodkowska, 2003). Therefore, the authors assume that the studied sequence must be younger than the lower part of the upper Oligocene.

Below, individual sites and fossil assemblages are characterized in their presumed stratigraphic order (starting with the oldest). However, the authors must note that the stratigraphic position of some fossiliferous layers was problematic (samples I/8 vs. VI or sites VII vs. III/6) and therefore their chronological position is unclear.

**Site IV.** The richest group at this site is represented by "enduring" species (late Paleogene to Miocene or Pliocene): *Actinidia faveolata* (Fig. 18H–J; Tab. 2), *Alnus lusatica* (Fig. 14A, B, F), *Betula* cf. *dryadum* (Fig. 13T), *Eurya stigmosa* (Fig. 15K, M), *Fagus decurrens* (Fig. 13A–C), *Liquidambar europaea* (Fig. 9J, 10A), *Liriodendron geminata* (Fig. 7K–M), *Meliosma pliocaenica* (Fig. 9D, E), *Oxydendrum europaeum* (Fig. 18K1, K2; Tab. 3), *Pseudolarix schmidtgenii* (Fig. 5A–I), *Rubus semirotundatus* (Fig. 11C, E), *R. microspermus* (Fig. 11F, G), *Sequoia abietina* (Fig. 7A, B), *Symplocos casparyi* (Fig. 15N–P), *Symplocos schereri* (Fig. 16D, E), *Tetraclinis salicornioides* (Fig. 5J, K, N, L). The second-largest group consists of "old" species (Eocene or Oligocene to Middle Miocene), including *Acer hercynicum* (Fig. 14O, Q, R), *Aralia intermedia* (Fig. 20E), *A. lusatica* (Figs 19E, 20D), *A. rugosa* (Fig. 19G, H), *Decaisnea bornensis* (Fig. 9C; Tab. 2), *Distylium prologaeum* (Fig. 10B, C), *Dulichium hartzianum* (Fig. 8H1, H2), *"Fortunearia" altenburgensis* (Fig. 10F), *Meliosma miessleri* (Fig. 9I1, I2), *Pterocarya margaritana* (Fig. 13H, J, K, P), *Pterostyrax coronatus* (Fig. 18A–E), *Schefflera dorofeevi* (Fig. 20F), and *Sparganium pusilloides* (Fig. 8E). As most are relatively rarely found, their time ranges may not be fully known, but *Distylium prologaeum* and *Sparganium pusilloides* are quite common and regarded as late Oligocene and Early Miocene index fossils (Mai, 1997). "Young" elements, including *Cephalotaxus miocenica* (Fig. 7D, H), *Cinnamomum costatum* (Fig. 8A, B), *Ilex ovidrupacea* (Fig. 19C1, C2, F1, F2), and *Prunus scharfii* (Fig. 11D1, D2; Tab. 1) are relatively scarce.

Considering floristic composition, assemblages of site IV (Tabs 1–3) best correspond with the Rott-Thierbach floristic complex floras from the Horka-Kausche graben in Upper Lusatia. Particularly close are the fossil assemblages, described by Mai (1997) from the cores NSL 35/1965 near Niederheide, NSL 36/1965 near Hirschwinkel, NSL 42/1965 near Jahmen, NSL 43/1965 near Kringelsdorf, and Spremberg 37/1960. The most characteristic features of these floras are the relatively high contribution of old elements and the coexistence of *Fagus* with a diverse group of conifers, especially *Picea beckii* Mai, 1987. In Tetta, *Picea* has not been found, but *Pseudolarix, Sequoia*, and *Tetraclinis* are very common.

It should be noted that there is a slight discrepancy in age between the floras of the Rott-Thierbach floristic complex from Rott near Bonn and the Horka-Kausche graben (Upper Lusatia) floras. The Rott-Thierbach floras are assigned to the Neochattian (MP 30 zone; Mai, 1995, 1997), whereas the age of the Horka-Kausche floras could not be estimated with such precision. The Horka-Kausche floras occurred mostly in sediments of the lower part of the Spremberg Formation and, to a lesser extent, the Cottbus Formation (Mai, 1997; Escher *et al.*, 2020), which would represent the Lower Miocene (Standke and Rascher, 2005).

In the palynological assemblage, such taxa as *Cornaceaepollis satzveyensis*, *Cupuliferoipollenites pusillus*, *Fususpollenites* sp., *Intratriporopollenites insculptus*, *Momipites quietus*, *M. punctatus*, *Platanipollis ipelensis*, *Platycaryapollenites* sp., *Quercoidites henricii*, *Q. microhenricii*, *Tricolporopollenites dolium*, *T. pseudocingulum*, *T. staresedloensis* and *T. villensis* were recorded. Palaeotropical and palaeotropical/warm-temperate taxa are well represented (Tab. S4). Their composition is most similar to Oligocene palynofloras (Krutzsch *et al.*, 1992; Grabowska, 1996). In particular, there are many similarities between the palynoflora from site IV and palynoassemblages from the upper Oligocene of the Thierbach member exposed in Tagebau Bockwitz, Saxony, Germany (Gastaldo *et al.*, 1998) and Enspel, western Germany (Herrmann *et al.*, 2009, 2010; Uhl and Herrmann, 2010) as well as the upper Oligocene palynoflora from Rębiszów, Lower Silesia, Poland (Kowalski *et al.*, 2020). The lack of lower Oligocene elements and presence of some "new" elements (for example relatively frequent *Faguspollenites*) suggests that this assemblage dates to the late Oligocene.

In addition, fossil fungal microremains of *Pesavis tagluensis* were found in sample IV/3 (Tab. S4; Fig. 22Z–BB). This probably aero-aquatic fungus (Smith and Crane, 1979) represents a good stratigraphic proxy because it is practically found only in the Paleogene, ranging from Paleocene to late Oligocene (Smith and Crane 1979; Kalgutkar and Sweet, 1988; Ediger and Alişan, 1989; Pole *et al.*, 1993; Macphail and Hill, 1994; Kalgutkar and Jansonius, 2000). The only Neogene record of *Pesavis tagluensis* concerns the Middle Miocene Brassington Formation, United Kingdom (Pound *et al.,* 2022). However, it cannot be ruled out that the remains of *Pesavis tagluensis* found in the Brassington Formation are in fact redeposited from older sediments. On the contrary, the excellent state of preservation of *Pesavis tagluensis* microremain from Tetta appears to exclude redeposition of it.

**Site II.** The presence of *Cyperus leptodermis* (Fig. 8D1, D2), *Laportea nemejci* (Fig. 12O), *Microdiptera lusatica* (Fig. 14K1, K2, L1, L2), *M. minor* (Fig. 14G), *Sparganium pusilloides* and *Fagus castaneifolia* leaves (Fig. 21A) in sample II/5 (Tab. 4) indicate that this part of the sequence represents the transition between the Oligocene and Miocene or Lower Miocene, but cannot be younger than the Early Miocene. Therefore, from a macrofloristic perspective, it appears close in age to the site IV floras. However, the biostratigraphic position of the site II floras cannot be estimated with the same precision as site IV because of the low number of taxa present (Tabs 1–5).

The palynological assemblages from site II are similar to site IV palynoflora (Tab. S4). The main differences are the absence of *Fususpollenites* and the more frequent pollen grains of *Faguspollenites* at site II. This is evidence that the site II assemblages are slightly younger than those at site IV and indicates their Miocene age. In the opinion of the present authors, the palynoflora is most similar to Lower Miocene assemblages (Piwocki and Ziembińska-Tworzydło, 1997; Krutzsch, 2000), but the authors did not find taxa that clearly indicate an Early Miocene age of this assemblage.

**Site VI.** This fossil assemblage shares most species with sample IV/1–3, particularly the presence of conifers (Tab. 6). The position of the fossiliferous layers of site VI, approx. 7–9 m above sites II and IV in the sedimentary succession, indicates that they may be younger than those sites. Some elements of site VI make it resemble the Lower Miocene floras, but the presence of *Tectocarya elliptica* (Fig. 17O) indicates that this fossil assemblage cannot be older than the floras of the Brandis-Bilina floristic complex (see Mai, 2000).

The composition of the palynological spectrum of sample VI/7 (Tab. S4), i.e., the co-occurrence of relatively frequent spores of *Cicatricosisporites* cf. *chattensis* and pollen grains of *Cornaceaepollis satzveyensis*, *Cupuliferoipollenites*, *Momipites*, *Platycaryapollenites*, *Quercoidites henricii*, *Tricolporopollenites dolium*, *T. pseudocingulum*, *T. villensis* and *Faguspollenites*, also indicates an Early Miocene age.

**Site V.** The composition of the palynological spectrum of sample V/10 (Tab. S4), including pollen grains of Cupressaceae, *Cathayapollis*, *Cornaceaepollis satzveyensis*, *Cupuliferoipollenites*, *Cyrillaceaepollenites megaexactus*, *Edmundipollis*, *Periporopollenites*, *Quercoidites henricii*, *Reevesiapollis*, *Symplocoipollenites vestibulum*, *Tricolporopollenites dolium*, *T. pseudocingulum* and *Faguspollenites*, is generally similar to Lower to Middle Miocene palynofloras.

**Site I.** Approximately a third of the 37 taxa encountered among macroremains at this site represent the enduring species, *Eurya stigmosa*, *Moehringia miocaenica* (Fig. 15J, 15L), *Ostrya scholtzii* (Fig. 14C, D), *Pentapanax tertiaries* (Fig. 20G), *Pyracantha acuticarpa* (Fig. 12A-C, G), *Rubus microspermus* (Fig. 11F, G), *Sambucus lucida*, *Symplocos casparyi*, *Symplocos minutula* (Fig. 16G), *Ternstroemia sequoioides* (Fig. 15Q). "Old" elements (Eocene or Oligocene to Middle Miocene) are numerous and include *Alnus latibracteosa* (Figs 13O, 14E–J), *Aralia rugosa*, *Carpinus cordataeformis* (Fig. 13N, R), *Comptonia goniocarpa* (Fig. 12N1, N2), *Distylium protogaeum*, *Urospathites visimensis* (Fig. 8G), *Ilex saxonica* (Fig. 16H), *Laportea europaea* (Fig. 12K), *Meliosma miessleri*, *Microdiptera* cf. *parva* (Fig. 14M1, M2). Index taxa from the late Oligocene and Early Miocene are limited to *Carpinus cordataeformis*, *Comptonia goniocarpa* and *Distylium protogaeum* (Mai, 1997, 2000). "Young" elements are in a minority: *Betula* cf. *longisquamosa* (Fig. 13M), *Frangula solitaria* (Fig. 12F), *Ilex ovidrupacea* (Fig. 8D1, D2), *I. lotschii* (Fig. 20A), *Paliurus favonii* (Fig. 12D, H), *Vitis parasilvestris* (Fig. 10K1, K2, N1, N2), *V.* aff. *teutonica* (Fig. 10O, P1, P2).

The feature that distinguishes sample I/8 (Tab. 7) flora from samples IV, II and VI is the low proportion of conifer macroremains (*Cephalotaxus*). This may be caused by taphonomic, ecological, or climatic factors. Macroflora from this sample resembles the floras of the Bitterfeld-Münzenberg floristic complex, where many common conifers, including *Quasisequoia couttsiae*, *Cunninghamia miocenica*, *Glyptostrobus europaeus*, and *Sequoia abietina* are lacking. However, *Taxodium* is also lacking in sample I/8, whereas in the Bitterfeld-Münzenberg floristic complex this tree occurs regularly (Mai, 2000). The high proportion of *Fagus* is also rather unusual for floras of the Bitterfeld-Münzenberg floristic complex.

The combination of *Fagus* and *Carpinus cordataeformis* is one of the characteristic features of the Rott-Thierbach floristic complex (Mai and Walther, 1991). Among the Horka-Kausche graben sites, particularly similar to site I are floras from Horka 3/1962, NSL 42/1965 near Jahmen, and NSL 36/1965 near Hirschwinkel, both assigned to the Rott-Thierbach floristic complex (Mai, 1997). *Fagus*, *Carpinus cordataeformis*, and *Frangula solitaria* have also been reported together in some floras of the Brandis-Bilina floristic complex, e.g., "Flora B" of Spremberg 29/57 (Mai, 2000, p. 134).

The biostratigraphic position of the sample I/8 fossil assemblage is therefore uncertain, although it can be confidently stated that it is older than the Wiesa-Eichelskopf floristic complex.

Palynological analysis does not provide much more information. In sample I/9, *Fagus* pollen grains make up about 50% of the pollen spectrum (Tab. S4), with the remaining 50% composed mainly of pollen grains and spores of taxa with long stratigraphic ranges.

**Sites III and VII**. Similarities in geological characteristics and general floristic composition between site III and VII assemblages indicate that they may represent the same biostratigraphic unit. However, closer study of the floristic composition reveals subtle differences. Compared with sample III/11 (Tab. 8), sample VII/12 (Tab. 9) is much less species-rich and lacks the late Oligocene and Early Miocene elements, including *Alnus latibracteosa*, *Aralia rugosa*, *Carpinus cordataeformis*, *Distylium protogaeum*, *Pterostyrax coronatus*. On the other hand, some taxa, such as *Morella stoppii*, *Prunus scharfii* and *Trigonobalanopsis* (Fig. 13D–F), were present in sample VII/12 and absent from sample III/11. These discrepancies may have a wide variety of causes, including habitat or climatic fluctuation or taphonomic processes.

Distinctive for these samples is the mass occurrence of various Mastixiaceae, including *Mastixia amygdalaeoformis* (Figs 15R–T, 17F, H–J), *Eomastixia saxonica* (Fig. 17A–C) and *Tectocarya*, as well as a small addition of other "younger mastixioid floras" elements, such as *Morella stoppii*, several species of *Symplocos*, *Rehderodendron ehrenbergii* (Fig. 17K, L) and *Zanthoxylum giganteum* (Fig. 15H; Tabs 8, 9). In the Lusatia region, these represent typical Neogene elements, mostly associated with the uppermost Lower Miocene floras of the Wiesa-Eichelskopf floristic complex. They may also occur in younger Middle Miocene floras, especially of the Kleinleipisch-Františkove Lázně and Klettwitz – Salzhausen floristic complexes, as well as the Upper Miocene floras of the "Schipkau-Konin" floristic complex but become increasingly rare and less diverse in younger deposits (Mai, 2000). Some have been documented in the Upper Miocene, as in Gozdnica (Poland; Zastawniak, 1992), and outside Lusatia in the Lower Rhenish Basin floras (Germany; Van der Burgh, 1987), or even in Lower Pliocene floras [see *Eomatixia saxonica* in Ungstein/Upper Rhine Graben; Gregor and Schumann (1987)]. On the other hand, *Eomatixia saxonica* and *Mastixia amygdalaeoformis* are known in older floras of the Brandis-Bilina (Mai, 1995; Czaja, 2003), or even Rott-Thierbach floristic complex (*Mastixia*; Mai and Walther, 1991).

Nevertheless, the presence of *Carpinus cordataeformis*, *Alnus latibracteosa*, and *Distylium protogaeum* at site III excludes the possibility of this fossil assemblage representing Middle or Upper Miocene floristic complexes. The aforementioned taxa have been reported together only in the Lower Miocene floras (Mai, 1995, 1999). The presence of *Trigonobalanopsis* in sample VII/12 is also of great importance because, in the Lusatian region, this taxon appears to be absent after the Wiesa-Eichelskopf floristic complex (Mai, 2001). The presence of *Fagus* and *Mastixia amygdalaeformis* instead of *M. lusatica* is rather unusual for this floristic complex, although *Fagus* has been reported in Berzdorf (Czaja, 2003), Dauban and Spremberg (Mai, 2000b), Oberdorf (Meller, 1998). Minimal participation of the "young" elements (*Fothergilla europaea* – Fig. 10E) further support an Early Miocene age.

Fossil assemblages from sites III and VII resemble to a large extent the flora described by Czaja and Berner (1999). According to their report and also considering Adam (1964), the plant remains studied by Czaja and Berner were extracted from fine to coarse sands above the 1st (C1) clay seam (Fig. 2, site "1999"). This indicates either that site III and VII fossil assemblages and the flora described by Czaja and Berner come from two distinct lithostratigraphical units, or that sites III and VII include redeposited fossil material. The latter possibility is supported by the high altitude of both sites and their clear glaciotectonic deformation (mixing with Pleistocene material and the glacial anticline with the local downward structure). However, there is one important difference between these fossil assemblages: the floras studied by Czaja and Berner include a taxonomically diverse group of conifers, which is absent at sites III and VII. This may be a result of taphonomical differences, or the flora described by Czaja and Berner representing more than one fossiliferous layer (owing to methods employed in fossil collection, especially that specimens were gathered over 1.5 years). Czaja and Berner compared their fossil assemblage to the Middle Miocene floras of the Klettwitz-Salzhausen floristic complex and rejected the relationship with the Wiesa-Eichelskopf floristic complex, because of the lack of *Mastixia lusatica* (see Mai, 1995). However, the presence of *Carpinus cordataeformis* and *Meliosma messleri* among the remains documented by Czaja and Berner (1999) indicates an Early Miocene age for this flora.

The fossil flora documented by Leder (2007, 2009) occurs much lower in the sedimentary sequence than the fossil flora documented by Czaja and Berner (1999; Fig. 2, site "2006"), it was also correlated with the Klettwitz-Salzhausen floristic complex (Langhian, Serravallian, Middle Miocene), although an Early Miocene to Middle Miocene age was also considered by this author. However, the present authors raise doubts about the identification of remains and conclusions regarding their age. In the view of the authors, *Fagus* leaves assigned by Leder (2007) to *Fagus* cf *menzelii* most probably belong to *F. castaneifolia*, which would indicate that this flora is not younger than the Early Miocene (Denk, 2004). In contrast, the presence of *Carpinus betulus* L. foss would indicate an age not older than the Late Miocene (Mai, 1995). The gap in stratigraphic range between *F. castaneifolia* and *C. betulus* foss makes the age of the flora described by Leder (2007, 2009) difficult to estimate.

In conclusion, floras from the lowest part of the sedimentary sequence studied here, represented by samples from site IV, can be securely regarded as dating to the latest Oligocene, supported by the presence of the Paleogene fossil fungus taxon *Pesavis tagluensis*. The biostratigraphic affiliation of floras from the middle part of the sedimentary sequence (clay seam C2, samples II/4–5, VI/6–7 and I/8–9) is less certain, probably between the Oligo/Miocene and the Early Miocene, while the dating of floras from the upper part of the sequence (samples III/11 and VII/12, DB2) are younger, yet still the (latest?) Early Miocene.

### Discussion on palaeoclimatic signals

Owing to the strong floristic resemblance, the three site-IV fossil assemblages are considered together. Only site IV and site III assemblages are analyzed, as they are the most floristically distinct.

The present authors considered canopy trees as the best indicators for climatic reconstruction, because they experience more climatic influence than plants of the other forest layers (Kolakovskiy, 1964). The most probable canopy trees from site IV are *Acer*, *Betula*, *Fagus*, *Liriodendron*, *Mastixia*, *Paranothotsuga*, *Pinus*, *Pseudolarix*, *Sequoia*, *Tetraclinis*, and *Tsuga*. However, *Pseudolarix*, *Sequoia*, and *Tetraclinis* are today relictual or monotypic plants and therefore less reliable as climatic indicators (see Kvaček, 2007; Grimm and Denk, 2012; Utescher *et al*., 2014). Most remaining taxa are temperate, deciduous, or conifers. *Mastixia*, which probably represents the only broad-leaved evergreen tree in this fossil assemblage, is traditionally regarded as a warm climate indicator in the palaeobotanical literature. This indicates a mean annual temperature (MAT) of 15–19 °C, cold month mean temperature (CMMT) above 10 °C and annual precipitation (AP) >1000 mm (Mai and Walther, 1978; Mai, 1995). However, considering climatic preferences most living species of *Fagus*, cold month mean temperature of above 10 °C, as indicated by the presence of *Mastixia* would appear too high for the development of a luxuriant beech forest. Except for *F. grandifolia,* for which this represents the upper limit, most modern beeches exist in much cooler climates (Fang and Lechowicz, 2006). The present authors have not found an example of the coexistence of *Fagus* and *Mastixia* today (Hukusima *et al.*, 2013). *Fagus* generally represents a temperate zone tree, except *Fagus grandifolia* subsp. *mexicana* (Rodriguez-Ramirez *et al.*, 2013), while *Mastixia* occurs mainly in the tropical zone, entering subtropical zone only in some areas of SE (Myanmar, China) and S (India, Bhutan) Asia (Matthew, 1976).

Accepting the climatic preferences of modern *Fagus* and *Mastixia*, their coexistence in time and space at Tetta might appears unlikely. Nevertheless, the co-occurrence of tropical and temperate elements in Cenozoic floras is common and has long been debated in the palaeobotanical literature with various explanations (Mai, 1995). The authors believe that, as the geographic range of modern *Mastixia* is significantly reduced in comparison to the Neogene, it is very likely that its climatic preferences could have changed. Furthermore, European mastixias in the form of shrubs, may have benefited from the protective function of canopies (Ferguson *et al.*, 1998). The role of canopies in regulating the microclimate for understory plants has been highlighted in younger Neogene floras, where one observes a relatively high percentage of evergreen elements, despite climatic deterioration (see Mai, 1995).

Considering the uncertainties regarding *Mastixia*, *Fagus* represents the most reliable climatic indicator, although it provides only a very wide climatic parameters: MAT 4.2–19.5 °C, CMMT -11.4–10.4 °C (Fang and Lechowicz, 2006). Nevertheless, the presence of evergreen taxa, especially broad leaved, indicates that the temperature did not drop below -15°C (Box and Fujiwara, 2012).

In the older literature, *Tetraclinis* and *Pyracantha* were proposed as periodic (summer?) drought indicators of semi-humid/semi-arid climate (Andreánszky, 1963a, b; Palamarev, 1967; Krutzsch *et al.*, 1992). However, according to more modern views, *T. salicornioides* unlike living *Tetraclinis* existed in humid climates (Mai, 1994; Kunzmann and Mai, 2005). In Tetta, the authors observe *Tetraclinis*, *Fagus* and *Cercidiphyllum* in one fossil assemblage. If one accepts that all three were components of the same plant community, it is clear that drought in any part of the year can be completely excluded. *Fagus* indicates high humidity and precipitation (see Mai, 1995), often far in excess of 1000 mm annually (Fang and Lechowicz, 2006).

Estimations based on vegetation provide more precise indications of climate than those based on preferences of individual taxa. Intuitive vegetation analysis suggests that zonal vegetation from site IV could represent an ecotone between MMF and BLEF. Wolfe (1979) established general boundary values for the ecotone between MMF and BLEF vegetation of a MAT of approx. 13 °C and a CMMT of approx. 1 °C. Ge and Xie (2017) indicate optimal climatic conditions for sites with equal proportions of evergreen and deciduous species are characterized by a MAT of approx. 14 °C, CMMT of approx. -1 °C and MAP of approx. 1150 mm. Additionally, based on the intuitive method, the authors concluded that site IV vegetation could resemble some modern beech forests in Japan, for which the optimal MAT is suggested as being around 10 °C and annual precipitation above 1300 mm (Hukusima *et al.*, 2013).

According to Mai and Walther (1991; see also Mai, 1997; Krutzsch *et al.*, 1992), the Rott-Thierbach floristic complex floras, with which we compare site IV floras, indicate a perhumid, temperate climate (Cfa/Cfb), with a MAT of approx. 10 °C and CMMT of approx. 0°C. The occurrence of *Fagus*, *Picea*, *Trigonobalanopsis* and *Mastixia* evidences a MAP far in excess of 1,000 mm/y or even 2,000 mm/y. The estimation of the authors for site IV overlaps with or is slightly warmer than the values, proposed for the Rott-Thierbach floristic complex.

The abundance of thermophilous taxa in sample III distinguishes it from site IV and indicates significant climate warming at the time of deposition of this part of the sequence. Climatic estimation, based on canopy trees for sample III, would be comparable to that obtained for site IV. However, intuitive vegetation reconstruction suggests a broad-leaved evergreen forests (see vegetation reconstruction). According to Wang (1961), broad-leaved evergreen forests develop today when MAT is between 13–19 °C, CMMT is above 6 °C, minimum temperature does not drop below -6 °C and for more than 9 months mean temperature is above 10 °C. Contrastingly, Wolfe (1979) proposed a MAT of 13–20 °C and a CMMT above 1 °C, and according to Ohsawa (1990), the lower limit for BLEF is a CMMT of around -1 °C and precipitation is evenly distributed throughout the year and exceeds 1,000 mm/y. However, owing to the presence of *Fagus,* the authors would expect MAT to be closer to the lower limit suggested for broad-leaved evergreen forests. Furthermore, participation of broad-leaved deciduous trees rapidly decreases when MAT exceeds 13 °C(Wolfe, 1979). On the basis of the intuitive method, the authors concluded that site III vegetation could resemble modern beech forests from China and Taiwan, for which the optimal MAT is 10–16 °C and AP 900–1600 mm (Hukusima *et al.*, 2013).

Epiphyllous fungal taxa (*Phragmothyrites* cf. *concentricus* and *Plochmopeltinites* cf. *masonii* – Fig. 21H–J) found on cuticles of *Tsuga* sp. (Fig. 21C, F, G) needles could indicate a humid climate as modern epiphyllous fungi (namely Microthyriaceae and Micropeltidaceae) are most abundant and diverse in humid regions since high precipitation and air humidity are crucial factors for their growth (Selkirk, 1975; Johnson and Sutton, 2000; Limaye *et al.*, 2007).

Site III flora was compared here with the Wiesa-Eichelskopf floristic complex, which is considered extremely warm, with a MAT of 18–21 °C, CMMT around 4–10 °C and AP of 800–2000 mm. The climatic condition suggested for site III flora are cooler than those typical for the Wiesa-Eichelskopf floristic complex, but this may result from differences in methods used in the reconstruction.

## CONCLUSIONS

Extensive exploration of the newly exposed section of the Tetta Clay Pit provided many new fossil plant remains. These new materials, coupled with palynological analysis, enabled a new interpretation of the stratigraphy, palaeoclimate, and palaeoenvironment of the site.

Twelve fossiliferous horizons provided 109 taxa, belonging to 45 families. Three were recognized as new fossil-taxa and three new combinations were proposed. Fossil assemblages consist mostly of arborescent plants, which represent riparian and mesophytic habitats. Aquatic vegetation and swamp forests were absent or marginal, probably a result of the local topography or environmental dynamics. The most widespread vegetation type was beech forest. Fossil plant assemblages from the lower part of the profile display marked similarities to late Oligocene/Early Miocene floras from the Horka-Kausche rift system (Saxony). The clearest biostratigraphic units in the studied sedimentary sequence are the Rott-Thierbach floristic complex in the lowest part of the profile and the Wiesa-Eichelskopf floristic complex in the uppermost part. The biostratigraphic affinity of the fossil assemblages from the middle part of the sedimentary sequence is equivocal. The presence of *Pesavis tagluensis* fungus in the lowermost part of the profile (site IV) indicates a minimum age of latest late Oligocene. Index taxa, such as *Carpinus cordataeformis, Cyperus leptodermis, Distylium prologaeum, Laportea nemejci, Microdiptera lusatica, Sparganium pusilloides*, and *Fagus castaneifolia*, indicate that the overlying deposits are no younger than Early Miocene. Fossil floras from the lowest part of the profile (site IV) indicate a cooler climate with MAT 13–14 °C and MAP >1,000 mm/y, while those in the uppermost part of the profile (sites III and VII) indicate a warmer climate with MAT 13–20 °C and MAP >1,000 mm/y.

The present investigation showed that sedimentary succession exposed in the Tetta Clay Pit most probably represents the upper Oligocene to the Lower Miocene. Out of five biostratigraphic units (floristic complexes) recognized so far in Lusatia for the time range between the latest Oligocene and the Early Miocene, at least two can be indicated at Tetta. Taking into account previous studies by Czaja and Berner (1999) and Leder (2007, 2009), the profile exposed so far may extend to the Middle Miocene and may include up to two additional floristic complexes. The stratigraphic time span, represented by this locality, is unique for Central Europe (comp. Czaja, 2003).

**Acknowledgements**

We would like to thank Michael Zschau (Operations Manager of the Buchholz Clay Pit, Germany) for granting access to the Buchholz Clay Pit and providing a map of the mine and other helpful information. We also thank former operations managers Siegfried Mönnig and Peter Löwenig for approving and supporting four exploratory drillings in 2004. Thanks also go to the Saxon State Office for Environment, Agriculture and Geology (Germany) for providing unpublished exploration reports. We are especially grateful to Alexander Czaja for the inspiration to undertake this study and for offering extensive support and providing information about the historical fossil sites. Furthermore, special thanks are extended to Błażej Błażejowski and Cyprian Kulicki (Institute of Paleobiology, PAS) for their help in preparing SEM pictures. Part of this work (mainly palynological and paleomycological investigations) was supported by the W. Szafer Institute of Botany, Polish Academy of Sciences, through the statutory funds (EW, GW). Steven Manchester (Florida Museum of Natural History, University of Florida) and Torsten Utescher (Senckenberg Research Institute, University of Bonn) are acknowledged for their careful and critical reviews and journal editor P. Filipiak (Faculty of Earth Sciences, University of Silesia, Sosnowiec) for helpful comments and suggestions.

## REFERENCES

Adam, C., 1964. *Ergebnisbericht über die vom VEB geologische Erkundung Süd 1962/63 durchgeführte Sucharbeiten und Vorerkundung auf Ton im Raum Großsaubernitz (Kreise Bautzen, Niesky und Görlitz)*. Unpubl. Report, VEB GFE Halle/Saale, Halle, pp. 61, 47 app.

Adam, C., 1974. Beiträge zur Kenntnis der Kaoline und Tertiärtone in Nordostsachsen. *Abhandlungen des Zentralen Geologischen Instituts*, 17: 1–181.

Alexowsky, W. & Leonhardt, D., 1994. *Geologische Übersichtskarte des Freistaates Sachsen 1 : 400.000, Karte ohne quartäre Bildungen.* Sächsisches Landesamt für Umwelt und Geologie, Freiberg.

Andreánszky, G., 1963a. Das Trockenelement in der jungtertiären Flora Mitteleuropas. *Vegetatio*, 11: 113–129.

Andreánszky, G., 1963b. Das Trockenelement in der jungtertiären Flora Mitteleuropas. *Vegetatio*, 11: 155–172.

Baillon, H. E., 1866. Mémoire sur la famille des Magnoliacées. *Adansonia*, 7: 1–16, 65–69.

Blume, C. L., 1823. Beschrijving van eenige gewassen, waargenomen op eenen togt naar den Salak, in den jare 1822. *Verhandelingen van het Bataviaasch Genootschap van Kunsten en Wetenschappen*, 9: 149–153. [In Duch.]

Blume, C. L., 1825. *Bijdragen tot de flora van Nederlandsch-Indië*. Lands Drukkerij, 284 pp. [In Duch.]

Bouchal, J. M. & Denk, T., 2020. Low taxonomic resolution ofpapillate Cupressaceae pollen (former Taxodiaceae) impairs their applicability for palaeo-habitatreconstruction. *Grana*, 59: 71–93.

Box, E. O. & Fujiwara, K., 2012. A comparative look at bioclimatic zonation, vegetation types, tree taxa and species richness in Northeast Asia. *Botanica Pacifica*, 1: 5–20.

Brause, H., 1990. Beiträge zur Geodynamik des Saxothuringikums. *Geoprofil*, 2: 1–88.

Burns, R. M. & Honkala, B. H., 1990. *Silvics of North America: 1. Conifers*. *Agriculture Handbook 654*. U.S. Department of Agriculture, Forest Service, Washington, D.C., 675 pp.

Candolle, A. P. & Sprengel, C. P. J., 1821. *Elements of the Philosophy of Plants: Containing the Principles of Scientific Botany; Nomenclature, Theory of Classification, Phytography, Anatomy, Chemistry, Physiology, Geography and Diseases of Plants: with a History of the Science, and Practical Illus*. W. Blackwood and T. Cadell, Edinburgh, 486 pp.

Chen, T., 1995. *Changiostyrax*, a new genus of Styracaceae from China. *Guihaia*, 15: 289–292.

Chen, T. & Li, G., 1997. A new species of *Sinojackia* Hu (Styracaceae) from Zhejiang, East China. *Novon1*, 7: 350–352.

Chevalier, A., 1901. Monographie des Myricaceae; anatomie et histologie, organographie, classiWcation et description des espèces, distribution géographique. *Mémoires de la Société nationale des sciences naturelles de Cherbourg*, 32: 82–340.

Collinson, E. M., Manchester, S. R. & Wilde, V., 2012. Fossil fruits and seeds of the Middle Eocene Messel biota, Germany. *Abhandlungen der Senckenberg Gesellschaft für Naturforschung*, 570: 1–251.

Czaja, A., 2000. *Pseudotsuga jechorekiae* sp. nova, der erste fossile Nachweis der Gattung *Pseudotsuga* Carrière nach Zapfen aus dem Miozän der Oberlausitz, Deutschland. *Feddes Repertorium*, 111: 129–133.

Czaja, A., 2001. Koniferen aus dem Mittelmiozän der Tongrube Tetta-Buchholz in der Oberlausitz (Sachsen). *Veröffentlichungen des Museums der Westlausitz Kamenz*, 23: 23–38.

Czaja, A., 2003. Paläokarpologische Untersuchungen von Taphozönosen des Unter- und Mittelmiozäns aus dem Braunkohlentagebau Berzdorf/Oberlausitz (Sachsen). *Palaeontographica Abteilung B*, 265: 1–148.

Czaja, A. & Berner, T., 1999. Tetta-Buchholz – eine neue Fundestelle tertiärer Pflanzenreste in der Oberlausitz. *Abhandlungen und Berichte des Naturkundemus*, 71: 435–463.

Dandy, J. E., 1927. The genera of Magnoliaceae. *Bulletin of Miscellaneous Information, Royal Gardens, Kew*, 1927: 257–264.

Denk, T., 2004. Revision of *Fagus* from the Cenozoic of Europe and southwestern Asia and its phylogenetic implications. *Documenta Naturae*, 150: 1–72.

Dietrich, H. & Liebscher, W., 1972. *Ergebnisbericht über Ton Buchholz, Kreis Görlitz, Bez. Dresden*. VEB GFE Halle Saale, Freiberg, 82 pp.

Dorofeev, P. I., 1979. K sistematike tretichnykh *Sparganium.* In: Goretskiy G. I. & Grichuk V. P. (eds), *Sovetskaya Paleocarpologiya*. Izdatel'stvo Nauka, Moskva, pp. 53–75. [In Russian.]

Ediger, V. Ş. & Alişan, C., 1989. Tertiary fungal and algal palynomorph biostratigraphy of the northern Thrace basin, Turkey. *Review of Palaeobotany and Palynology*, 58: 139–161.

Elias, T. S., 1971. The genera of Myricaceae in the southeastern United States. *Journal of the Arnold Arboretum*, 52: 305–318.

Escher, D., Gerschel, H., Geißler, M., Hartmann, A., Rascher, J., Rascher, M., Richter, L. & Wittwer, S., 2020. *Lithofazieskarten Tertiär Lausitz 1 : 50.000 (LKT50 Lausitz)*. Sächsisches Landesamt für Umwelt, Landwirtschaft und Geologie, Dresden, 96 pp.

Fang, J. & Lechowicz, M. J., 2006. Climatic limits for the present distribution of beech (*Fagus* L.) species in the world. *Journal of Biogeography*, 33: 1804–1819.

Farjon, A., 2010. *A Handbook of the World's Conifers (2 Vols.)*. Brill, Leiden & Boston, 1112 pp.

Ferguson, D. K., Pingen, M., Zetter, R. & Hofmann, C.-C., 1998. Advances in our knowledge of the Miocene plant assemblage from Kreuzau, Germany. *Review of Palaeobotany and Palynology*, 101: 147–177.

Figlar, R. B. & Nooteboom, H. P., 2004. Notes on Magnoliaceae IV. *Blumea: Journal of Plant Taxonomy and Plant Geography*, 49: 87–100.

Frankis, M. P., 1988. Generic inter-relationship in Pinaceae. *Notes Royal Botanic Garden Edinburgh*, 45: 527–548.

Friis, E. M., 1975. Climatic implications of microcarpological analyses of the Miocene Fasterholt flora, Denmark. *Bulletin of the Geological Society* of *Denmark,* 24: 179–191.

Fritsch, P. W., Yao, X., Simison, W. B., Cruz, B. C. & Chen, T., 2016. *Perkinsiodendron*, a new genus in the Styracaceae based on morphology and DNA sequences. *Journal of the Botanical Research Institute of Texas*, 10: 109–117.

Fu, L., Li, N., Elias, T. S. & Mill, R. R., 1999. Pinaceae. In: Wu, Z. Y. & Raven, P. H. (eds), *Flora of China, Volume 4*. St. Louis, Science Press, Beijing, and Missouri Botanical Garden Press, pp. 11–52.

Gastaldo, R. A. & Ferguson, D. K., 1998. Reconstructing Tertiary plant communities: introductory remarks. *Review of Palaeobotany and Palynology*, 101: 3–6.

Gastaldo, R. A., Riegel, W., Püttmann, W., Linnemann, U. G. & Zetter, R., 1998. A multidisciplinary approach to reconstruct the Late Oligocene vegetation in central Europe. *Review of Palaeobotany and Palynology*, 101: 71–94.

Ge, J. & Xie, Z., 2017. Geographical and climatic gradients of evergreen versus deciduous broad-leaved tree species in subtropical China: Implications for the definition of the mixed forest. *Ecology and Evolution*, 7: 3636–3644.

Göthel, M., 2004. Stratigraphie des Känozoikums in Brandenburg mit spezieller Berücksichtigung des Braunkohlenreviers Lausitz. *Brandenburgische Geowissenschaftliche Beiträge*, 11: 149–168.

Grabowska, I., 1996. Flora sporowo-pyłkowa. In: Malinowska, L. & Piwocki, M. (eds), *Budowa Geologiczna Polski 3. Atlas Skamieniałości Przewodnich i Charakterystycznych 3a. Kenozoik, Trzeciorzęd, Paleogen*. Polska Agencja Ekologiczna, Warszawa, pp. 395–431. [In Polish.]

Grabowska, I. & Słodkowska, B., 2003. Paleogen. In: Dybova-Jachowicz, S. & Sadowska, A. (eds), *Palinologia*. W. Szafer Institute of Botany, Polish Academy of Sciences, Kraków, pp. 177–182. [In Polish.]

Gregor, H.-J. & Schumann, F., 1987. Eine neue Diasporen-Flora aus dem „Weißen Pliozän" von Ungstein. *Documenta Naturae*, 41: 19–29.

Grimm, G. W. & Denk, T., 2012. Reliability and resolution of the coexistence approach – a revalidation using modern-day data. *Review of Palaeobotany and Palynology*, 172: 33–47.

Handel-Mazzetti, H., 1921. Plantae novae Sinenses. *Anzeiger der Akademie der Wissenschaften in Wien*, 59: 101–112.

Herrmann, M., Ashraf, A. R., Uhl, D. & Mosbrugger, V., 2009. Die oberoligozäne Palynoflora der Bohrung Enspel 1996/1 (Westerwald, WDeutschland) – Teil 1: Sporen und Gymnospermen. *Mainzer Geowissenschaftliche Mitteilungen*, 37: 33–76.

Herrmann, M., Ashraf, A. R., Uhl, D. & Mosbrugger, V., 2010. Die oberoligozäne Palynoflora der Bohrung Enspel 1996/1 (Westerwald, WDeutschland) – Teil 2: Angiospermen und Paläökologie. *Mainzer Geowissenschaftliche Mitteilungen*, 38: 9–60.

Hu, H. H., 1928. *Sinojackia*, a new genus of Stracaceae from southeastern China. *Contributions from the Biological Laboratory of the Science Society of China*, 4: 1–4.

Hukusima, T., Matsui, T., Nishio, T., Pignatti, S., Yang, L., Lu, S.-Y., Kim, M.-H., Yoshikawa, M., Honma, H. & Wang, Y., 2013. *Phytosociology of the Beech (Fagus) Forests in East Asia*. Springer, Berlin, Heidelberg, 257 pp.

Hwang, S. & Grimes, J., 1996. Styracaceae. In: Wu, Z. Y. & Raven, P. H. (eds), *Flora of China, Volume 15*. Science Press & Missouri Botanical Garden Press, Beijing St. Louis, pp. 253–271.

Janssen, R., Doppler, G., Grimm, K., Grimm, M., Haas, U., Hiss, M., Köthe, A., Radtke, G., Reichenbacher, B., Salamon, M., Standke, G., Teipel, U., Thomas, M., Uffenorde, H., Wielandt-Schuster, U. & Subkommission Tertiär-Stratigraphie, 2018. The Tertiary in the Stratigraphic Table of Germany 2016 (STG 2016). *Zeitschrift der Deutschen Gesellschaft für Geowissenschaften*, 169: 267–294.

Johnson, E. M. & Sutton, T. B., 2000. Response of two fungi in the apple sooty blotch complex to temperature and relative humidity. *Phytopathology*, 90: 362–367.

Jussieu, A.-L., 1789. *Genera plantarum : secundum ordines naturales disposita, juxta methodum in Horto regio Parisiensi exaratam*. Viduam Herissant et Theophilum Barrois, Paris, 498 pp.

Kalgutkar, R. M. & Jansonius, J., 2000. Synopsis of fossil fungal spores, mycelia and fructifications. *AASP Contribution Series*, 39: 1–428.

Kalgutkar, R. M. & Sweet, A. R., 1988. Morphology, taxonomy and phylogeny of the fossil fungal genus *Pesavis* from northwestern Canada. *Geological Survey of Canada Bulletin*, 379: 117–133.

Kirchheimer, F., 1941. Ein neuer Beitrag zur Kenntnis der Braunkohlenflora in der Lausitz. *Beitrag zur Biologie der Pflanzen*, 27: 189–231.

Kirchheimer, F., 1942. Zur Kenntnis der Alttertiärflora von Wiesa bei Kamenz. *Planta*, 32: 418–446.

Kirchheimer, F., 1943a. Über den Nachweis der Styracaceen-Gattung *Halesia* Ellis im Tertiär Mitteleuropas. *Planta*, 33: 505–515.

Kirchheimer, F., 1943b. Bemerkenswerte Frucht- und Samenreste besonders aus den Braunkohlenschichten der Lausitz. *Botanisches Archiv*, 44: 362–430.

Kolakovskiy, A. A., 1964. *A Pliocene Flora of the Kodor River*. Izdatielstwo Akademii Nauk Gruzinskoy SSR, Sukhumi, 208 pp. [In Russian, with English summary.]

Kovar-Eder, J. & Kvaček, Z., 2007. The integrated plant record (IPR) to reconstruct Neogene vegetation: the IPR-vegetation analysis. *Acta Palaeobotanica*, 47: 391–418.

Kovar-Eder, J. & Meller, B., 2001. Plant assemblages from the hanging wall sequence of the opencast mine Oberdorf N Voitsberg, Styria (Austria, Early Miocene, Ottnangian). *Palaeontographica Abteilung B*, 259: 65–112.

Kowalski, R., Worobiec, G., Worobiec, E. & Krajewska, K., 2020. Oligocene plant assemblage from Rębiszów (Lower Silesia): first "volcanic flora" from Poland. *Acta Palaeontologica Polonica*, 65: 273–290.

Krutzsch, W., 1957. Sporen- und Pollengruppen aus der Oberkreide und dem Tertiär Mitteleuropas und ihre stratigraphische Verteilung. *Zeitschrift für angewandte Geologie*, 3: 509–548.

Krutzsch, W., 2000. Stratigraphische Tabelle Oberoligozän und Neogen (marin-kontinental). *Berliner geowissenschaftliche Abhandlungen*, 34: 153–165.

Krutzsch, W., Blumenstengel, H., Kiesel, Y. & Rüffle, L., 1992. Paläobotanische Klimagliederung des Alttertiärs (Mitteleozän bis Oberoligozän) in Mitteldeutschland und das Problem der Verknüpfung mariner und kontinentaler Gliederungen (klassische marine Biostratigraphien – paläobotanische, ökologische Klimastratigraphie – Evolutions-Stratigraphie Vertebraten). *Neues Jahrbuch für Geologie und Paläontologie*, 186: 137–253.

Kunth, K. S., 1817. *Nova Genera et Species Plantarum*. Librariae Graeco-Latino-Germanicae, Paris, 404 pp.

Kunzmann, L., 2014. On the fossil history of *Pseudotsuga* Carr. (Pinaceae) in Europe. *Palaeobiodiversity and Palaeoenvironments*, 94: 393–409.

Kunzmann, L. & Mai, D. H., 2005. Die Koniferen der Mastixioideen-Flora von Wiesa bei Kamenz (Sachsen, Miozän) unter besonderer Berücksichtigung der Nadelblätter. *Palaeontographica Abteilung B*, 272: 67–135.

Kvaček, Z., 2007. Do extant nearest relatives of thermophile European Cenozoic plant elements reliably reflect climatic signal? *Palaeogeography, Palaeoclimatology, Palaeoecology*, 253: 32–40.

Kvaček, Z. & Walther, H., 2004. Oligocene flora of Bechlejovice at Děčín from the neovolcanic area of the České Středohoří Mountains, Czech Republic. *Acta Musei Nationalis Pragae, B, Historia Naturalis*, 60: 9–60.

Landesamt für Geobasisinformation Sachsen (GeoSN): WebatlasSN, digitale Orthofotos RGB. https://geoportal.sachsen.de/cps/karte.html?showmap=true [Accessed on 05/01/2021].

Leder, R., 2007. Mitteilung über die Entdeckung eines fossilen Blatthorizontes aus dem Mittelmiozän der Tongrube Tetta-Buchholz in der Oberlausitz (Sachsen). *Veröffentlichungen des Museums der Westlausitz Kamenz*, 27: 59–80.

Leder, R., 2009. Karpologische Belege aus dem fossilen Blätterhorizont der Tongrube Tetta-Buchholz. *Veröffentlichungen des Museums der Westlausitz Kamenz*, 29: 51–74.

Limaye, R. B., Kumaran, K. P. N., Nair, K. M. & Padmalal, D., 2007. Non-pollen palynomorphs as potential palaeoenvironmental indicators in the Late Quaternary sediments of the west coast of India. *Current Science*, 92: 1370–1382.

Linnaeus, C., 1753. *Species plantarum: exhibentes plantas rite cognitas, ad genera relatas, cum differentiis specificis, nominibus trivialibus, synonymis selectis, locis natalibus, secundum systema sexuale digestas*. Laurentius Salvius, Stockholm, 1200 pp.

Linnaeus, C., 1759. *Systema Naturae. Vol. 2*. Laurentii Salvi, Stockholm, pp. 825–1384.

Linnemann, U., Romer, R. L., Gerdes, A., Jeffries, T. E., Drost, K. & Ulrich, J., 2010. The Cadomian Orogeny in the Saxo-Thuringian Zone. In: Linnemann, U. & Romer, R. L. (eds), *Pre-Mesozoic Geology of Saxo-Thuringia: From the Cadomian Active Margin to the Variscan Orogen*. Schweizerbart, pp. 37–58.

Lotsch, D., Krutzsch, W., Mai, D. H., Kiesel, Y. & Lazar, E., 1969. Stratigraphisches Korrelationsschema für das Tertiär der Deutschen Demokratischen Republik. *Abhandlungen des Zentralen Geologischen Instituts*, 12: 1–438.

Loureiro, J., 1790. *Flora cochinchinensis: sistens plantas in regno Cochinchina nascentes. Quibus accedunt aliæ observatæ in Sinensi imperio, Africa Orientali, Indiæque locis variis. Omnes dispositæ secundum systema sexuale Linnæanum. Volume 2*. Academicis, Lisboa, pp. 357–744.

Macphail, M. K. & Hill, R. S., 1994. K-Ar dated palynofloras in Tasmania 1: Early Oligocene, Proteacidites tuberculatus Zone sediments, Wilmot Dam, northwestern Tasmania. *Papers and Proceedings of the Royal Society of Tasmania*, 128: 1–15.

Mai, D. H., 1965. Der Florenwechsel im jüngeren Tertiär Mitteleuropas. *Feddes Repertorium*, 70: 157–169.

Mai, D. H., 1967. Die Florenzonen, der Florenwechsel und die Vorstellungen über den Klimaablauf im Jungtertiär der Deutschen DDR. *Abhandlungen des Zentralen Geologischen Instituts*, 10: 55–81.

Mai, D. H., 1971. Fossile Funde von *Manglietia* Blume (Magnoliaceae). *Feddes Repertorium*, 82: 441–448.

Mai, D. H., 1985. Entwicklung der Wasser- und Sumpfpflanzen-Gesellschaften Europas von der Kreide bis ins Quartär. *Flora*, 176: 449–511.

Mai, D. H., 1987. Neue Arten nach Früchten und Samen aus dem Tertiär von Nordwestsachsen und der Lausitz. *Feddes Repertorium*, 98: 105–126.

Mai, D. H., 1994. Two conifers – *Tetraclinis* Mast. (Cupressaceae) and *Metasequoia* Miki (Taxodiaceae) – relics or palaeoclimatic indicators of the Past. *NATO ASI Series, Serie I. Global Environmental Change*, 27: 199–213.

Mai, D. H., 1995. *Tertiäre Vegetationsgeschichte Europas. Methoden und Ergebnisse.* G. Fisher Verlag, Jena, Stuttgart, New York, 691 pp.

Mai, D. H., 1997. Die oberoligozänen Floren am Nordrand der Sächsischen Lausitz. *Palaeontographica Abteilung B*, 244: 1–124.

Mai, D. H., 1999. Die untermiozänen Floren aus der Spremberger Folge und dem 2. Flözhorizont in der Lausitz. II: Polycarpicae and Apetalae. *Palaeontographica, Abteilung B*, 251: 1–70.

Mai, D. H., 2000. Die untermiozänen Floren aus der Spremberger Folge und dem 2. Flözhorizont in der Lausitz. IV: Fundstellen und Paläobiologie. *Palaeontographica, Abteilung B*, 254: 65–176.

Mai, D. H., 2001. Die mittelmiozänen und obermiozänen Floren aus der Meuroer und Raunoer Folge in der Lausitz. III: Fundstellen und Paläobiologie. *Palaeontographica Abteilung B*, 258: 1–85.

Mai, D. H., 2008. Paläokarpologische Untersuchungen im Ober-Oligozän von Oberleichtersbach bei Bad Brückenau (Unterfranken). *Courier Forschungsinstitut Senckenberg*, 260: 31–77.

Mai, D. H. & Walther, H., 1978. Die Floren der Haselbacher Serie im Weisselster Becken. *Abhandlungen des Staatlichen Museums für Mineralogie und Geologie zu Dresden*, 28: 1–200.

Mai, D. H. & Walther, H., 1991. Die oligozänen und untermiozänen Floren NW Sachsens und des Bitterfelder Raumes. *Abhandlungen des Staatlichen Museums für Mineralogie und Geologie zu Dresden*, 38: 1–230.

Matthew, K. M., 1976. A revision of the genus *Mastixia* (Cornaceae). *Blumea*, 23: 51–93.

Meller, B., 1998. Systematisch-taxonomische Untersuchungen von Karpo-Taphocoenosen des Köflach-Voitsberger Braunkohlenrevieres (Steiermark, Österreich; Untermiozän) und ihre paläoökologische Bedeutung. *Jahrbuch der Geologischen Bundesanstalt*, 140: 497–655.

Merrill, E. D., 1937. Miscellanea Sinensia. *Sunyatsenia*, 3: 246–262.

Moore, P. D., Webb, J. A. & Collinson, M. E., 1991. *Pollen Analysis*. Blackwell, Oxford, 216 pp.

Nooteboom, H. P., 1985. Notes on Magnoliaceae. *Blumea 1*, 31: 65–121.

Office of Communications and Publishing, 2016. EarthWord – Tertiary. https://www.usgs.gov/communications-and-publishing/news/earthword-tertiary [04.04.2023].

Ohsawa, M., 1990. An interpretation of latitudinal patterns of forest limits in south and east Asian mountains. *Journal of Ecology*, 78: 326–339.

Page, C. N., 1989. New and maintained genera in the conifer families Podocarpaceae and Pinaceae. *Notes from the Royal Botanic Garden Edinburgh*, 45: 377–395.

Palamarev, E., 1967. Xerotherme Elemente in der Tertiärflora Bulgariens und Aspekte zum Problem der Formierung der mediterranen Flora auf der Balkanhalbinsel. *Abhandlungen des Zentralen Geologischen Instituts, Berlin*, 10: 167–175.

Perkins, J., 1907. Styracaceae. In: Engler, A. (ed.), *Das Pflanzenreich: regni vegetablilis conspectus*, W. Engelmann, Leipzig, IV, 214: pp. 1–111.

Piwocki, M. & Ziembińska-Tworzydło, M., 1997. Neogene of the Polish Lowlands – lithostratigraphy and pollen-spore zones. *Geological Quarterly*, 41: 21–40.

Pole, M. S., Hill, R. S., Green, N. & Macphail, M. K., 1993. The Oligocene Berwick Quarry flora-rainforest in a drying environment. *Australian Systematic Botany*, 6: 399–427.

Pound, M. J., Nuñez Otaño, N. B., Romero, I. C., Lim, M., Riding, J. B. & O'Keefe, J. M. K., 2022. The fungal ecology of the Brassington Formation (Middle Miocene) of Derbyshire, United Kingdom, and a new method for palaeoclimate reconstruction. *Frontiers in Ecology and Evolution*, 10: 947623.

Rodriguez-Ramirez, E. C., Sanchez-Gonzalez, A. & Angeles-Perez, G., 2013. Current distribution and coverage of Mexican beech forests *Fagus grandifolia* subsp. *mexicana* in Mexico. *Endangered Species Research*, 20: 205–216.

Rudolphi, F., 1830. *Systema orbis vegetabilium: quod gratiosi medicorum ordinis consensu et auctoritate*. Gryphiae. Typis F. Guil, Kunike, 80 pp.

Selkirk, D. R., 1975. Tertiary fossil fungi from Kiandra, New South Wales. *Proceedings of the Linnean Society of New South Wales*, 97: 141–149.

Siebold, P. F. & Zuccarini, J. G., 1835. *Flora Japonica; sive, Plantae Quas in Imperio Japonico Collegit, Descripsit, ex Parte in Ipsis Locis Pingendas Curavit. Sectio Prima Continens Plantas Ornatui vel Usui Inservientes*. Apud auctorem, Leiden, 193 pp.

Siebold, P. F. & Zuccarini, J. G., 1846. Flora Japonicae. Familiae naturales, adjectis generum et specierum exemplis selectis. Plantae Dicotyledoneae et Monocotyledoneae. *Abhandlungen der Mathematisch-Physikalischen Classe der Königlich Bayerischen Akademie der Wissenschaften*, 4: 123–239.

Smith, P. H. & Crane, P. R., 1979. Fungal spores of the genus *Pesavis* from the Lower Tertiary of Britain. *Botanical Journal of the Linnean Society*, 79: 243–248.

Standke, G., 1998. Zur Stratigraphie der Tertiärvorkommen in der nördlichen Oberlausitz. *Veröffentlichungen des Museums der Westlausitz Kamenz*, 20: 23–64.

Standke, G., 2008. Tertiär. In: Pälchen, W. & Walther, H. (eds), *Geologie von Sachsen*. Schweizerbarth, Stuttgart, pp. 358–419.

Standke, G. & Rascher, J., 2005. *Geologischer Atlas Tertiär Nordwestsachsen 1 : 250.000*. GEOmon-tan GmbH Freiberg, Sächsisches Landesamt für Umwelt, Freiberg, Dresden, 22 pp.

Steding, D. & Brause, H., 1969. Beziehungen zwischen Grund- und Deckgebirge in der Oberlausitz. In: Hirschmann, G. & Brause, H. (eds), *Exkursionsführer Zum Treffen Des Fachverbandes Geologie vom 7. bis 10. September 1969 in Görlitz „Alt- Und Vorpaläozoikum des Görlitzer Schiefergebirges und der westlichen Westsudeten" mit Kurzreferaten*. Deutsche Gesellschaft für Geologische Wissenschaften, Berlin, pp. 35–48.

Stuchlik, L., Ziembińska-Tworzydło, M., Kohlman-Adamska, A., Grabowska, I., Słodkowska, B., Ważyńska, H. & Sadowska, A., 2009. *Atlas of Pollen and Spores of the Polish Neogene. Volume 3 – Angiosperms (1).* W. Szafer Institute of Botany, Polish Academy of Sciences, Kraków, 233 pp.

Stuchlik, L., Ziembińska-Tworzydło, M., Kohlman-Adamska, A., Grabowska, I., Słodkowska, B., Worobiec, E. & Durska, E., 2014. *Atlas of Pollen and Spores of the Polish Neogene. Volume 4 – Angiosperms (2).* W. Szafer Institute of Botany, Polish Academy of Sciences, Kraków, 466 pp.

Stuchlik, L., Ziembińska-Tworzydło, M., Kohlman-Adamska, A., Grabowska, I., Ważyńska, H. & Sadowska, A., 2002. *Atlas of Pollen and Spores of the Polish Neogene. Volume 2 – Gymnosperms.* W. Szafer Institute of Botany, Polish Academy of Sciences, Kraków, 237 pp.

Stuchlik, L., Ziembińska-Tworzydło, M., Kohlman-Adamska, A., Grabowska, I., Ważyńska, H., Słodkowska, B. & Sadowska, A., 2001. *Atlas of Pollen and Spores of the Polish Neogene.*

*Volume 1 – Spores*. W. Szafer Institute of Botany, Polish Academy of Sciences, Kraków, 158 pp.

Tang, C. Q. & Ohsawa, M., 1997. Zonal transition of evergreen, deciduous and coniferous forests along the altitudinal gradient on humid subtropical mountain, Mt. Emei, Sichuan, China. *Plant Ecology*, 133: 63–78.

Teodoridis, V., Kovar-Eder, J. & Mazouch, P., 2011. Integrated Plant Record (IPR) vegetation analysis applied to modern vegetation in South China and Japan. *Palaios*, 26: 623–638.

Teodoridis, V., Mazouch, P. & Kovar-Eder, J., 2020. The Integrated Plant Record (IPR) analysis: Methodological advances and new insights into the evolution of European Palaeogene/Neogene vegetation. *Palaeontologia Electronica*, 23: a16.

Thunberg, C. P., 1784. *Flora Japonica sistens plantas insularum japonicarum*. Bibliopolio I. G. Mülleriano, Leipzig, 419 pp.

Tiffney, B. H., 1977. Fruits and seeds of the Brandon Lignite: Magnoliaceae. *Botanical Journal of the Linnean Society*, 75: 299–323.

Uhl, D. & Herrmann, M., 2010. Palaeoclimate estimates for the Late Oligocene taphoflora of Enspel (Westerwald, W-Germany) based on palaeobotanical proxies. *Palaeobiodiversity and Palaeoenvironments*, 90: 39–47.

Utescher, T., Bruch, A. A., Erdei, B., François, L., Ivanov, D., Jacques, F. M. B., Kern, A. K., Liu, Y-S. (C.), Mosbrugger, V. & Spicer, R. A., 2014. The coexistence approach – theoretical background and practical considerations of using plant fossils for climate quantification. *Palaeogeography, Palaeoclimatology, Palaeoecology*, 410: 58–73.

Van der Burgh, J., 1987. Miocene floras in the Lower Rhenish Basin and their ecological interpretation. *Review of Palaeobotany and Palynology*, 52: 299–366.

Wang, C.-W., 1961. *The Forests of China, with a Survey of Grassland and Desert Vegetation.* Maria Moors Cabot Foundation, Cambridge, 313 pp.

Wang, Y., Liu, B., Nie, Z., Chen, H., Chen, F., Figlar, R. B. & Wen, J., 2020. Major clades and a revised classification of *Magnolia* and Magnoliaceae based on whole plastid genome sequences via genome skimming. *Journal of Systematics and Evolution*, 58: 673–695.

Wilbur, R. L., 1994. The Myricaceae of the United States and Canada: genera, subgenera, and Series. *Sida*, 16: 93–107.

Winterscheid, H. & Gossmann, R., 2017. Validation of *Cathaya vanderburghii* (Pinaceae) from European Neogene. *Phytotaxa*, 302: 188–192.

Wolfe, J. A., 1979. Temperature parameters of humid to mesic forests of Eastern Asia and relation to forests of other regions of the northern hemisphere and Australasia. *Geological Survey Professional Paper*, 1106: 1–37.

Xu, F.-X., 2003. Sclerotesta morphology and its systematic implications in magnoliaceous seeds. *Botanical Journal of the Linnean Society*, 142: 407–424.

Yao, X., Ye, Q.-G., Ge, J.-W., Kang, M. & Huang, H., 2007. A new species of *Sinojackia* (Styracaceae) from Hubei, central China. *Novon*, 17: 138–140.

Ying, T.-S., Zhang, Y.-L. & Boufford, D. E., 1993. *The Endemic Genera of Seed Plants of China*. Science Press, Beijing, 824 pp.

Zastawniak, E., 1992. Age of the macrofossils from Gozdnica and Gozdnica-Stanisław localities and their comparison with other Neogene floras. In: Zastawniak, E. (ed.), *The Younger Tertiary Deposits in the Gozdnica Region (SW Poland) in the Light of Recent Palaeobotanical Research*. *Polish Botanical Studies*, 3: 49–53.